UNIVERSITY OF SOUTHAMPTON

FACULTY OF ENGINEERING, SCIENCE AND MATHEMATICS

School of Mathematics

When is a Stokes line not a Stokes line?

by

Philip J. Langman

Supervised by Dr C. J. Howls

Thesis for the degree of Doctor of Philosophy

December 2005

UNIVERSITY OF SOUTHAMPTON

ABSTRACT

FACULTY OF ENGINEERING, SCIENCE AND MATHEMATICS
SCHOOL OF MATHEMATICS

Doctor of Philosophy

WHEN IS A STOKES LINE NOT A STOKES LINE?

by Philip John Langman

During the course of a Stokes phenomenon, an asymptotic expansion can change its form as a further series, prefactored by an exponentially small term and a Stokes multiplier, appears in the representation. The initially exponentially small contribution may nevertheless grow to dominate the behaviour for other values of the asymptotic or associated parameters.

We introduce the concept of a higer order Stokes phenomenon, at which a Stokes multiplier itself can change value. We show that the higher order Stokes phenomenon can be used to explain the apparent sudden birth of Stokes lines at regular points, why some Stokes lines are irrelevant to a given problem and why it is indespensible to the proper derivation of expansions that involve three or more possible asymptotic contributions. We provide an example of how the higher order Stokes phenomenon can have important effects on the large time behaviour of linear partial differential equations.

Subsequently we apply these techniques to Burgers equation, a non-linear partial differential equation developed to model turbulent fluId flow. We find that the higher order Stokes phenomenon plays a major, yet very subtle role in the smoothed shock wave formation of this equation.

Contents

List of Figures

Acknowledgements

I would like to thank my supervisor, Doctor Chris Howls, first and foremost for his unfailing support, patience, enthusiasm, encouragement and friendship throughout my time as a research student. I extend my gratitude to Doctor Adri Olde Daalhuis, Professor Jon Chapman and to Doctor David Mortimer for many helpful discussions. Thanks also to Doctor Nils Andersson, Professor James Vickers and Professor Eric Delabaere for their comments and advice. I thank the E.P.S.R.C for funding my studies.

I am eternally grateful to my friends and fellow postgraduate students, who made my time with them memorable and enjoyable. In no particular order, thanks to Princi, Bhey, Tone, Beeroy, CJ, JC, Pacey, D, JD, the MK Massive, The Man from Del Monte and Lo*Chine. Thanks to the academic and administrative staff at the School of Mathematics.

I extend my heartfelt thanks to Sarah - without her love and support I would have lost the plot a long time ago. Finally a big thank you to my family, especially Jonno, Linda, Mr and Mrs Harold, George, Mannfred, Chicken, Stig, Nanny Caff, Nanny Betty, Sheila and the Saaf Landan Krew, Unky Matt, Stellar, BigCrash, Tula, Ben, Billie, Charm, Tigger, Leo, Isaac and Otis.

Without all of the people mentioned above, I would not be where I am today. Cheers.

Chapter 1

Introduction

The question posed by the title of this thesis, "When is a Stokes line not a Stokes line?", requires a mixture of accepted asymptotic techniques and subtle new extensions of these ideas in order to be answered. In doing so, this thesis intends to highlight the importance of the seemingly insignificant: the small exponential term.

Poincaré's initial definition of an asymptotic series is well known to have neglected terms of this nature. This was not necessarily a bad thing; an approximation with an exponentially small error term is not always necessary. We only really see how exponentially small terms being forgotten in an asymptotic approximation can be a mistake when we consider how a Poincaré asymptotic approximation cannot account for what is known as the Stokes phenomenon. This is characterised by the sudden introduction or removal of asymptotic terms in an expansion prefactored by a small exponential as the asymptotic parameter is varied.

Once it was acknowledged that these 'subdominant' exponentials existed, alternative approaches to asymptotics were introduced, where small exponentials were explicitly included in an approximation. The most recent and most accurate method for handling these small exponentials (and the Stokes phenomenon) is called hyperasymptotics, developed by Berry and Howls. Not only does hy-

perasymptotics give exponential accuracy over a Poincaré approximation, it also culminates in an exact remainder term.

It is the hyperasymptotic techniques developed by, in particular, Berry & Howls and Olde Daalhuis that leads to the main result of this thesis, which we have called the Higher Order Stokes Phenomenon. This occurs across a Higher Order Stokes curve, and changes the potential for a regular Stokes phenomenon to occur. This is a subtle effect, and we show that as a result, initially sub-subdominant terms (those which might normally be neglected in an asymptotic approximation) can grow to dominate the behaviour of some asymptotic expansions, the neglect of which would lead to incorrect assumptions about the long-term behaviour. This is a general result which is not only confined to the examples we have chosen.

The layout of the thesis is as follows.

Chapter 2 will give a brief historical summary of asymptotic analysis. We will begin by looking at infinite series. We will summarise Dingle's philosophy regarding divergent series, and via a theorem due to Darboux we will see that in general, the late terms of a divergent series have a general form of a factorial over a power. Knowledge of the form of the late terms leads to the development of optimal truncation, which allows the truncation point of an asymptotic series to vary. This provides an advantage over Poincaré's asymptotic series which has strictly fixed truncation points. By allowing the truncation point to vary, exponential accuracy can be achieved over a Poincaré asymptotic series truncation. We define the Stokes phenomenon and explore its relevance through the Airy function $\mathrm{Ai}(z)$. We show how the explicit inclusion of exponential terms in an asymptotic approximation ("exponential asymptotics") can make calculations simpler, and we compare this approach with matching techniques. We show how a "ladder" of exponentials is necessary to improve the accuracy of an approximate solution to boundary layer ODEs, which often leave one boundary condition only approximately satisfied. We review hyperasymptotics, and introduce the notion of the Borel plane; a vital technique used throughout the rest of the thesis.

Chapter 3 explains the higher order Stokes phenomenon, both in a general case and via a PDE example. This chapter contains new results.

Chapter 4 extends the work of the previous chapter to a nonlinear PDE, and we find that the higher order Stokes phenomenon contributes to some very subtle behaviour. We show how it has a *real* effect on the behaviour of a nonlinear PDE.

Chapter 5 offers some suggestions for future work, and reviews the results of the thesis.

Chapter 2

Asymptotics and Small Exponentials

This thesis is primarily interested in exploring the role of exponentially small terms in asymptotic analysis, particularly when applied to differential equations (both linear and non-linear). This chapter is intended to introduce the necessary topics within the broad field of asymptotic analysis to the reader. We shall also discuss briefly the historical development of the tools which we will be implementing throughout the work within this thesis.

Some new ideas to improve the accuracy of solutions of boundary layer ODEs are also included in this chapter.

2.1 Infinite Series

The history of divergent series has been fraught with antagonism amongst mathematicians. Hardy [1] wrote an account of the "fall and rise" of divergent series in analysis. He says that there was a disinclination amongst mathematicians to give formal definitions, combined with an inadequate theory of complex variables and analytic continuation at the time. Perhaps the most famous quote on this subject

is attributed to Abel (1828): *"The divergent series are the intention of the devil, and it is a shame to base on them any demonstration whatsoever"*. Of course, Abel's view has since been shown to have been somewhat blinkered, as divergent series now have many applications in analysis.

Let a_n be an infinite sequence $a_1, a_2, a_3, \ldots, a_n, \ldots$. Then

$$S_n = \sum_{n=1}^{\infty} a_n \tag{2.1}$$

is called an infinite series. The task of computing the sum of such a series presents many problems. We cannot add up all the infinitely many terms, so instead we sum an ever increasing number of terms; a new sequence called the partial sum of the original series. The expression

$$\lim_{n\to\infty} S_n = \sum_{n=1}^{N} a_n, \quad N = 1, 2, 3, \ldots \tag{2.2}$$

is the Nth partial sum of the series (2.1) [2].

If $\lim S_n$ exists and is finite, the series a_n is said to converge to this limit (a_n is a convergent series). If $\lim S_n$ is infinite, or does not exist, then the series a_n is said to diverge (a_n is a divergent series).

Historically, it seems mathematicians disliked divergent series due to the problems in assigning meaningful values to them. The sum of a convergent series can be computed to arbitrarily high accuracy (subject to the necessary effort and sufficient computing power), but the approximation of a divergent series is restricted to only a finite number of terms in the series, before the series tends to its divergent limit.

In 1849, G.G. Stokes [3] wrote a paper in which he implied that infinite series that do not converge are useful as "symbolic" representations of functions (an idea later embraced by Dingle [4]). He suggested that a divergent series could be employed as an abbreviated way of expressing the limit of a convergent series. The problem lay in how to correctly interpret divergent series expansions of functions.

In 1886, Poincaré [5] was the first to wrote down his definition for an asymptotic series:

Let $f(z)$ be a function of the real or complex variable z, and $\sum a_s z^{-s}$ be a formal power series (convergent or divergent). Then, if

$$f(z) \sim \sum_{s=0}^{\infty} a_s z^{-s} \tag{2.3}$$

for $|z| \to \infty$, then for every fixed *integer $n \geq 0$ the remainder term*

$$R_n(z) = f(z) - \sum_{s=0}^{n-1} a_s z^{-s} \tag{2.4}$$

is $O(z^{-n})$ as $|z| \to \infty$ in some sector S.

The series $\sum a_s z^{-s}$ is said to be a Poincaré asymptotic expansion of $f(z)$. If the series $\sum a_s z^{-s}$ converges, then it is an asymptotic expansion of its sum [6].

Poincaré's definition allows basic formal manipulations. Addition, subtraction, multiplication and division of Poincaré expansions of functions can be carried out as if these procedures were being performed on the parental functional representations, with the asymptotic nature of the result itself being assured [6]. Term-by-term integration of expansions is allowed (subject to f being an integrable function), the result being Poincaré asymptotic to the integrated function (see [6] for further detail). Differentiation may not always be possible. For example [6], if

$$f(x) = e^{-x} \sin(e^x) \tag{2.5}$$

(x real and positive), then since

$$f(x) \sim 0 + \frac{0}{x} + \frac{0}{x^2} + \cdots \quad \text{as } x \to \infty, \tag{2.6}$$

(for reasons that we shall see shortly, see equation 2.21). But $f'(x) \equiv \cos(e^x) - e^{-x}\sin(e^x)$ oscillates as $x \to \infty$, and so $f(x)$ cannot be written in the form of (2.4). Differentiation is legitimate when $f'(x)$ is continuous and its asymptotic expansion exists. Series reversion (or "inversion") is possible as well. For examples, see [6], [7] or [8].

A Poincaré expansion guarantees a result accurate in magnitude to the order of the first term neglected, ie. the $(n+1)^{th}$ term. However, (2.4) only states that the

remainder is algebraically decreasing in $|1/z|$. It gives no information about the optimal point numerically to truncate the series, when $|R_n(z)|$ is at a minimum. Only if the behaviour of the a_r in (2.3) is known is it possible to determine an optimal truncation point N.

Berry [9] illustrated this idea. Consider an infinite series expansion which takes the form of a factorial-over-a-power; that is,

$$|a_r| \approx K\frac{(r-1)!}{|x|^r},\ K > 0. \tag{2.7}$$

Note that we will use the "$\approx$" symbol whenever an approximation has been made in the formal analysis. We have

$$\frac{|a_{r+1}|}{|a_r|} \approx \frac{r}{|x|}, \tag{2.8}$$

thus the minimum term is $r = N \approx |x|$. It is expected that the minimum remainder term will be at this point also. Therefore

$$|a_N| \approx K\frac{(|x|-1)!}{|x|^{|x|}}. \tag{2.9}$$

Stirling's formula for a factorial [4] is

$$x! = \sqrt{2\pi}x^{x+1/2}e^{-x}, \tag{2.10}$$

which, upon substitution into (2.9) gives

$$|a_N| \approx \sqrt{2\pi}K\frac{e^{-|x|}}{|x^{\frac{1}{2}}|}. \tag{2.11}$$

Poincaré asymptotics fixes N to be a constant for all z. If the above series were Poincaré asymptotic to a function, stopping at the first term would give an error of $O(1/|z|)$. We see that by varying N with $|z|$ to find the least term, we can obtain exponential accuracy for this series over the lowest order result. This idea was termed "superasymptotics" by Berry [9].

Figure 2.1 shows how terms in a power-over-factorial type series increase initially, before rapidly converging to a point. Terms in a divergent factorial-over-power series typically decrease initially before reaching a minimum and swiftly increasing, as shown in Figure 2.2.

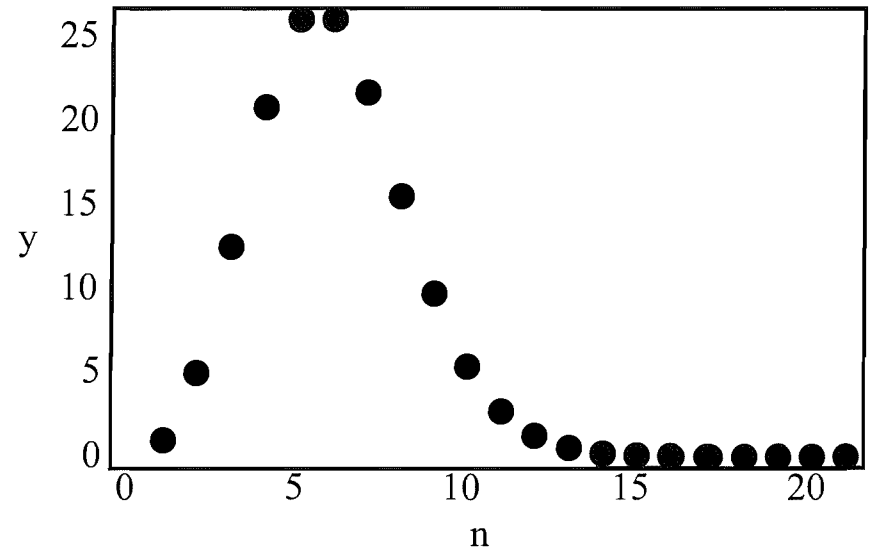

Figure 2.1: A plot of the terms $y = \frac{x^n}{n!}$ with $x = 5$. Notice that in this power-over-factorial series the size of the terms initially increase, before converging to as n becomes larger.

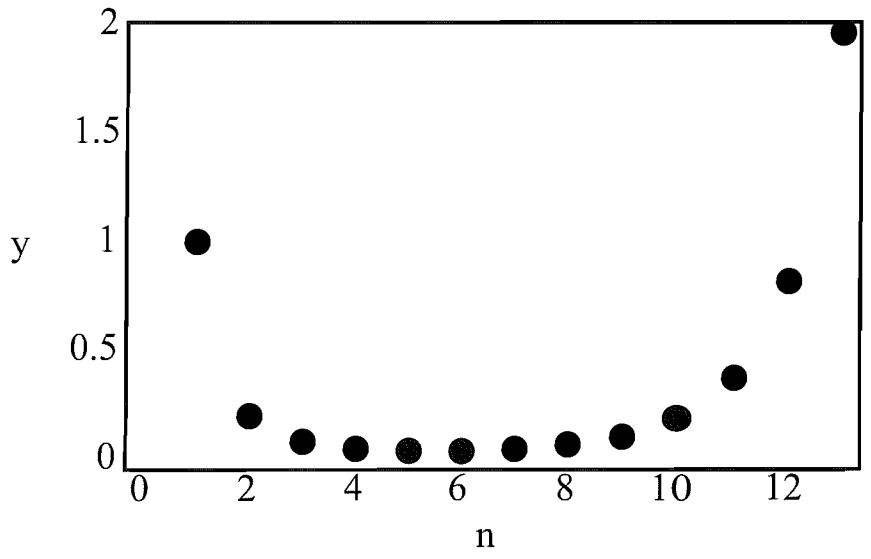

Figure 2.2: A plot of the terms $y = \frac{n!}{x^n}$ with $x = 5$. This factorial-over-power series is divergent, yet initially the size of the terms is decreasing.

The specific form of the series (2.7) allowed us to specify N above. This factorial-over-power form of series may appear a very particular choice, but in fact series of this type arose in a theorem due to Darboux [4]. It is necessary to know the form of the general term in an asymptotic expansion not only to be able to gain greater accuracy, but also to guarantee that an expansion is of the expected asymptotic form [4]. The Darboux theorem relates the behaviour of terms in a series to the singularity structure of the functions they represent, and shows how the late terms of a series diverge.

Suppose $\phi(f)$ converges within a circle, and that it can be expanded within a Taylor series $\sum_0^\infty a_r f^r$. Let f_i be a pole or branch point on or outside this circle of convergence. In the vicinity of this point we can write

$$\phi(f) = (f_i - f)^{-p_i}\phi_i(f), \tag{2.12}$$

where p_i is a positive integer for a pole and fractional (positive or negative) for a branch point, and where $\phi(f)$ is expansible as a Taylor series

$$\phi_i(f) = \phi_i(f_i) - (f_i - f)\phi_i'(f_i) + (f_i - f)^2\phi_i''(f_i)/2! - \ldots. \tag{2.13}$$

Now, the coefficient of f^r in $(f_i - f)^{-p_i}$ is $(r + p_i - 1)!/r!(p_i - 1)!f_i^{r+p_i}$ so the contribution to a_r from the singularity at $f = f_i$ is

$$\frac{(r + p_i - 1)!}{r!(p_i - 1)!f_i^{r+p_i}}\left(\phi_i - \frac{p_i - 1}{r + p_i - 1}f_i\phi_i' + \ldots\right), \tag{2.14}$$

an expansion suitable for late coefficients $r \gg p_i$. For such large r the factor f^r in the denominator ensures dominant contributions from those f_i with smallest modulus, ie. from singularities lying on the circle of convergence.

The Darboux theorem shows how late terms in a Taylor series for a given function will depend on the behaviour of that function in the neighbourhood of the singularity closest to the origin of expansion. We also find that the late terms of any asymptotic power series can be expressed in a standard factorial-over-power form.

Borel (1899) [4] wrote that the sum of a divergent series could be defined as

$$\sum_{r=0}^{\infty} \frac{a_r}{x^r} = \int_0^{\infty} e^{-u} du \sum_{r=0}^{\infty} \frac{a_r}{r!} \left(\frac{u}{x}\right)^r, \tag{2.15}$$

provided the summation on the right converges for some range of u/x (it can then be extended by analytic continuation) and the integral converges. This is known as Borel summation. Dingle wanted to find a general procedure for the termination of an asymptotic series. He developed what he called "terminants" using Borel summation techniques. We have seen that late terms of asymptotic series behave like factorial-over-power, so let

$$\sum_{r=n}^{\infty} \frac{a_r}{x^r} = \int_0^{\infty} e^{-u} du \sum_{r=n}^{\infty} \frac{a_r}{(r+\alpha)!} \left(\frac{u}{x}\right)^{r+\alpha}. \tag{2.16}$$

The series on the RHS is assumed to be convergent, and the sum to infinity of a geometric progression is easily found as

$$\frac{a}{1-r} \tag{2.17}$$

where a is the initial term and r is the ratio between terms. Therefore we have a unique termination to the asymptotic series. Dingle showed that we can express a large class of functions as "first N terms of asymptotic expansion + Nth term $\times$ terminant". The advantage of this is that the terminants take a universal form of either

$$\Lambda_s(z) = \frac{1}{s!} \int_0^{\infty} du \frac{e^{-u} u^s}{1 + u/z} \tag{2.18}$$

or

$$\Pi_s(z) = \frac{1}{s!} \int_0^{\infty} du \frac{e^{-u} u^s}{1 + u^2/z^2}. \tag{2.19}$$

2.2 The Stokes Phenomenon

For a given function $f(z)$ in a region S, there is at most one expansion of the form

$$f(z) \sim a_0 + \frac{a_1}{z} + \frac{a_2}{z^2} + ...(|z| \to \infty). \tag{2.20}$$

However, the converse of this is false [6]. Consider for example, the asymptotic expansion of e^{-z} with $Re(z) > 0$. From the definition (2.4) and the fact that $z^n e^{-z} \to 0$ as $|z| \to \infty$, e^{-z} has a Poincaré expansion

$$e^{-z} \sim 0 + \frac{0}{z} + \frac{0}{z^2} + ..., \quad z \to +\infty, \tag{2.21}$$

the coefficients of each term being identically zero. Hence an arbitrary constant multiple of e^{-z} (or e^{+z} if $Re(z) < 0$) may be added to the function $f(z)$ without altering the Poincaré asymptotic expansion (2.20). Therefore an isolated Poincaré expansion can represent infinitely many functions.

Asymptotic representations which are the sum of several uniquely determined formal series, each multiplied by small exponential prefactors switching in dominance depending on the region in question are, by definition, not Poincaré asymptotic. A truncated and bounded Poincaré representation of this might discard the series prefixed by the small exponentials, leading to misinterpretations in the Poincaré asymptotics of a function if this representation is extended into a domain where the initially discarded and retained exponentials swap dominance. The Poincaré definition therefore introduces ambiguities by failing to represent a function outside a sector of the complex plane. Poincaré's failure to capture small exponential terms in his asymptotic series is highlighted by what is known as the Stokes phenomenon [4].

A function f can have different asymptotic representations in different sectors of the complex plane. As these sectors are crossed, an asymptotic expansion can change discontinuously as a parameter is varied. In this way, exponentially small terms may be introduced into, or removed from, the expansion in question. This change happens across a Stokes line, where the imaginary parts of two contributing asymptotic terms are equal. Let $f_i(x), f_j(x)$ be the asymptotic contributions in question. Then, a Stokes line is defined as

$$S_{i>j} = \{x \in \mathbb{C} : f_j(x) - f_i(x) > 0\}. \tag{2.22}$$

On this line, one exponential is maximally dominant over another. (Lines where

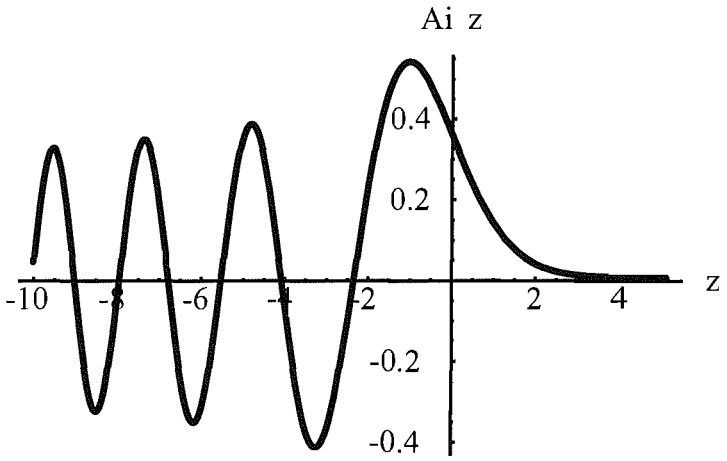

Figure 2.3: A plot of the Airy function Ai(z).

the exponentials are equal in size are known as anti-Stokes lines.)

A well studied example of a Stokes phenomenon taking place is in the Airy function Ai(z) [4], represented by the integral

$$\mathrm{Ai}(z) = \frac{1}{2\pi}\int_{-\infty}^{+\infty} e^{i(zt+t^3/3)}dt. \tag{2.23}$$

From the plot shown in Figure 2.3, we can see that the Airy function Ai(z) oscillates for $z < 0$ and decays quickly for $z > 0$.

The integral in (2.23) has stationary points at $t = \pm i\sqrt{z}$. By making the substitution $t = i\sqrt{z} + x$ into the exponent of the integrand, (2.23) becomes

$$\mathrm{Ai}(z) = \frac{e^{-\frac{2}{3}z^{3/2}}}{2\pi}\int_{-\infty}^{+\infty} dz e^{-(z^2\sqrt{z}-iz^3/3)}. \tag{2.24}$$

Thus, as $|z| \to \infty$, the lowest order approximation to Ai(z) is

$$\mathrm{Ai}(z) \approx \frac{e^{-\frac{2}{3}z^{3/2}}}{2z^{\frac{1}{4}}\sqrt{\pi}}. \tag{2.25}$$

If the $e^{iz^3/3}$ term in (2.24) is not neglected, the asymptotic form of Ai(z) for large, real z is

$$\mathrm{Ai}(z) = \frac{e^{-\frac{2}{3}z^{3/2}}}{2z^{1/4}\sqrt{\pi}}\sum_{r=0}^{\infty} a_r, \tag{2.26}$$

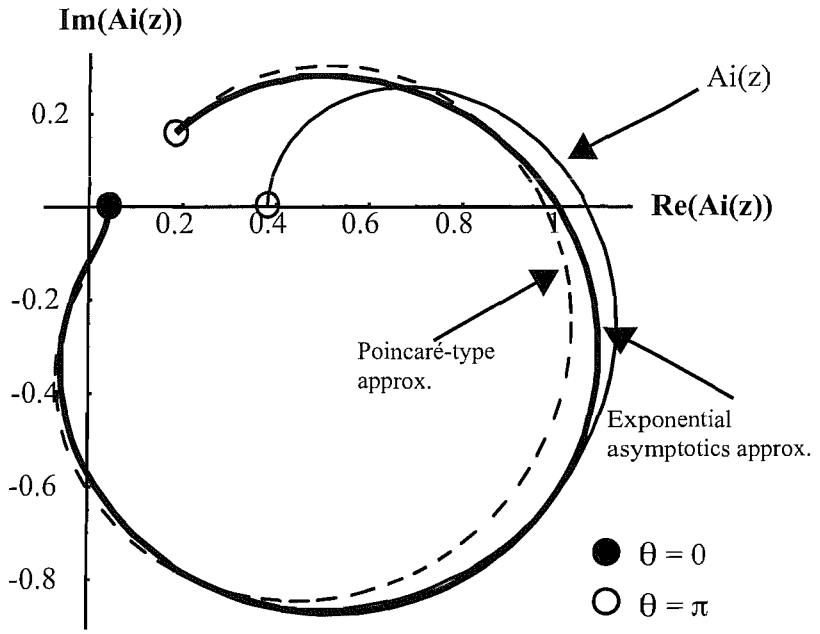

Figure 2.4: A comparison of the Poincaré-type asymptotic expansion (2.25) of the Airy function $\mathrm{Ai}(z)$ in the upper half-plane (the dashed line) and the lowest order exponential asymptotics expansion (2.26) (the thick line). The exact Airy function is also shown as the thin black line. We have taken $|z| = \sqrt{3}$. As we walk around the complex plane in an anti-clockwise sense, the agreement between the approximations and the exact value of the Airy function begins well but becomes less accurate as $\theta \to \pi$.

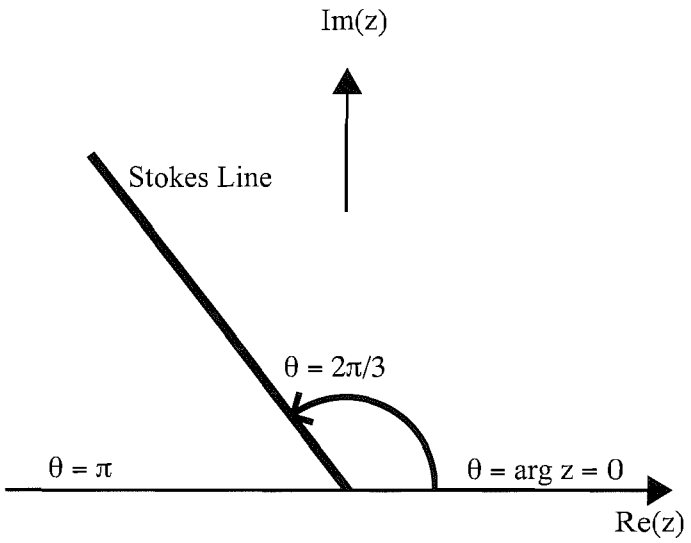

Figure 2.5: The Stokes lines of the Airy function $\mathrm{Ai}(z)$ in the upper-half z-plane.

where

$$a_r = (-1)^r \frac{\Gamma(r+\frac{1}{6})\Gamma(r+\frac{5}{6})}{2\pi\Gamma(r+1)(\frac{4}{3}z^{3/2})^r}. \tag{2.27}$$

Figure 2.4 [11] shows a comparison between the numerical results obtained from expansions (2.25) and (2.26) (using the terms generated by $r = 0$ and $r = 1$), and the exact value of the Airy function at various points in the complex plane. We see that expansion (2.26) agrees far better with the exact Airy function than the Poincaré-type expansion (2.25), though both are poor as $\arg z \to \pi$.

Consider now what happens when $z \to -|z|$ (that is, purely real, negative z). We find that here the Airy function may be approximated by

$$\mathrm{Ai}(-|z|) \approx \frac{1}{\sqrt{\pi}(|z|^{1/4})} \sin\left(\frac{2}{3}(|z|^{3/2}) + \frac{\pi}{4}\right), \ |z| \to -\infty. \tag{2.28}$$

Since we may write

$$\sin z = \frac{e^{iz} - e^{-iz}}{2i}, \tag{2.29}$$

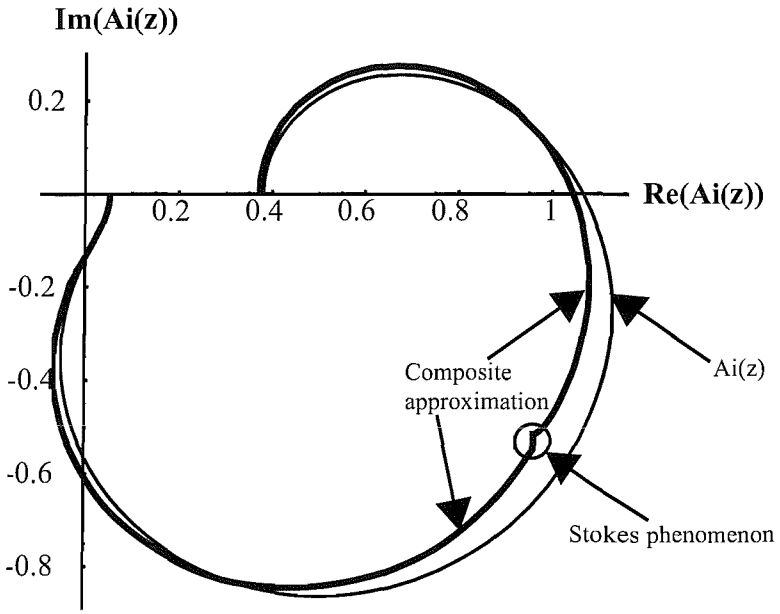

Figure 2.6: A comparison between the exact values of the Airy function Ai(z), and the "composite" asymptotic approximation including the Stokes phenomenon (shown in bold). We can observe the Stokes phenomenon taking place as the 'jump' visible in the bold line. There is considerable improvement in the accuracy of the approximation, except in the locality of the Stokes phenomenon.

we see that an extra exponential term has been introduced as we move from the positive real z-axis to the negative real z-axis in the complex plane. Further investigation reveals a Stokes line at $\theta = \frac{2\pi}{3}$ (Figure 2.5). As this line is crossed an new exponential term is 'born', hence the form of expansion (2.28). The discrepancies shown in Figure 2.4 between the real values of the Airy function and the approximations to it can be explained by this. Neither approximation (2.25) or (2.26) has more than one exponential term, so we could not have reproduced a good approximation to Ai(z) throughout the complex plane. Figure 2.6 shows the results of a numerical comparison between the exact Airy function and the correct approximations throughout the upper-half z-plane. The accuracy of the approximations

are vastly improved. Figure 2.6 also shows the Stokes discontinuity, represented by the small 'jump' in the bold line.

The discontinuous jump between asymptotic representations which is the signature of a Stokes phenomenon can be misinterpreted; that is, sometimes we think we see a Stokes phenomenon when in fact there is none. It is important that we consider the entire asymptotic expansion of a function in a given sector. An example given in Ablowitz and Fokas [12] highlights this fact.

They consider the asymptotic behaviour of

$$I(z) = \sinh z^{-1}, \quad z \to 0, \tag{2.30}$$

for complex z. Since we have

$$\sinh z^{-1} = \frac{e^{z^{-1}} - e^{-z^{-1}}}{2}, \tag{2.31}$$

and letting $z = re^{i\theta}$, then the dominant behaviour in each sector is

$$I(z) \sim \frac{e^{z^{-1}}}{2}, \quad |\arg z| < \pi/2, \tag{2.32}$$

$$I(z) \sim -\frac{e^{-z^{-1}}}{2}, \quad \pi/2 < \arg z < 3\pi/2. \tag{2.33}$$

The authors conclude that there is a discontinuous change in the asymptotic expansion of $\sinh z^{-1}$ across the ray $\theta = \pi/2$, which they say must be a Stokes line. This can be seen to be incorrect when we realise that, in fact, there is no change at all in the asymptotic expansions across this ray. The only reason this appears to be so from equations (2.32) and (2.33) is because in each of the respective sectors of the complex plane, the exponentially small terms have been neglected, so that there appears to be a 'switching' occurring between them. This does not happen; either side of this ray, both the exponentials $e^{z^{-1}}$ and $e^{-z^{-1}}$ are present. There is no Stokes phenomenon at $\theta = \pi/2$. In fact, the ray $\theta = \pi/2$ is an anti-Stokes line, since both exponentials have the same magnitude at this point.

Berry [9] showed that across a Stokes line, the multiplier of the small exponential (called the Stokes constant) could be approximated by a smooth function. He

did this using a combination of Borel summation techniques and what Dingle [4] called "singulants". Dingle's singulants are defined as the difference between the exponents of the dominant and sub-dominant exponentials. Berry showed that the Stokes multiplier in a general problem where an asymptotic expansion has just two exponentials could be approximated by an error function. The result was rigorously analyzed and proved by McLeod [13].

This smoothing of the Stokes phenomenon was interpreted using matched asymptotic expansion methods. Olde Daalhuis *et al.* [14] gave an account of the activity of the Stokes lines directly from a differential equation. In particular they considered solutions of a class of homogeneous linear second order differential equations. They found that, in agreement with Berry's result, the behaviour across a Stokes line was described by an error function. However, their methods were not generally applicable to higher order or inhomogeneous equations (for reasons explained in [14]).

Chapman [15] showed that in fact not all Stokes lines are described locally by error functions. Working within the same framework as Olde Daalhuis *et al.* [14], he demonstrated this by way of an example of a Stokes phenomenon with smoothing function of the form

$$\int_{-\infty}^{\phi} e^{-u^{2m}} du \tag{2.34}$$

for each integer $m \geq 2$. He considered the delay equation

$$f(z) = f(z - 1/k) + \frac{e^{k^m z^{2m}}}{\sqrt{k}} \tag{2.35}$$

for $m \geq 2$, where k is a (real) large parameter. He showed that the transition at the Stokes line $\mathrm{ph} z = 0$ was not an error function, but was in fact

$$\int_{-\infty}^{\phi} \exp[-(\mathrm{cosec}(\pi/2m))^{2m} u^2 m] du. \tag{2.36}$$

This result showed the non-universality of the error function in Stokes smoothing. For a wide class asymptotic approximations though, it will be the case that an error function does describe the local behaviour of a Stokes line.

2.3 The Importance of Exponentially Small Terms

We have seen how Poincaré's definition alone cannot include the effects of or explain the results of a Stokes phenomenon. The inclusion of exponentially small terms in an asymptotic expansion is crucial to improving the accuracy of an approximation.

Motivated by the Stokes phenomenon, expansions of the form (2.3) alone are no longer satisfactory for all problems. We will now define an asymptotic series for a function depending on a large parameter k as

$$y(k;x) \sim \sum_{r=0}^{\infty} \frac{a_r(x)}{k^r} + e^{-kf(x)} \sum_{r=0}^{\infty} \frac{b_r(x)}{k^r}, \quad k \to \infty. \tag{2.37}$$

The advantage of doing this is that we are explicitly including the exponentially small terms that would be missed from the remainder term of the first sum in (2.37) under a Poincaré regime. We refer to (2.37) as an exponential asymptotic expansion.

Exponentially small terms are often disregarded because of their subdominant behaviour in certain regions of solutions. This can lead to misinterpretation of the asymptotics because subdominant exponentials can sometimes grow to dominate solutions of time-dependent equations for large time (we will show an example of this in the next chapter). Including exponential terms in an asymptotic expansion can therefore extend the range of validity for the solution, can give increased numerical accuracy (as shown in the previous section, see Figures (2.4) and (2.6)), and can often simplify calculations, as we will now show with a simple example.

Consider for example the linear ODE

$$\epsilon y''(x) + y'(x) + y(x) = 0, \tag{2.38}$$

$$y(0) = \alpha, \tag{2.39}$$

$$y(1) = \beta, \tag{2.40}$$

as $\epsilon \to 0^+$. This boundary layer equation can be solved trivially exactly, but we are using it as a 'toy' model to illustrate some important ideas. A simple perturbation expansion of the form

$$y(x) \sim \sum_{n=0}^{\infty} a_n(x)\epsilon^n \tag{2.41}$$

cannot satisfy all of the boundary conditions. So, initially we attempt to solve this problem by finding suitable scalings, considering the inner and outer solutions, and matching using Van Dyke's rule [19]. The outer solution expansion can be found by using a simple perturbation expansion

$$y(x) = y_0(x) + \epsilon y_1(x) + O(\epsilon^2), \tag{2.42}$$

which, when substituted into (2.38), followed by a balancing at $O(\epsilon^0)$, gives

$$y_0' + y_0 = 0 \tag{2.43}$$

$$\Rightarrow y_0 = Ae^{-x}. \tag{2.44}$$

We now apply the appropriate boundary condition, which for the outer expansion is (2.40), so we have

$$y_0 = \beta e^{1-x}. \tag{2.45}$$

To find the inner solution expansion, we need to rescale. The boundary layer is $O(\epsilon)$ so we write

$$X = \frac{x}{\epsilon}, \quad \Rightarrow \partial_X = \frac{\partial X}{\partial x}\partial x = \frac{1}{\epsilon}\partial_x, \tag{2.46}$$

and let $y(\epsilon x;\epsilon) = Y(X;\epsilon)$. Substituting these new variables into (2.38) gives us the equation

$$Y'' + Y' + \epsilon Y = 0, \quad Y(0) = \alpha. \tag{2.47}$$

We substitute an expansion of the form

$$Y(X;\epsilon) = Y_0(X) + \epsilon Y_1(X) + \epsilon^2 Y_2(X) + O(\epsilon^3) \tag{2.48}$$

into (2.47). Balancing at $O(\epsilon^0)$ we obtain

$$Y_0'' + Y_0' = 0, \; Y_0(0) = \alpha, \tag{2.49}$$

which we solve to find

$$Y_0 = (\alpha - C) + Ce^{-x}, \tag{2.50}$$

where C is a constant, left in our solution because we only had one boundary condition to apply to our equation. We use Van Dyke's matching rule to find C, which says that the outer limit of the inner expansion equals the inner limit of the outer expansion. When we do this, we find

$$C = \alpha - \beta e. \tag{2.51}$$

Thus, the (composite) matched approximate solution to the problem is

$$y \approx \beta e^{1-x} + (\alpha - \beta e)e^{-x/\epsilon} + O(\epsilon), \quad 0 \leq x \leq 1, \quad \epsilon \to 0^+. \tag{2.52}$$

Sometimes this is can be an over complicated procedure. This is true for this case, as we will now see. Matching is only required here because the small exponential term has been neglected.

We will start with the ansatz

$$y \sim \sum_{n=0}^{\infty} a_n(x)\epsilon^n + \exp\left\{-\frac{f(x)}{\epsilon}\right\} \sum_{n=0}^{\infty} b_n(x)\epsilon^n, \quad \epsilon \to 0. \tag{2.53}$$

Substituting this back into (2.38) and balancing at different orders of ϵ^r and $\epsilon^r \exp(-f(x)/\epsilon)$ for arbitrary x, we generate the following equations:

$$O(\epsilon^0) \quad : \quad a_0' + a_0 = 0, \tag{2.54}$$

$$O(\epsilon^1) \quad : \quad a_1' + a_1 = -a_0'', \tag{2.55}$$

$$O(\epsilon^{-1}e^{-f/\epsilon}) \quad : \quad (f'^2 - f')b_0 = 0, \tag{2.56}$$

$$O(\epsilon^0 e^{-f/\epsilon}) \quad : \quad b_0' - b_0 = 0. \tag{2.57}$$

Equation (2.56) has the non-trivial consequence (that is, taking b_0 to be non-zero) that $f' = 1$, so

$$f(x) = x. \tag{2.58}$$

Now we look to the boundary values of x, which we write as

$$x = 0 : \begin{cases} a_0(0) + b_0(0) = \alpha \\ a_n(0) + b_n(0) = 0 \end{cases}, \quad x = 1 : \begin{cases} a_0(1) = \beta \\ a_n(1) = 0 \end{cases}. \tag{2.59}$$

Note that the exponential contribution is ignored at the right-hand boundary. Equation (2.54) gives

$$a_0(x) = \beta e^{1-x}, \tag{2.60}$$

and equation (2.57) gives

$$b_0(x) = (\alpha - \beta e)e^x. \tag{2.61}$$

The approximate solution for (2.38) is then

$$y \approx \beta \exp(1-x) + (\alpha - \beta e)\exp(x - x/\epsilon) + O(\epsilon), \quad 0 \leq x \leq 1. \tag{2.62}$$

This example shows that the "exponential" method above arrives at a similar answer to that of matching (compare (2.62) and (2.52)) in a quicker and easier fashion, without the need for knowledge of matching techniques.

This is not a new idea; we have used a WKB-type ansatz, also known as Latta's method [19]. We have shown that in simple cases such as this it might pay to use exponential asymptotics over Van Dyke matching methods.

The example above shows the role a single exponential can play in the asymptotic approximation of a linear system. We will now look at what happens in a problem where many exponentials are present. Chapman *et al.* [16] were the first to look at a method for finding subdominant exponentials arising from singularly perturbed (nonlinear) ODE's. Their method was based on Dingle's method of making the exponentials visible by optimally truncating the algebraic asymptotic series obtained from the equation. We will use our exponential asymptotics approach to tackle this problem.

Consider the following linear ODE boundary layer problem [19]:

$$\begin{aligned} \epsilon y''(x) + (2x+1)y'(x) + 2y(x) &= 0 \\ y(0) = \alpha, \ y(1) &= \beta, \end{aligned} \tag{2.63}$$

$$0 < \epsilon \ll 1.$$

The Van Dyke matching algorithm is the same as for the previous example. When we apply this to (2.63) we recover a matched approximate solution

$$y \approx \frac{3\beta}{2x+1} + (\alpha - 3\beta)\exp(-x/\epsilon), \quad 0 \le x \le 1. \tag{2.64}$$

In comparison, we try the simple exponential asymptotics approach

$$y \sim \sum_{n=0}^{\infty} f_n(x)\epsilon^n + \exp(-F(x)/\epsilon)\sum_{n=0}^{\infty} h_n(x)\epsilon^n. \tag{2.65}$$

Automatically we have the condition $F(0) = 0$ so that the terms in the two series (the f_n and h_n) can balance at $x = 0$. We now substitute (2.65) into equation (2.63) and balance at powers of ϵ^r and $e^{-F/\epsilon}\epsilon^r$. We obtain the following:

$$\begin{aligned} O(\epsilon^0): &\qquad (2x+1)f_0' + 2f_0 = 0 \\ O(\epsilon^1): &\qquad f_0'' + (2x+1)f_1' + 2f_1 = 0 \\ O(e^{-F/\epsilon}\epsilon^{-1}): &\qquad F'^2 h_0 - (2x+1)F'h_0 = 0. \end{aligned} \tag{2.66}$$

The last equation, coupled with the condition $F(0) = 0$, gives

$$F(x) = x^2 + x. \tag{2.67}$$

The boundary conditions in (2.63) can now be written

$$f_n(0) + h_n(0) = \delta_{n0}\alpha, \tag{2.68}$$

$$f_n(1) + O(e^{-F(1)/\epsilon}) = \delta_{n0}\beta, \tag{2.69}$$

where $\delta_{n0} = 1$ if $n = 0$, and 0 otherwise. By solving the first equation in (2.66) for f_0 using (2.69), ignoring the exponential error, we find

$$f_0(x) = \frac{3\beta}{(2x+1)}. \tag{2.70}$$

Equation (2.68) now gives

$$h_0(x) = \alpha - 3\beta. \tag{2.71}$$

By looking at higher orders of ϵ^r we can generate the following recurrence relations:

$$f_n(x) = \frac{f'_{n-1}(1) - f'_{n-1}(x)}{2x+1}, \quad h'_n(x) = \frac{h''_{n-1}(x)}{2x+1}. \tag{2.72}$$

The leading order behaviour of the solution is

$$y(x) \sim \frac{3\beta}{2x+1} + (\alpha - 3\beta)\exp\left(-(x^2+x)/\epsilon\right). \tag{2.73}$$

Both procedures produce a similar result, but we have shown how matching requires more work than is necessary. However, from an exponential asymptotic viewpoint, both matching and the Latta method leaves the right hand condition only approximately satisfied.

This error at the RHS is exponentially small. We now present a exponential asymptotic method which can account for this exponential error. Importantly, we find that an infinite number of exponentials are required, even for a simple linear problem.

2.3.1 Beyond WKB

The exponential prefactors of the f-series and h-series in (2.65) match up at $x = 0$ by design; to leading order we have

$$y(0) \approx f_0(0) + e^{-F(0)/\epsilon} h_0(0) = f_0(0) + h_0(0). \tag{2.74}$$

At the $x = 1$ boundary, we have

$$y(1) \approx f_0(1) + e^{-F(1)/\epsilon} h_0(1). \tag{2.75}$$

In order for the exponential prefactors to balance, there must also be a factor of $e^{-F(1)}$ in front of the f-series. But, if this were the case, things would not balance up at the $x = 0$ boundary. Thus, we deduce there must also be an extra exponential prefactor included at $x = 0$, of the form

$$y(0) \approx e^{-F(1)} f_0(0) + e^{-(F(0)+F(1))} h_0(0), \tag{2.76}$$

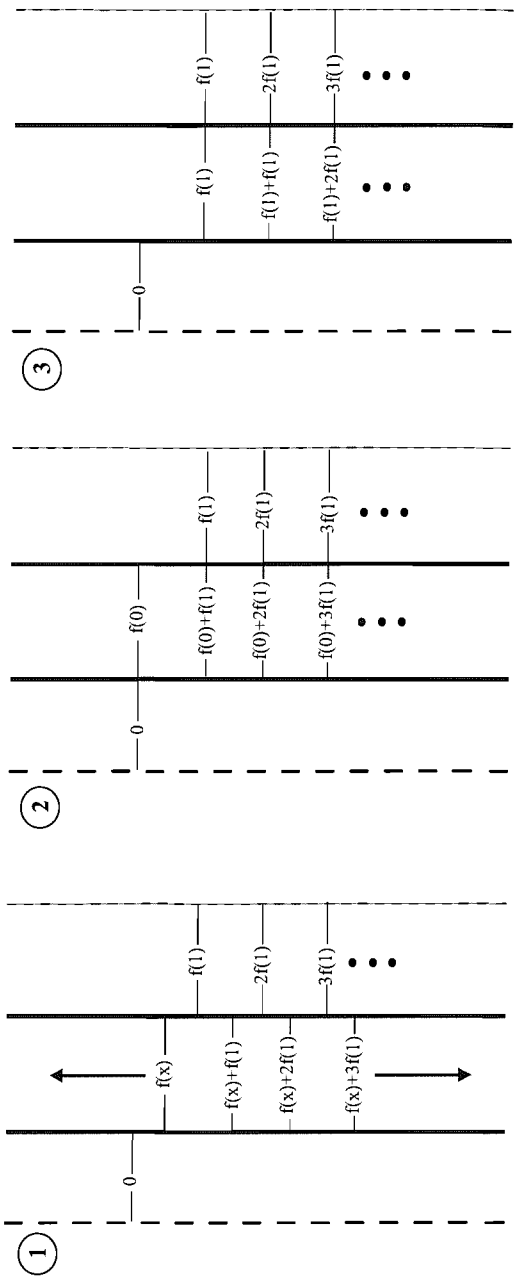

Figure 2.7: Figurative explanation of the 'ladder' of exponentials. The middle column in each of the three diagrams can be visualised as a sliding scale which is used to match up each exponential scale, represented as one 'rung' on the ladder. Refer to the text for a full explanation.

ensuring that the exponentials balance. Of course, this then means that there is a need for a prefactor $e^{-2F(1)}$ in front of the f-series at $x = 1$, and so on and so forth. In summary, the boundary values generate a ladder of series with exponential prefactors with arguments as follows. The middle column of Figure 2.7(1) can be visualised as a sliding scale that can be used to line up different exponential scales. Each 'rung' of the ladder represents one such exponential scale in the complete expansion. The left ladder represents scales which must be satisfied at the left hand boundary; the right ladder represents scales which must be satisfied at the right hand boundary. The middle ladder must be shifted up and down via $f(x)$ as x goes from 0 to 1.

At $x = 0$, the middle ladder lines up with the 0 at the LHS and also the scales at $pF(1)$, for integer $p \geq 0$. This ensures that the boundary conditions at $x = 0$ are satisfied (Figure 2.7(2)) . As x travels from 0 to 1 this scale slides down so as to line up with $pF(1)$ ($p \geq 1$) series so that the boundary data at $x = 1$ can be satisfied exactly (Figure 2.7(3)). With this ladder, the zero-prefactored series exactly satisfies the boundary condition at $x = 1$, without an exponential error. The template for the full expansion is then

$$\begin{aligned} y &\sim \sum_{n=0}^{\infty} f_n(x)\epsilon^n + \sum_{p=1}^{\infty} e^{-pF(1)/\epsilon} \sum_{n=0}^{\infty} f_n^{(p)}(x)\epsilon^n + \sum_{p=0}^{\infty} e^{-(F(x)+pF(1))/\epsilon} \sum_{n=0}^{\infty} h_n^{(p)}(x)\epsilon^n, \\ &\sim \sum_{p=0}^{\infty} e^{-p\frac{F(1)}{\epsilon}} \sum_{n=0}^{\infty} f_n^{(p)}(x)\epsilon^n + \sum_{p=0}^{\infty} e^{-\frac{1}{\epsilon}(F(x)+pF(1))} \sum_{n=0}^{\infty} h_n^{(p)}(x)\epsilon^n. \end{aligned} \tag{2.77}$$

Substitute (2.77) into (2.63). By balancing at orders of $e^{-pF(1)/\epsilon}\epsilon^n$ and $e^{-(F(x)+pF(1))/\epsilon}\epsilon^n$, we again find that $F(x) = x^2 + x$. The boundary conditions are

$$f_n^{(p)}(0) + h_n^{(p)}(0) = \delta_{n0}\delta_{p0}\alpha, \tag{2.78}$$

$$f_n^{(p)}(1) + h_n^{(p-1)}(1) = \delta_{n0}\delta_{p0}\beta, \tag{2.79}$$

where $\delta_{n0} = 1$ if $n = 0$, and 0 otherwise. Solving the equations, we find

$$f_0^{(0)}(x) = \frac{3\beta}{2x+1};\ f_0^{(p)}(x) = \frac{-3^p(\alpha - 3\beta)}{2x+1};\ h_0^{(p)}(x) = 3^p(\alpha - 3\beta). \tag{2.80}$$

The lowest order solution can then be written as

$$y(x) \sim \frac{3\beta}{2x+1} - \frac{\alpha-3\beta}{2x+1}\sum_{p=1}^{\infty} 3^p e^{-pF(1)/\epsilon} + (\alpha-3\beta)\sum_{p=0}^{\infty} 3^p e^{-(F(x)+pF(1))/\epsilon}. \quad (2.81)$$

This is a new form of solution for an exponential asymptotics approach to a problem such as this. The series in (2.81) take the form of transseries ([20], [23]). This method is related to the method of multiple scales, but we will not explore this here.

Summing the p-series, we obtain:

$$\begin{aligned} y(x) &= \frac{3}{(2x+1)}\left\{\frac{\beta-\alpha\exp(-F(1)/\epsilon)}{1-3\exp(-F(1)/\epsilon)}\right\} \\ &\quad + \left\{\frac{\alpha-3\beta}{1-3\exp(-F(1)/\epsilon)}\right\} e^{-F(x)/\epsilon} + O(\epsilon). \qquad (2.82) \\ &= \frac{3}{(2x+1)}\left\{\frac{\beta-\alpha e^{-2/\epsilon}}{1-3e^{-2/\epsilon}}\right\} + \left\{\frac{\alpha-3\beta}{1-3e^{-2/\epsilon}}\right\} e^{-(x^2+x)/\epsilon} + O(\epsilon). \\ & \qquad (2.83) \end{aligned}$$

Note that if the terms in $\exp(-2/\epsilon)$ are neglected then we have the simple leading order result (2.73), as we should expect. However, whereas (2.73) only satisfied one of the boundary conditions, the approximation (2.82) satisfies both, without exponential error at the right boundary. The $O(\epsilon)$ error is therefore accounting for everything.

Note that if the exponentials in the denominator of the terms in curly brackets in (2.82) depend on x, then the generation of singularities will change; we will in fact be dealing with infinite arrays of exponentials. We will see this later on in Chapter 4.

2.4 Hyperasymptotics and the Borel Plane

It had been suggested as far back as Stieltjes (1886) [4] that improvement may be made to an optimally truncated asymptotic approximation by looking at the remainder from that truncation. We have seen that Dingle carried out his work

based on Borel summation and developed a systematic method of gaining his terminants. Airy [24], Miller [25] and Boyd [26] took steps towards developing similar ideas. We will look at a method which was developed by Berry & Howls for systematically studying the remainder of an asymptotic series, which they called hyperasymptotics.

Hyperasymptotics is defined as the systematic improvement to the exponentially small remainder of an optimally truncated series. Berry and Howls [27] discussed Helmholtz-type second order linear ODE's. They were able to re-expand the late terms in the expansion of one formal solution in terms of the early terms of a second. A Borel summation, followed by iteration of the method, led to a sequence of finite "hyperseries". Each of these hyperseries contained early terms from one of the formal solutions multiplied by certain multiple integrals called "hyperterminants", which had a universal form. This method produces an exponential improvement in accuracy over the first term of the original expansion. It relied on truncating each successive hyperseries at its least term, which led to the termination of the iteration when one of the hyperseries had just one term. Several papers followed this one, extending the method to other special cases; see in particular [28], [29], [30], [31], [32], and [33].

It is more instructive at this point for us to review some of the ideas in Berry & Howls' second paper. They set out a method of applying hyperasymptotics to a specific class of integrals [28] (a rigorous proof of the approach was given by Boyd [34]).

Consider an integral of the form

$$I^{(n)}(k) = \int_{C_n(\theta_k)} dz g(z) e^{-kf(z)}. \tag{2.84}$$

where $|k|$ is the large asymptotic parameter and the functions f and g are analytic, at least in a strip containing the contour $C_n(\theta_k)$. A saddle of f is defined to be where

$$f'(z) = 0, \tag{2.85}$$

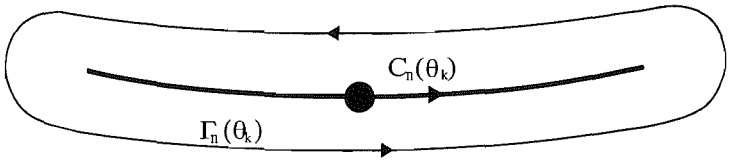

Figure 2.8: The steepest path $C_n(\theta_k)$ (the thick line) through saddle z_n, with the loop $\Gamma_n(\theta_k)$ enclosing it.

with $f''(z) \neq 0$ (this constraint is added for simplicity, and may be removed later on). If f is an mth order polynomial, there will be $(m-1)$ saddles. The infinite oriented contour $C_n(\theta_k)$ is the path of steepest descent through the nth saddle $z = z_n$, define as

$$\mathrm{Re}[k(f(z) - f_n)] > 0, \tag{2.86}$$

where $f_n \equiv f(z_n)$. Now let

$$I^{(n)}(k) \equiv k^{-\frac{1}{2}} e^{-kf_n} T^{(n)}(k), \tag{2.87}$$

$$T^{(n)}(k) = k^{\frac{1}{2}} \int_{C_n(\theta_k)} dz g(z) e^{-k[f(z)-f_n]} \tag{2.88}$$

The coefficients $T_r^{(n)}$ are required in the formal (divergent) asymptotic expansion

$$T^{(n)}(k) \sim \sum_{r=0}^{\infty} \frac{T_r^{(n)}}{k^r}. \tag{2.89}$$

It can be shown (refer to details in Appendix B) that

$$T^{(n)}(k) = \sum_{r=0}^{N-1} \frac{1}{k^r} \int_0^{\infty} du \frac{e^{-u} u^{r-1/2}}{2\pi i} \oint_{\Gamma_n(\theta_k)} dz \frac{g(z)}{(f(z) - f_n)^{r+1/2}} + R^{(n)}(k, N) \tag{2.90}$$

$$\Rightarrow T^{(n)}(k) = \sum_{r=0}^{N-1} \frac{T_r^{(n)}}{k^r} + R^{(n)}(k, N), \tag{2.91}$$

where the coefficients $T_r^{(n)}$ are defined as

$$T_r^{(n)} = \frac{(r - 1/2)!}{2\pi i} \oint_n dz \frac{g(z)}{(f(z) - f_n)^{r+1/2}}. \tag{2.92}$$

Crucially, the remainder $R^{(n)}$ in (2.91) is *exact*:

$$R^{(n)}(k,N) = \frac{1}{2\pi i k^N}\int_0^\infty du e^{-u}u^{N-\frac{1}{2}} \times \oint_{\Gamma_n(\theta_k)} dz \frac{g(z)}{[f(z)-f_n]^{N+\frac{1}{2}}\{1-u/k(f(z)-f_n)\}}. \quad (2.93)$$

Consider all of the steepest paths through the saddle z_n, as θ_k is varied. Some of them will encounter other saddles m. These saddles are said to be adjacent to n (see Figure 2.9). To specify these paths through adjacent saddles, Dingle's singulants are used, in the form

$$F_{nm} \equiv |F_{nm}|e^{i\sigma_{nm}} \equiv f_m - f_n. \quad (2.94)$$

These special steepest paths correspond to where

$$\mathrm{Re}[kF_{nm}] > 0, \quad (2.95)$$

$$\mathrm{Im}[kF_{nm}] = 0, \quad (2.96)$$

that is

$$\mathrm{Im}[e^{i\theta_k}e^{i\sigma_{nm}}] = 0, \quad (2.97)$$

$$\mathrm{Im}[e^{i(\theta_k+\sigma_{nm})}] = 0. \quad (2.98)$$

Thus it follows that

$$\theta_k = -\sigma_{nm}, \quad (2.99)$$

where $\sigma_{nm} = \arg F_{nm}$. The steepest path $C_n(-\sigma_{nm})$ turns sharply through a right angle at z_m to continue descending into a valley of $e^{-k[f(z)-f_n]}$. This is the signature of the occurrence of a Stokes phenomenon.

If we are able to write an integral in the form (2.84), then we can find out about the presence of singularities and their position with respect to others by looking in the complex kf-plane, also known as the Borel plane. The singularities are represented in the Borel plane as branch points with cuts running from them to infinity at constant values of $\mathrm{Im}(kf)$ ([35], [33]).

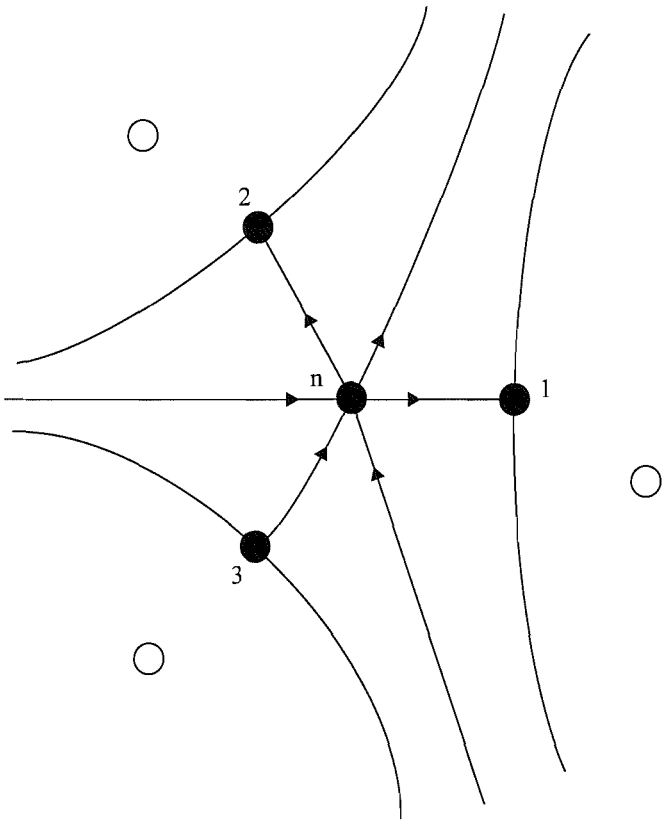

Figure 2.9: A simple schematic adjacency diagram. Saddle n is adjacent to Saddles 1,2, and 3 (and vice-versa); for example, n and 1 lay on the same steepest path (i.e the same phase contours of $f(z) - f_n$). None adjacent saddles (empty circles) are also shown.

This method introduces a Riemann sheet structure. For two singularities to be lying on the same Riemann sheet is for the same singularities to be adjacent to each other and is what leads to divergent saddle expansions ([33], [10]). The Stokes phenomenon can be well illustrated in the Borel plane (Figure 2.10); it corresponds to a singularity passing through the contour of integration emanating from another singularity as $\arg k$ is varied. If the two points are adjacent, the singularity passing through the cut can "drag" the integration contour with it, creating an extra contribution to the expansion. If the singularities are not adjacent, then they are not on the same Riemann sheet; no new contributions arise as a result of the crossing. The Borel plane approach applies equally to the asymptotics of differential equations as to integrals [33].

The algorithm for using the Borel plane method of approach is summarised as follows:

(i) Locate the singularities in the Borel plane,

(ii) Categorise each singularity (saddle, endpoint, pole etc.),

(iii) Calculate the values of the F_{nm},

(iv) Calculate the adjacency of the singularities,

(v) Find the position of the Stokes lines.

In the next chapter, we shall see that this simple template can handle complicated and subtle behaviour.

The loop $\Gamma_n(\theta_k)$ (Figure 2.8) is expanded in such a way that symbolically we can write

$$\oint_{\Gamma_n(\theta_k)} dz \ldots = \sum_m K_{nm} \int_{C_m(-\sigma_{nm})} dz \ldots . \tag{2.100}$$

The K_{nm} are known as Stokes constants, and these (in general) take the value

$$|K_{nm}| = \begin{cases} 1 & \text{if m adjacent to n} \\ 0 & \text{m not adjacent to n} \end{cases} \tag{2.101}$$

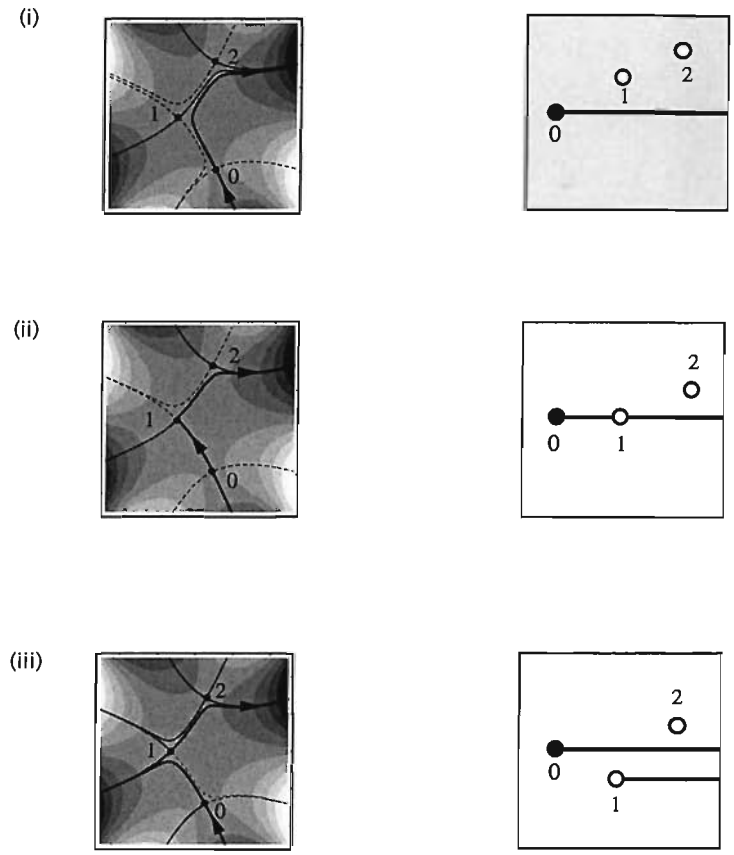

Figure 2.10: The Stokes phenomenon as seen from steepest descent plots and simultaneously in the Borel plane. (i) The steepest descent plot shows saddle 0 is the only contributing singularity. In the Borel plane we see the branch cut emanating form 0 accordingly. (ii) A Stokes phenomenon occurs between saddles 0 and 1. This is signified in the Borel plane by saddle 1 crossing the cut from 0. (iii) Since they are adjacent, saddle 1 'drags' on the cut from saddle 0 as it passes through, introducing a new asymptotic contribution.

We will discuss the significance of these constants shortly. Via a transformation of variables, the remainder term (which is *exact*) is

$$R^{(n)}(k,N) = \frac{1}{2\pi i}\sum_m \frac{K_{nm}}{(kF_{nm})^N}\int_0^\infty dv \frac{v^{N-1}e^{-v}}{1-\frac{v}{kF_{nm}}} T^{(m)}\left(\frac{v}{F_{nm}}\right), \tag{2.102}$$

and thus an exact resurgence formula is obtained in the form

$$T^{(n)}(k) = \sum_{r=0}^{N-1}\frac{T_r^{(n)}}{k^r} + \frac{1}{2\pi i}\sum_m \frac{K_{nm}}{(kF_{nm})^N}\int_0^\infty dv \frac{v^{N-1}e^{-v}}{1-\frac{v}{kF_{nm}}} T^{(m)}\left(\frac{v}{F_{nm}}\right). \tag{2.103}$$

This is called a resurgence formula since the 'closest' saddle n is connected to 'later' saddles m [36]. This is exact for all finite $N \geq 0$, and $|F_{nm}| > 0$.

The form of these results means that resurgence formula (2.103) can be iterated. After m iterations this results in being able to write

$$\begin{aligned}
T^{(n)}(k) &= \sum_{r=0}^{N_n-1} T_r^{(n)} K_r^{(n)} \\
&+ \sum_{m_1} K_{nm_1} \sum_{r=0}^{N_{nm_1}-1} T_r^{(m_1)} K^{(nm_1)} \\
&+ \sum_{m_1}\sum_{m_2} K_{nm_1}K_{nm_2} \sum_{r=0}^{N_{nm_1m_2}-1} T_r^{(m_2)} K_r^{(nm_1m_2)} \\
&+ \cdots \\
&+ \sum_{m_1}\cdots\sum_{m_M} K_{nm_1}\ldots K_{nm_1\ldots m_M} \\
&\times \left(\sum_{r=0}^{N_{n\ldots m_M}-1} T_r^{(m_M)} K_r^{(n\ldots m_M)} + R^{(n\ldots m_M)}(N_n,\ldots,N_{m_M})\right).
\end{aligned} \tag{2.104}$$

The K_r's represent hyperterminants, an extension of Dingle's terminants. In the notation of Berry and Howls, these are

$$K_r^{(0)} = \frac{1}{k^r}, \tag{2.105}$$

$$K_r^{(01\ldots s)} = \left(\prod_{p=0}^{s-1}\int_0^\infty dv_p\right) J_r^{(01\ldots s)}, \tag{2.106}$$

$$J_r^{(01)} = \frac{K_{01}}{2\pi i k^{N_0} F_{01}^{N_0-r}} \frac{v_0^{N_0-r-1} e^{-v_0}}{1 - v_0/kF_{01}} \tag{2.107}$$

$$J_r^{(01\ldots s)} = \frac{K_{s-1,s}}{2\pi i F_{s-1,s}^{N_{s-1}-r}} \times \frac{v_{s-1}^{N_{s-1}-r-1} e^{-v_{s-1}}}{1 - (v_{s-1}/v_{s-2})(F_{s-2,s-1}/F_{s-1,s}).} \tag{2.108}$$

The superscript (0) represents the starting saddle n_0, (1) represents the saddles n_1 which are adjacent to n_0, etc., so that (s) represents the saddles that are reached in the sth iteration. In [37] and [38], Olde Daalhuis showed how to compute the numerical values of these hyperterminants.

After $s+1$ iterations, the remainder is

$$R^{(0\ldots s)} = \left(\prod_{p=0}^{s} \int_0^\infty dv_p \right) \sum_{s+1} J_0^{(0\ldots s+1)} T^{(s+1)} \left(\frac{v_s}{F_{s,s+1}} \right). \tag{2.109}$$

Berry & Howls determined that the optimal truncation points in their procedure were

$$N_0 = |kF_{01^*}|, \tag{2.110}$$

$$N_s = \frac{N_{s-1}}{1 + |F_{s-1,s}/F_{s,(s+1)^*}|}. \tag{2.111}$$

Here, 1^* stands for the nearest saddle to saddle 0, and is not necessarily adjacent to it. Also,

$$|F_{s-1,s}/F_{s,(s+1)^*}| \geq 1, \tag{2.112}$$

so that the nearest saddle to s cannot be more distant than the previous saddle $s-1$, and

$$N_s \leq \frac{1}{2} N_{s-1}, \tag{2.113}$$

so each hyperseries is no more than half the length of its predecessor.

In [31], [32] and [33] (see also [35]) it was shown that the numerically optimal truncation scheme was not that of truncating every hyperseries at its least term. The updated algorithm was derived from locally minimizing the estimate for the remainder after M iterations. From [28] (cf. [33]) we have

$$|R^{(n)}| \approx \frac{N_0^{N_0-1/2} e^{-N_0}}{\sqrt{2\pi} |kF_{01^*}|^{N_0}} |T_0^{(1^*)}|, \tag{2.114}$$

$$|R^{(0\ldots s)}| \approx \frac{N_s^{N_s-1/2}e^{-N_0}}{(2\pi)^{(s+1)/2}|k|^{N_0}|F_{s,(s+1)*}|^{N_s}} \prod_{p=0}^{s-1} \frac{(N_p - N_{p+1})^{(N_p-N_{p+1}-1/2)}}{|F_{p,p+1}|^{N_p-N_{p+1}}} |T_0^{(s+1)^*}|, \tag{2.115}$$

where $|T_0^{(1^*)}|$ is the first term of the asymptotic expansion about the closest adjacent saddle. Berry & Howls only allowed the last truncation $N_{0\ldots s}$ to vary, with the previous $N_{0\ldots s-1}$ fixed. If this restriction is relaxed so that all values of $N_{0\ldots s-1}$ are allowed to vary, globally minimizing the remainder, then for M stages of hyperasymptotics the optimal truncation scheme is shown below (in the notation of Howls).

$$\begin{aligned}
N_n &= \left\{ \begin{array}{l} \text{shortest directed path of } M+1 \text{ steps in the} \\ kf \text{ plane between singularities, starting at } n \end{array} \right\} \\
N_{nm_1} &= \max\{0, N_n - |kF_{nm_1}|\}, \\
N_{nm_1m_2} &= \max\{0, N_{nm_1} - |kF_{m_1m_2}|\}, \\
&\vdots \\
N_{nm_1m_2\ldots m_M} &= \max\{0, N_{nm_1\ldots m_{M-1}m_M} - |kF_{m_{M-1}m_M}|\}.
\end{aligned} \tag{2.116}$$

Here, m_1 represents the first adjacent saddles to n, m_2 the second, and so on.

In his papers (particularly [33]), Olde Daalhuis tackled hyperasymptotics from a different viewpoint, culminating in similar results. He studied linear ordinary differential equations. His method was based on the properties of the Borel transform, which proved to be a very useful breakthrough, since it meant that hyperasymptotic analysis could be performed on any function that possessed a Borel transform regardless of whether they originated from differential equations or not. A formal (divergent) series of the form (2.3) becomes a convergent series under a Borel transform. A Laplace transform of this series would then give us the integral form presented in [28], and the hyperasymptotic method proceeds from there as before.

The hyperasymptotic techniques discussed above were applied to multidimen-

sional integrals by Howls [35], the results of which implied that dimensionality has little effect on the general form of the exact remainder term. By using the Borel plane method, all references to the dimension d of the integral

$$I^{(n)}(k) = \int \cdots \int_{S_n} dz^{(1)} dz^{(2)} \ldots dz^{(d)} g(z^{(1)}, \ldots, z^{(d)}) exp\{-kf(z^{(1)}, \ldots, z^{(d)})\} \tag{2.117}$$

are incorporated into the $T^{(n)}(k)$ and $T^{(m)}(v/F_{nm})$ factors, and the result is an identical resurgence formula to (2.103). Thus, the case for $d = 1$ is the same as for all cases $d > 1$. More complicated examples of the use of hyperasymptotic techniques can be found in [39], [40] and [41].

2.5 Stokes Constants

A factorial-over-power approximation for the late terms of a series is very good for leading order results, but this alone cannot include more distant singularities. This is because, as we have seen, only the closest singularity to an expansion point will be included. For singularities further away, no Stokes information would be found. Hyperasymptotics makes it possible to look further away and include more distant singularities. The Stokes constant allows us to determine which singularities are adjacent to others, and which are not.

The problem of determining whether or not two saddles are adjacent, and also the Riemann sheet structure of the f plane, comes down to the calculation of the K_{nm}. These are related to the so called 'intersection numbers' (Pham 1967) [35] prescribing whether or not two singularities lie on the same Riemann sheet. Olde Daalhuis [33] introduced the following method of calculating these constants. It proceeds (in the notation of Howls) by noting that

$$T^{(n)}(k) = \sum_{r=0}^{N_n - 1} \frac{T_r}{k^r} + R^{(n)}(N_n), \tag{2.118}$$

$$T^{(n)}(k) = \sum_{r=0}^{N_n} \frac{T_r}{k^r} + R^{(n)}(N_n + 1), \tag{2.119}$$

thus

$$\begin{aligned}
\frac{T_{N_n}}{k^{N_n}} &= R^{(n)}(N_n) - R^{(n)}(N_n+1) \\
&= -\sum_{m_1} K_{nm_1} \sum_{r=0}^{N_{nm_1}-1} T_r^{(m_1)} \Delta K_r^{(nm_1)} \\
&\quad -\sum_{m_1}\sum_{m_2} K_{nm_1} K_{nm_2} \sum_{r=0}^{N_{nm_1m_2}-1} T_r^{(m_2)} \Delta K_r^{(nm_1m_2)} \\
&\quad -\cdots \\
&\quad -\sum_{m_1}\cdots\sum_{m_M} K_{nm_1}\ldots K_{nm_1\ldots m_M} \\
&\quad \times \left(\sum_{r=0}^{N_{n\ldots m_M}-1} T_r^{(m_M)} \Delta K_r^{(n\ldots m_M)} + \Delta R^{(n\ldots m_M)} \right),
\end{aligned} \tag{2.120}$$

where

$$\begin{aligned}
\Delta K_r^{(nm_1\cdots m_p)} &= K_r^{(nm_1\cdots m_p)}(N_n+1, N_{nm_1}, \ldots, N_{nm_1\cdots m_p}) \\
&\quad -K_r^{(nm_1\cdots m_p)}(N_n, N_{nm_1}, \ldots, N_{nm_1\cdots m_p})
\end{aligned} \tag{2.121}$$

with a similar expression for $\Delta R^{(nm_1\cdots m_p)}$. Knowledge of the coefficients $T_r^{(m_p)}$ and the hyperterminants $K_r^{(n\cdots m_p)}$ means that each expression of the form (2.120) reduces to an equation for the K_{nm} with an exponentially small error coming from the unevaluated remainder term. Using the truncation method (2.116), then numerically solving a system of algebraic equations, it is then possible to determine very good approximations to the K_{nm}. If any of the K_{nm} in (2.120) are individually zero then all hyperseries containing it can be terminated at the earliest possible stage. Once sufficiently many K_{nm} have been calculated, the full expansion (2.104) gives the hyperasymptotic expansion of the integral to the accuracy required.

The most general form for a tree-structure of a hyperseries, expanded about a singularity 0 is

$$T^{(0)}(k) = \sum_{r=0}^{N_0-1} \frac{T_r^{(0)}}{k^r} + \left\{ \begin{array}{l} K_{01} \sum_{r=0}^{N_{01}-1} T_r^{(1)} K_r^{(01)} + \left\{ \begin{array}{l} K_{01}K_{10} \sum_{r=0}^{N_{010}-1} T_r^{(0)} K_r^{(010)} + \ldots \\ K_{01}K_{12} \sum_{r=0}^{N_{012}-1} T_r^{(2)} K_r^{(012)} + \ldots \\ K_{01}K_{13} \sum_{r=0}^{N_{013}-1} T_r^{(3)} K_r^{(013)} + \ldots \end{array} \right. \\ K_{02} \sum_{r=0}^{N_{02}-1} T_r^{(1)} K_r^{(02)} + \left\{ \begin{array}{l} K_{02}K_{20} \sum_{r=0}^{N_{020}-1} T_r^{(0)} K_r^{(020)} + \ldots \\ K_{02}K_{21} \sum_{r=0}^{N_{021}-1} T_r^{(1)} K_r^{(021)} + \ldots \\ K_{02}K_{23} \sum_{r=0}^{N_{023}-1} T_r^{(3)} K_r^{(023)} + \ldots \end{array} \right. \\ K_{03} \sum_{r=0}^{N_{03}-1} T_r^{(1)} K_r^{(03)} + \left\{ \begin{array}{l} K_{03}K_{30} \sum_{r=0}^{N_{030}-1} T_r^{(0)} K_r^{(030)} + \ldots \\ K_{03}K_{31} \sum_{r=0}^{N_{031}-1} T_r^{(1)} K_r^{(031)} + \ldots \\ K_{03}K_{32} \sum_{r=0}^{N_{032}-1} T_r^{(2)} K_r^{(032)} + \ldots \end{array} \right. \end{array} \right. \tag{2.122}$$

We can obtain an equivalent expansion for a term $T_{N_0}^{(0)}/k^{N_0}$ by replacing $T^{(0)}(k)$ on the left of (2.122) with $T_{N_0}^{(0)}/k^{N_0}$ and removing the first sum on the right. We also replace the $K_r^{(01\cdots)}$ with $-\Delta K_r^{(01\cdots)}$ (see (2.121)).

Note that there is a difference in the literature between the Stokes Constants of Howls and those of Olde Daalhuis, resolved by the relation

$$K_{nm}|_{OD} = \frac{T_0^{(m)}}{T_0^{(n)}} K_{nm}|_{Howls}. \tag{2.123}$$

In the next chapter we will see further how calculating the Stokes constants

and understanding the adjacency of a singularity can be critical to understanding the underlying behaviour of a problem.

We have reviewed the development of the continually improved accuracy of asymptotic techniques. Has everything been studied, and is everything well understood, or is there perhaps some surprise still left to be found? The next chapter shows that the answer to this last question is yes; indeed we do discover a subtle, but general, new result.

Chapter 3

The Higher Order Stokes Phenomenon

In this chapter we apply some of the existing hyperasymptotic methods to a PDE example. Hyperasymptotics has been derived for linear equations ([31], [14]) and steepest descent expansions of single and multidimensional integrals ([35]); work has also been done on nonlinear ordinary differential equations by Costin (see, for example, [21] and also in [41]). Partial differential equations are still relatively unstudied in areas related to hyperasymptotics.

The Pearcey function ([42], [43])

$$P(x,y) = \int_{-\infty}^{+\infty} dz \exp\{-i(z^4 + yz^2 + xz)\} \tag{3.1}$$

satisfies the system

$$\frac{\partial^3 P}{\partial x^3} - \frac{1}{2} y \frac{\partial P}{\partial x} - ixP = 0, \tag{3.2}$$

$$-\infty < x < +\infty, \quad -\infty < y < +\infty$$

with suitable conditions given for $P(0,y)$, $P_x(0,y)$, $P_{xx}(0,y)$. The Pearcey function has been used by Berry and Howls [28] to demonstrate their hyperasymptotic techniques. In this chapter, we explicitly look at applying hyperasymptotics directly to a PDE.

We will demonstrate that for systems with additional parameters $\mathbf{a}$, knowledge of any Stokes phenomena alone is not sufficient to understanding the global connection problems when there are three or more possible asymptotic behaviours. Berk et al. [44] have shown that when more than two possible asymptotic behaviours are present, so-called 'new Stokes lines' [45] must be introduced to fully describe the analytic continuation. However, we shall demonstrate in this chapter that it is also necessary to introduce the concept of a 'higher order Stokes phenomenon'. At a higher order Stokes phenomenon, the potential for a 'regular' Stokes phenomenon to occur is changed. We show that without knowledge of the existence of a higher order Stokes phenomenon, it is possible to draw incorrect conclusions as to the existence of Stokes lines (or coalescences of singularities) as $\mathbf{a}$-space is traversed. This effect is much more subtle than a Stokes phenomenon, yet can generate terms that can grow to dominate the asymptotics, and can affect the possible occurrence of a Stokes phenomenon.

We introduce the higher order Stokes phenomenon by means of a simple integral example. This is followed by an explanation of how the higher order Stokes phenomenon fundamentally influences asymptotic expansions by reference to the remainder terms derived from hyperasymptotics. Finally, we will demonstrate the findings in the context of a PDE example.

3.1 Introduction to the Higher Order Stokes Phenomenon

In order to illustrate a higher order Stokes phenomenon occurring, we study the integral

$$P(k;a) = \int_C dz \exp\left\{ik\left(\frac{1}{4}z^4 + \frac{1}{2}z^2 + az\right)\right\}, \tag{3.3}$$

where C is a contour which runs from a valley $V_1 = \infty\exp(-3\pi i/8)$ to valley $V_2 = \infty\exp(\pi i/8)$, and k is a large positive parameter. This integral is clearly

related to the Pearcey integral (3.1). The parameter a is a complex variable and we shall look at specific points in the complex a-plane.

Since (3.3) is of the form

$$I(k) = \int_C dz g(z) e^{-kf(z)}$$

(with $g(z) = 1$), we define

$$f(z;a) = -i\left(\frac{1}{4}z^4 + \frac{1}{2}z^2 + az\right). \tag{3.4}$$

There are 3 saddle points, where $f'(z) = 0$ (but $f''(z) \neq 0$), i.e,

$$z_n^3 + z_n + a = 0, \quad n = 0, 1, 2.$$

The heights of the saddles, after re-writing equation (3.4) as

$$f(z_n) = f(z_n) - \frac{1}{4}z_n f'(z_n), \tag{3.5}$$

(where $' = d/dz_n$) are given by

$$f_n(a) \equiv f(z_n; a) = -\frac{1}{4}iz_n(z_n + 3a). \tag{3.6}$$

The steepest descent paths through the saddles z_n are the connected paths passing through the z_n that satisfy

$$C_n = \{z \in \mathbb{C} : k(f(z;a) - f_n(a)) \geq 0\}. \tag{3.7}$$

Let us choose a point $a = a_1$ and plot the corresponding steepest descent path in the z-plane (Figure 3.1).

Here, we take $C = C_0$ as the contour of integration, so that only the saddle z_0 will contribute to the large-k asymptotics of $P(k;a)$. Now we vary a and notice that the steepest path is deformed. At the value $a = a_3$, we have to choose $C = C_0 \cup C_1$ if the contour is still to be a steepest descent path. Hence, for this value of a, both saddles z_1 and z_0 contribute to the large-k asymptotics.

As we travelled from a_1 to a_3, an extra asymptotic contribution has been introduced; that is, a Stokes phenomenon has taken place. Therefore, somewhere

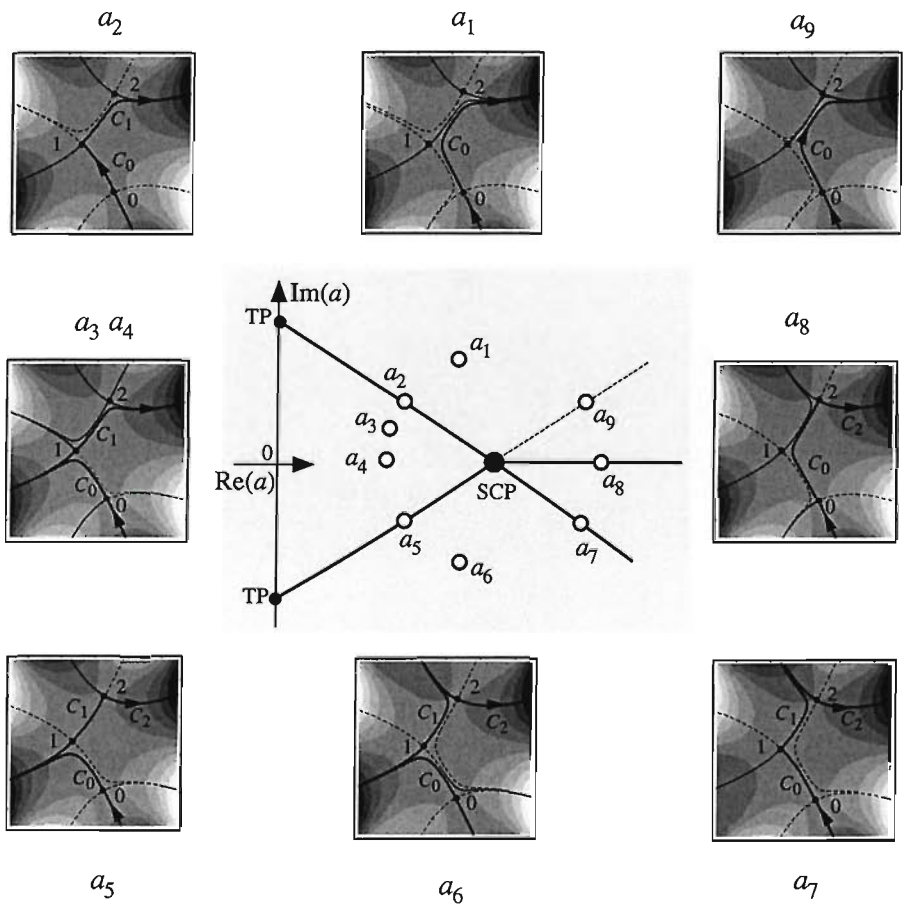

Figure 3.1: The Stokes curves in the a-plane and the steepest descent contours of integration in the integrand z-plane passing over saddles 0, 1 and 2 for selected values a_i for integral (3.3). The dashed Stokes line passing through a_9 is active, but irrelevant to the function defined by the integral.

between a_1 and a_3 there is a Stokes line, across which this change in asymptotic contribution occurs. As in Chapter 2 (equation (2.22)) this is defined as

$$S_{0>1} = \{a \in \mathbb{C} : f_1(a) - f_0(a) > 0\}. \tag{3.8}$$

The point a_2 lies on this Stokes line and we can see from the steepest descent paths that C must be made up from the part of C_0 running from V_1 to z_1, and the part of C_1 running from z_1 to V_2. This is the visual 'signature' of the Stokes phenomenon taking place.

For the three points z_n, we display the corresponding values for $f_j(a)$ in the complex f-plane (the Borel plane) in Figure 3.2. Mapping from the z to the f-plane generates singularities at the images $f_j(a)$. The steepest path maps to horizontal loop contours, starting and finishing at infinity, circling around the corresponding saddle images. By writing the integral in terms of the f-plane, it can be seen that it is precisely the presence of other such singularities on the same Riemann sheet that causes that saddle-point expansions about any of the $f_j(a)$ to diverge ([33], [10]). The Stokes phenomenon occurs at the point a_2 when $f_1(a)$ crosses the horizontal half-line emanating from $f_0(a)$, which corresponds to the image of C_0 in the f-plane.

It seems that all we need do is study the relative alignment of the $f_j(a)$ in the complex f-plane in order to locate the Stokes lines. However, in general more information is required. For example, the plot for the values of $f_j(a_4)$ shows that $f_2(a_4)$ is crossing the horizontal half-line starting from $f_0(a_4)$. Viewed in this plane, a Stokes phenomenon is occurring, yet there is obviously no Stokes phenomenon at this point in the z-plane. This apparent contradiction is resolved as follows: the branch point at $f_2(a_4)$ does not lay on the same Riemann sheet as $f_0(a_4)$ and thus cannot be seen from $f_0(a_4)$. (Equally we can say that saddle z_2 is not adjacent to z_0 at $a = a_4$ and so this crossing in the f-plane has no consequence.)

Having travelled from a_1 to a_4, we now continue to walk anti-clockwise around the a-plane. At a_5, a Stokes phenomenon occurs between saddles z_1 and z_2, so

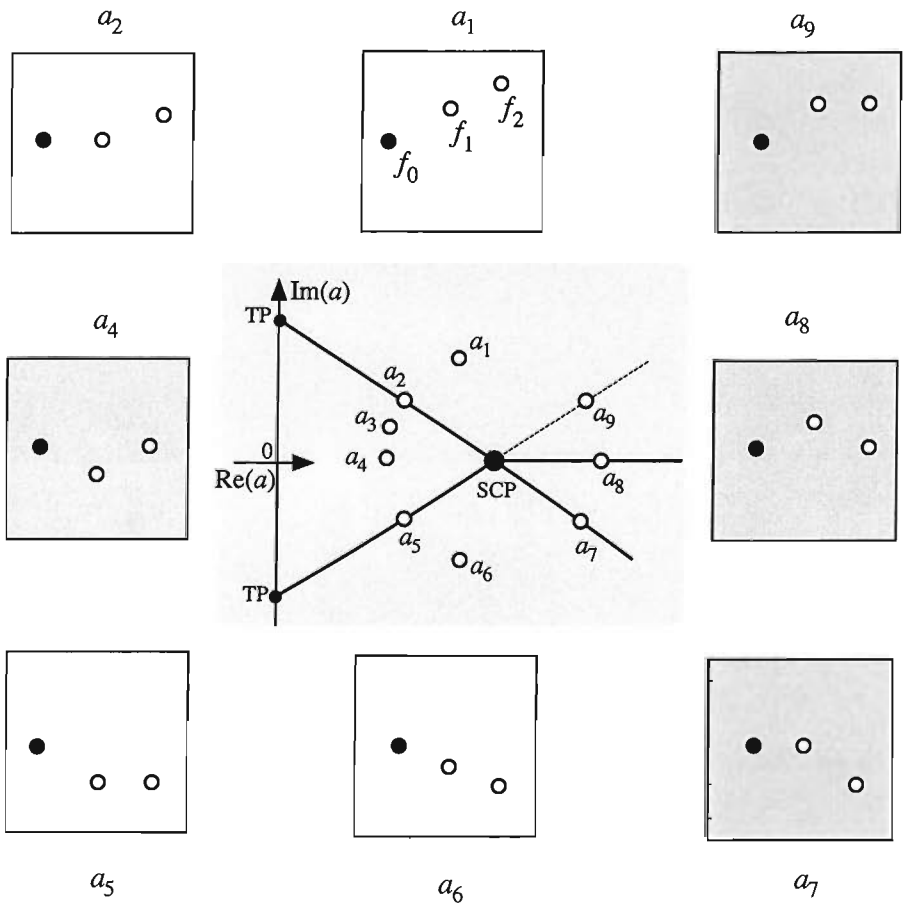

Figure 3.2: Sketches of the Borel planes for (3.3) at values of the a_i corresponding to those in figure 1. In each Borel plane the solid dot is the image of saddle 0. The other dots are the images of saddles 1 and 2. Note that a box labelled a_3 has been omitted as it is identical to a_4. At a Stokes phenomenon two or more solid dots are horizontally collinear as the steepest paths map to horizontal lines. At a higher order Stokes phenomenon (a_1 and a_6) three or more are collinear in any direction.

now all three saddles are involved in the large-k asymptotic contribution and, at a_6, $C = C_0 \cup C_1 \cup C_2$. Another Stokes phenomenon at a_7 removes the contribution from z_1; z_2 is removed at a_8. At this point we have the same contributions at a_8 as at a_1, but we have yet to cross the continuation of Stokes line $S_{1>2}$. Since saddle z_1 has been removed and no longer contributes to the asymptotics of $P(k;a)$ at this point, there is no Stokes phenomena at a_9. The Stokes line appears dotted in Figure 3.2 because it is irrelevant to our choice of contour in (3.3). (Note that this is different to the lack of a Stokes line at $a = a_4$, which was due to non-adjacency.)

We will call the point where all the Stokes lines meet in the a-plane the Stokes crossing point (SCP). The part of the positive real axis connecting the origin to the SCP is not an active Stokes line, as shown above, yet the portion to the right of the SCP is a Stokes line ($S_{0>2}$). If our point a lies on either part of the line, $f_2(a)$ is crossing the horizontal half-line emanating from $f_0(a)$. For a to the left of the SCP, $f_2(a)$ is not on the same Riemann sheet as $f_0(a)$. For a to the right of the SCP, it is.

We explain this change in the Riemann sheet structure with the higher order Stokes phenomenon, which takes place across a higher order Stokes curve (HSC) in the complex s-plane passing through the SCP.

In the example above, we have chosen to let a_1 lie on the HSC. We see that the steepest descent paths show nothing of interest happens at this point, however the Borel plane reveals something significant. Let the points a_1^+ and a_1^- be values of a lying slightly to the right and left of a_1 respectively. Figure 3.3 shows that $f_2(a_1)$ is actually crossing the continuation of line from $f_0(a_1)$ to $f_1(a_1)$. On the HSC, the three points $f_j(a)$ are collinear in the Borel plane. As collinearity occurs, the Riemann sheet structure of the Borel plane changes. For $a = a_1^+$, the point $f_2(a)$ lies on the principal Riemann sheet as seen from $f_0(a)$, but for $a = a_1^-$ it is not. This means that in order to walk from $f_0(a_1^-)$ to $f_2(a_1^-)$ we must first walk around $f_1(a_1^-)$, and then "drop" on to the relevant Riemann sheet.

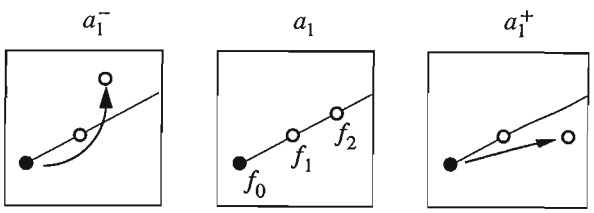

Figure 3.3: The higher order Stokes phenomenon in the Borel plane for values of a near to a_1. At the higher order Stokes phenomenon f_1 eclipses f_2 when viewed from f_0. The Riemann sheet structure of the Borel plane changes as f_2 passes through a radial cut from f_1. At a_1^-, f_2 is invisible from f_0 and so no Stokes phenomenon between f_0 and f_2 can take place. At a_1^+, f_2 is visible and so a Stoke phenomenon is then possible.

On a traditional Stokes line we have

$$\mathrm{Im}[k(f_m(a) - f_j(a))] = 0, \tag{3.9}$$

(k an arbitrary complex value) which means that the two points f_m, f_j can be joined by a horizontal line in the f-plane. The Stokes lines are only active when the relevant $f_j(a)$ are on the same Riemann sheet. Previously it was thought that in the a-plane Stokes lines could only emanate from turning points, where two or more $f_j(a)$ coalesce, or from other singularities. However, the example above shows that Stokes lines may start and end from other regular points in the a-plane, where two or more Stokes lines cross. This effect has also been observed by Berk *et al* [44] and Aoki *et al* [45].

We would like to stress at this point the difference between the SCP and the so called "new turning points" highlighted in [44] and [45]. This difference can be viewed best in the Borel plane. At a Stokes Crossing Point, no coalescence of the $f_j(a)$ is taking place, and there is no breakdown in the large k asymptotics there. Furthermore, no Stokes lines are actually born at this point, they just change their behaviour. In the Borel plane, the SCP will be signified by the $f_j(a)$ lying in a straight and horizontal line. This is obvious when one considers that the SCP will necessarily be part of the HSC. A higher order Stokes phenomenon requires that

the $f_j(a)$ are collinear (in any direction), and if the Stokes lines cross we must also have the simultaneous horizontal lining up (pair-wise) of the $f_j(a)$. Hence the resultant view in the Borel plane.

When viewed from the Borel plane, a new turning point (also known as a Virtual Turning Point) exhibits the apparent coalescence of the $f_j(a)$ with one another. In fact, at this point, there is no coalescence taking place, and the virtual turning points do not cause any breakdown of the large k asymptotics. This is because each of the f_j lie on mutually different Riemann sheets. Analogously, at a Virtual Turning Point, the values of the exponents of two different saddle points are identical, but the saddle points themselves have not coalesced as they would have done at a real turning point.

We will explain this and discuss these points at length in the next chapter. Here it suffices to draw the distinction between the SCP and the new turning points, and to correct the misunderstanding made by the authors in [49]. It is clear from the above descriptions that the SCP and the new turning points are not the same phenomena.

It is important to note the difference between an inactive Stokes line and an irrelevant Stokes line. We have seen that there is no Stokes line drawn between $a = 0$ and the SCP; this is because no Stokes phenomenon occurred as a result of the fact that $f_2(a)$ was not on the principle Riemann sheet as viewed from $f_0(a)$ (ie., they were not adjacent). Hence this Stokes line is inactive. In the case of the line from the SCP along the continuation of the Stokes line $S_{1>2}$ in the direction of a_9, we find that a Stokes phenomenon does in fact take place between the saddles at z_1 and z_2. However, this particular phenomenon is irrelevant to the saddle-point asymptotics of $P(k;a)$ due to our choice of valleys in (3.3); at this point, z_1 does not contribute to the asymptotics of $P(k;a)$ at all.

A higher order Stokes phenomenon requires that at least three of the $f_j(a)$ are collinear in the f-plane, as opposed to the traditional Stokes phenomenon which required only two of the $f_j(a)$ to differ by a real number. This suggests

that a higher order Stokes phenomenon is less common, due to the apparent extra constraint on the positioning of the third $f_j(a)$ relative to the other two. However, for a higher order Stokes phenomenon there is no constraint on the positioning of the first two $f_j(a)$ in the f-plane, since a straight line can join any two points. Therefore there is actually only a single constraint on the position of the third $f_j(a)$. Provided three or more $f_j(a)$ exist, a traditional Stokes line and a higher order Stokes curve have the same co-dimensionality.

When k takes an arbitrary complex value, the traditional Stokes line $S_{i>j}$ is defined by

$$S_{i>j} = \{a : k(f_j(a) - f_i(a)) > 0\}. \tag{3.10}$$

This means that the position of these lines in the a-plane depends on the phase of k. The collinearity condition in the f-plane for a higher order Stokes phenomenon does not depend on k. We require

$$\frac{f_j(a) - f_i(a)}{f_k(a) - f_j(a)} \in \mathbb{R}, \tag{3.11}$$

so the higher order Stokes curves are invariant under a change of k. This shows that the SCP is k-dependent whereas a traditional turning point is k-independent. A HSC will emanate from the same points as the traditional Stokes lines (turning points or singularities of the phase function f).

We have so far talked about the higher order Stokes phenomenon in terms of asymptotic expansions arising from saddle-point integrals. However, since we have expressed everything in terms of the $f_j(a)$, the ideas are more generally applicable. The ability to determine all the different types of exponential asymptotic behaviours $\exp(-kf_j(a))$ associated with an expansion is all that is required. For the saddle-point integral we have used steepest descent contours in the z-plane of the integrand to determine the activity of the Stokes lines. We could also look to compute the Stokes constants of the problem, as discussed earlier in the thesis.

The higher order Stokes phenomenon requires the collinearity of at least three $f_j(a)$, so we expect such a phenomenon to occur in any expansion involving more

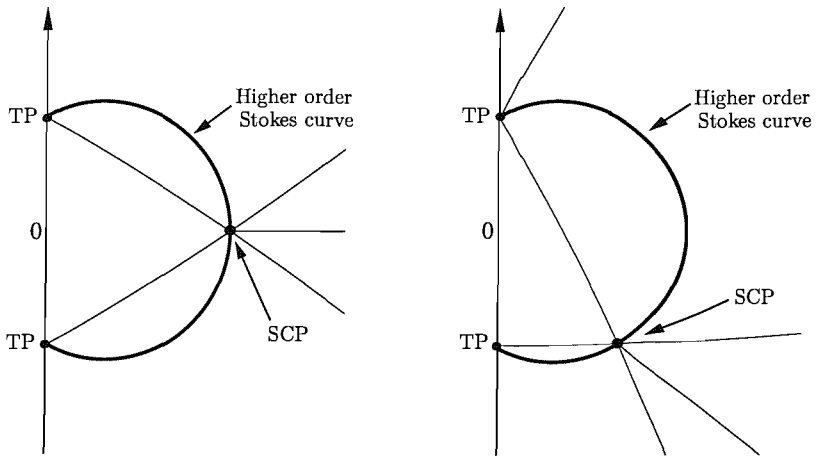

Figure 3.4: The Stokes geometry for ph $k = 0$ (left) and ph $k = \pi/4$ (right). The thin curves are the normal Stokes curves, and the bold curves are the higher order Stokes curves.

than two different asymptotic behaviours depending on an additional set of parameters $\mathbf{a}$. These expansions may arise from integrals (of any dimension), from the solutions of inhomogeneous second-order linear differential equations, higher order linear ODEs, non-linear ODEs, and especially partial differential equations.

3.2 Explanation of the Higher Order Stokes Phenomenon

We can explain the higher order Stokes phenomenon and why it gives rise to fundamental changes in the analytic structure of an expansion by using some of the hyperasymptotic procedures already developed ([28], [31], [35], [33], [46]). What follows is valid for any function that possesses a Borel transform representation.

Consider an integral of the form

$$I^{(n)}(k;\mathbf{a}) = \int_{C_n(\theta_k;\mathbf{a})} e^{-kf(z;\mathbf{a})} g(z;\mathbf{a}) dz. \tag{3.12}$$

It is assumed that f possesses at least three saddles situated at $z = z_n$ $(n = 0, 1, 2)$,

where $f'(z) = 0$ by definition; again we assume that the saddles are simple, ie., $f''(z) \neq 0$. As before, $f_n = f_n(\mathbf{a}) = f(z_n; \mathbf{a})$. The contour $C_n(\theta_k; \mathbf{a})$ is the steepest descent path running through (in general) a single specific saddle at z_n, between specified asymptotic valleys of $\mathrm{Re}\{f(z) - f_n\}$ at infinity ([47], [7]). The functions $f(z; \mathbf{a})$ and $g(z; \mathbf{a})$ are analytic at least in a strip including $C_n(\theta_k; \mathbf{a})$ and in the range of $\mathbf{a}$ values considered.

For the purpose of this explanation, and without loss of generality, we label the saddles such that $\mathrm{Re}\{f_0\} < \mathrm{Re}\{f_1\} < \mathrm{Re}\{f_2\}$ for the values of $\mathbf{a}$ under discussion. We consider the integral through saddle 0, and choose $\mathbf{a}$ such that saddle 2 is adjacent to saddle 1 but not to saddle 0.

Integral (3.12) may be rewritten to extract the exponential dependence at saddle 0 as

$$I^{(0)}(k; \mathbf{a}) = \frac{\exp(-kf_0(\mathbf{a}))}{\sqrt{k}} T^{(0)}(k; \mathbf{a}), \tag{3.13}$$

where

$$T^{(0)}(k) = \sum_{r=0}^{\infty} \frac{T_r^{(0)}(\mathbf{a})}{k^r}.$$

As we saw in the previous chapter, we can overcome the divergence of $T^{(n)}$ and gain an exact remainder term linking saddle 0 to saddle 1:

$$\begin{aligned} T^{(0)}(k) &= \sum_{r=0}^{N_0-1} \frac{T_r^{(0)}(\mathbf{a})}{k^r} \\ &+ \frac{1}{2i\pi} \frac{K_{01}}{(kF_{01}(\mathbf{a}))^{N_0}} \int_0^{\infty} dv \frac{e^{-v} v^{N_0-1}}{(1 - v/kF_{01}(\mathbf{a}))} T^{(1)}\left(\frac{v}{F_{01}(\mathbf{a})}; \mathbf{a}\right) \end{aligned} \tag{3.14}$$

where

$$F_{nm}(\mathbf{a}) = f_m(\mathbf{a}) - f_n(\mathbf{a}).$$

The Stokes multiplier K_{01} represents the contribution of saddle 1 to the expansion about saddle 0.

As a direct consequence of definition (3.10), a Stokes phenomenon will occur between saddle 0 and saddle 1 when $\arg(kF_{01}) = 2q\pi$ for any integer q. The

integral in the remainder encounters a pole at this phase, introducing a residue contribution of the form (up to a sign)

$$\frac{K_{01}}{(kF_{01}(\mathbf{a}))^{N_0}} \operatorname*{Res}_{v\to kF_{01}(\mathbf{a})} \left\{ \frac{e^{-v}v^{N_0-1}}{1-v/kF_{01}(\mathbf{a})} T^{(1)}\left(\frac{v}{F_{01}(\mathbf{a})};\mathbf{a}\right)\right\}$$

$$= K_{01}e^{-kF_{01}(\mathbf{a})}T^{(1)}(k;\mathbf{a}). \tag{3.15}$$

Combining this with the exponential prefactor $\exp(-kf_0)$ produces an exponentially small contribution

$$\exp(-kf_0)\exp(-kF_{01}) = \exp(-k\{f_0+f_1-f_0\}) = \exp(-kf_1), \tag{3.16}$$

leaving us with a $\exp(-kf_1)T^{(1)}(k)$ contribution. This is the integral over the steepest contour passing through z_1 (*cf.* equation (3.13)).

The remainder term in (3.14) is exact. However, it contains within it the term $T^{(1)}$, so it is implicit. We will in general know no more about $T^{(1)}$ than we do about $T^{(0)}$. Using the technique of Berry & Howls, we overcome this fact by writing down a similar expression for $T^{(1)}$ based on (3.14) in terms of its own adjacent terms:

$$\begin{aligned} T^{(1)}(\xi;\mathbf{a}) &= \sum_{r=0}^{N_1-1}\frac{T_r^{(1)}}{\xi^r} \\ &+ \frac{1}{2i\pi}\sum_{m=0,2}\frac{K_{1m}}{(\xi F_{1m}(\mathbf{a}))^{N_1}}\int_0^\infty dw \frac{e^{-w}w^{N_1-1}}{(1-w/\xi F_{1m}(\mathbf{a}))}T^{(m)}\left(\frac{w}{F_{1m}(\mathbf{a})};\mathbf{a}\right) \end{aligned} \tag{3.17}$$

($\xi = v/F_{01}(\mathbf{a})$) and then substituting it back in to (3.14). We now have a double integral term of the form

$$\begin{aligned} R^{012}(\xi;\mathbf{a}) &= \frac{1}{(2\pi i)^2}\frac{K_{01}K_{12}}{k^{N_0}(F_{01}(\mathbf{a}))^{N_0-N_1}(F_{12}(\mathbf{a}))^{N_1}} \\ &\times \int_0^\infty \frac{e^{-v}v^{N_0-N_1-1}dv}{1-v/kF_{01}(\mathbf{a})}\int_0^\infty \frac{e^{-w}w^{N_1-1}dw}{1-wF_{01}(\mathbf{a})/vF_{12}(\mathbf{a})}T^{(2)}\left(\frac{w}{F_{12}(\mathbf{a});\mathbf{a}}\right), \end{aligned} \tag{3.18}$$

which has a pole when the Stokes phenomenon takes place at

$$kF_{01}(\mathbf{a}) > 0. \tag{3.19}$$

There is also another potential pole if $\mathbf{a}$ is varied independently of k such that

$$\frac{F_{01}(\mathbf{a})}{F_{12}(\mathbf{a})} > 0, \tag{3.20}$$

which is identical to the collinearity condition (3.11). The occurrence of the pole and the higher order Stokes phenomenon are therefore intimately linked (an explicit calculation appears in the next section). The residue from this second pole is calculated to be (up to a sign)

$$\frac{K_{01}K_{12}}{2\pi i k^{N_0} F_{02}(\mathbf{a})^{N_0}} \int_0^\infty \frac{e^{-u}u^{N_0-1}}{1-u/kF_{01}(\mathbf{a})} T^{(2)}\left(\frac{u}{F_{02}(\mathbf{a})}\right) du \tag{3.21}$$

where $u = vF_{02}/F_{01}$. This new contribution to the remainder term is equivalent to the contribution that one would expect if saddle 2 were adjacent to saddle 0 (*cf.* (3.14) & (3.15), remembering that K_{01} and K_{12} are ± 1). If the parameters $\mathbf{a}$ (or k) are varied further so that kF_{02} becomes real and positive then a Stokes phenomenon can occur between saddle 2 and saddle 0, where before it could not. Equally, a coalescence could take place on a caustic. This change in the potential for a Stokes phenomenon to occur has arisen from a higher order hyperasymptotic expansion and is caused by the poles in the same way as a traditional Stokes phenomenon.

3.3 PDE Example

We can further illustrate the findings of the previous two sections via the following example. We show how an understanding of sub-subdominant terms can be vital in understanding the large time behaviour of a PDE.

We are interested in the large time behaviour of the following system

$$u_t - u_x = \epsilon^2 u_{xxx} - \frac{1}{1+x^2}, \tag{3.22}$$

$$-\infty < x < +\infty, \quad t > 0, \quad 0 < \epsilon \ll 1,$$

$$u(x,0) = \arctan x,$$

$$u, u_x, u_{xx} \to 0 \quad \text{as} \quad |x| \to \infty.$$

We can solve this exactly using Fourier transforms as follows.

Using Fourier's Theorem

$$u_x = (-ik)^n \bar{u} \tag{3.23}$$

where

$$\bar{u} = \int_{-\infty}^{\infty} e^{ikx} u(x) dx, \tag{3.24}$$

equation (3.22) becomes

$$\bar{u}_t - (-ik\bar{u}) = \epsilon^2(-ik)^3\bar{u} - \int_{-\infty}^{\infty} dx \frac{e^{ikx}}{1+x^2} \tag{3.25}$$

The integral in (3.25) can be evaluated in the following way. There are poles of the integral at $x = \pm 1$. We can navigate this pole in the complex x-plane in two ways depending on whether Re(k)>0 ($x > 0$) or Re(k)<0 ($x < 0$). When $x > 0$ then

$$\int_{-\infty}^{\infty} dx \frac{e^{ikx}}{1+x^2} = +2\pi i \lim_{x \to +i} (x-i) \frac{e^{ikx}}{1+x^2}, \tag{3.26}$$

$$= 2\pi i \lim_{x \to +i} \frac{e^{ikx}}{x+i}, \tag{3.27}$$

$$= \pi e^{-|k|}. \tag{3.28}$$

Similarly when $x < 0$ we find

$$\int_{-\infty}^{\infty} dx \frac{e^{ikx}}{1+x^2} = \pi e^{-|k|}. \tag{3.29}$$

Thus

$$\bar{u}_t + ik\bar{u} = \epsilon^2 ik^3 \bar{u} - \pi e^{-|k|}, \tag{3.30}$$

$$\bar{u} - t + ik(1 - \epsilon^2 k^2)\bar{u} = -\pi e^{-|k|}. \tag{3.31}$$

This can easily be solved, using an integrating factor $e^{ik(1-\epsilon^2k^2)t}$ and the initial condition

$$u(x,0) = \arctan x. \tag{3.32}$$

Under a Fourier transform this becomes

$$\bar{u}(k,0) = \int_{-\infty}^{\infty} dx e^{ikx} \arctan x, \tag{3.33}$$

$$= -\frac{1}{ik}\int_{-\infty}^{\infty} dx \frac{e^{ikx}}{1+x^2}, \tag{3.34}$$

which can be seen by using integration by parts. This last integral we have evaluated already in (3.28) and (3.29), hence

$$\bar{u}(k,0) = -\frac{\pi e^{-|k|}}{ik}. \tag{3.35}$$

Then the solution to (3.31) is

$$\bar{u} = \frac{\pi e^{-|k|}}{ik(1-\epsilon^2k^2)}\left(1-\epsilon^2k^2e^{-ik(1-\epsilon^2k^2)t}\right). \tag{3.36}$$

By applying an inverse Fourier transform, the solution takes the form of 2 time-dependent and 2 time-independent integrals

$$u(x,t;\epsilon) = \arctan x + \sum_{j=1}^{2} I_j(x,t;\epsilon) + \sum_{j=3}^{4} I_j(x;\epsilon), \tag{3.37}$$

where

$$I_1(x,t;\epsilon) \equiv \int_0^{\infty} dp \frac{ip\pi}{1-p^2}\exp\left[\frac{-p}{\epsilon}\{(1+ix)+i(1-p^2)t\}\right] = I_2^*(x,t;\epsilon), \tag{3.38}$$

$$I_3(x;\epsilon) \equiv \int_0^{\infty} dp \frac{i\pi}{p(1-p^2)}\exp\left[\frac{-p}{\epsilon}(1-ix)\right] = I_4^*(x;\epsilon). \tag{3.39}$$

(Stars denote complex conjugation.) Note that the integrals that appear in [49] for I_1 – I_4 are incorrect; those which appear above are the correct results.

The contours in I_1 and I_4 are taken around the poles at $p = +1$ in a clockwise direction; the contours in I_2 and I_3 taken around the poles at $p = +1$ in an anti-clockwise direction. This ensures that the initial conditions are satisfied; we

require no ϵ-dependence at $t = 0$, and in the sum of all four integrals there is no pole (hence we can neglect the $p = 0$ pole in I_3 and I_4).

Let

$$I_{total} = I_1 + I_2 + I_3 + I_4,$$

then at $t = 0$:

$$\begin{aligned} I_{total} &= \int_0^\infty dp \frac{ip\pi}{1-p^2} \exp\left[\frac{-p}{\epsilon}(1+ix)\right] \\ &\quad - \int_0^\infty dp \frac{ip\pi}{1-p^2} \exp\left[\frac{-p}{\epsilon}(1-ix)\right] \\ &\quad + \int_0^\infty dp \frac{i\pi}{p(1-p^2)} \exp\left[\frac{-p}{\epsilon}(1-ix)\right] \\ &\quad - \int_0^\infty dp \frac{i\pi}{p(1-p^2)} \exp\left[\frac{-p}{\epsilon}(1+ix)\right]. \end{aligned} \tag{3.40}$$

Thus, to cancel the ϵ-dependence for $u(x,0)$, we pair I_1 with I_4 and I_2 with I_3. Steepest descent plots at $t = 0$ indeed reveal that we traverse the poles in the manor stated above.

For $t > 0$, there are 3 possible asymptotic contributions to I_1 and I_2. These are an endpoint (at $p = 0$), a pole ($p = +1$) and a saddle point. For I_3 and I_4, contributions may only arise from the endpoint and the pole at $p = +1$. From this point on, we focus on the time-dependence of the problem; furthermore we may look only at the integral I_1, due to the symmetry of the integrals. I_1 is of the form (3.12) with

$$k = \frac{1}{\epsilon}, \quad \mathbf{a} = \{x, t\}, \quad f(p; x, t) = \left[\frac{-p}{\epsilon}\{(1+ix) + i(1-p^2)t\}\right], \tag{3.41}$$

plus the additional endpoint and pole contributions. We adopt the following labelling:

(i) e = endpoint at $p = 0$,

(ii) p_1 = poles at $p = +1$,

(iii) p_2 = poles at $p = -1$,

(iv) s_1 = saddle at $p = +\sqrt{\frac{1}{3it}(1+i(x+t))}$,

(v) s_2 = saddle at $p = -\sqrt{\frac{1}{3it}(1+i(x+t))}$.

The asymptotic behaviours are given by

$$e^{-f_j/\epsilon}T^{(j)}(\epsilon) \tag{3.42}$$

where $j = e,\ p_1$ or s_1 and

$$\begin{aligned}
f_e(x,t) &= 0, \qquad T^{(e)}(\epsilon;x,t) \sim \frac{1}{2i}\sum_{r=1}^{\infty}\left(\sum_{m=0}^{r-1}\frac{\Gamma(2r+1)(it)^m}{m!(1+i(x+t))^{2r+m}}\right)\epsilon^{2r};\\
f_{s_1}(x,t) &= \frac{2i(-i+t+x)^{3/2}}{3\sqrt{3t}}, \quad T^{(s_1)}(\epsilon;x,t) \sim \sum_{r=0}^{\infty} T_r^{(s_1)}\epsilon^{r+1/2};\\
f_{p_1}(x,t) &= 1+ix, \qquad T^{(p_1)}(\epsilon;x,t) = -\frac{\pi}{2}.
\end{aligned} \tag{3.43}$$

Notice that the contributions from the saddle and endpoint are both asymptotic infinite series. The pole contribution is exact. Since I_2 is the complex conjugate of I_1, it has an identical analytic structure and the relevant expansions are just the corresponding conjugates of (3.43). Expansions for I_3 (and I_4) may be obtained by setting $t = 0$ in the relevant expansions in (3.43) and multiplying by -1.

The real $(x, t > 0)$ half-plane is split into six regions by potential Stokes lines, separating areas of different asymptotic contributions. Three such lines are possible:

1. Along the line $x = 0$ where

$$F_{ep_1}(x,t) \equiv f_{p_1} - f_e = 1 + ix > 0,$$

the endpoint may switch on a pole (residue) contribution;

2. Along a line running forward in time from negative to positive x where

$$F_{s_1p_1}(x,t) \equiv f_{p_1} - f_{s_1} = 1 + ix - 2i\frac{(x+t-i)^{3/2}}{3\sqrt{3t}} > 0,$$

a saddle may switch on a pole contribution;

3. Along a line running forward in time from positive to negative x where

$$F_{es_1}(x,t) \equiv f_{s_1} - f_e = 2i\frac{(x+t-i)^{3/2}}{3\sqrt{3t}} > 0,$$

the endpoint may switch on a saddle.

A sequence of steepest descent contours as a function of x and t allows us to plot the Stokes lines and determine which contributions are made in each of the six regions between them. The endpoint e contributes for all x and t.

Numbering the regions as in Figure (3.5), we can interpret the diagram as follows:

In region 1, only e contributes. Across the Stokes line into 2, the *dominant* endpoint switches on a *subdominant* contribution from s_1. Across the Stokes line into 3, s_1 switches on a (relatively) subdominant contribution from p_1.

Moving now across the Stokes line from 1 to 6, e switches on a subdominant pole contribution from p_1. From 6 into 5 nothing changes, since there is no s_1 yet present to switch on contribution from p_1. Moving into 4 from 5, s_1 is finally switched on by e. Thus in both 3 and 4 there are contributions from e, s_1 and p_1.

Previously we calculated that the line $x = 0$, $t > 1/\sqrt{3}$ should be a Stokes line. However, the analysis above seems to suggest that the presence of such a line here would be a contradiction. The conclusion we draw is that despite the presence of the necessary dominant and subdominant terms, no Stokes phenomenon can take place. This is confirmed by the steepest descent analysis.

We resolve this apparent paradox via a U-shaped higher order Stokes line defined by

$$\frac{F_{es_1}}{F_{s_1p_1}} > 0 \tag{3.44}$$

that runs between infinities in 2 and 5 through the point $(0, 1/\sqrt{3})$ (see Figure 3.6).

In terms of a Borel transform, the higher order Stokes phenomenon may be observed by an extension of the arguments used above to include endpoints and poles. This requires a combination of techniques (see [28], [10], [34], [35]). A short

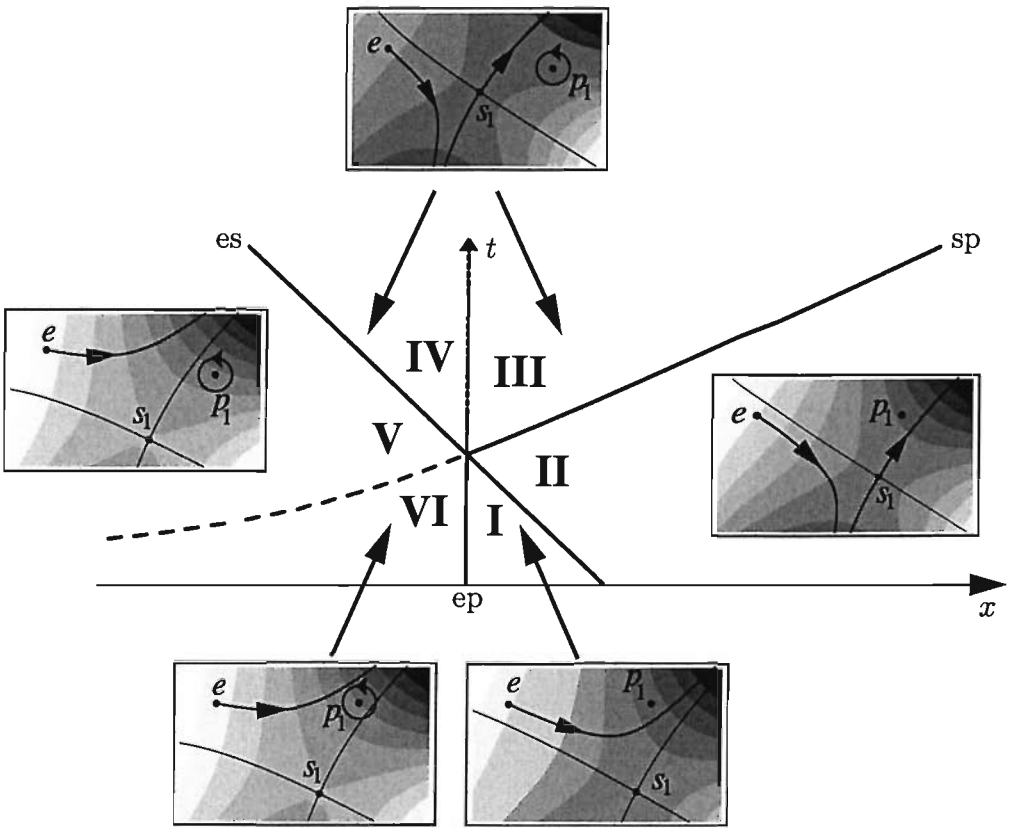

Figure 3.5: The six regions in the $(x, t > 0)$ half-plane in which different asymptotic behaviours for I_1 are possible. These regions are delineated by Stokes lines. The notation "es", for example, refers to an endpoint switching on a saddle contribution. The dashed Stokes line between **V** and **VI** is active, but irrelevant. The dotted line between regions **III** and **IV** is an inactive Stokes line.

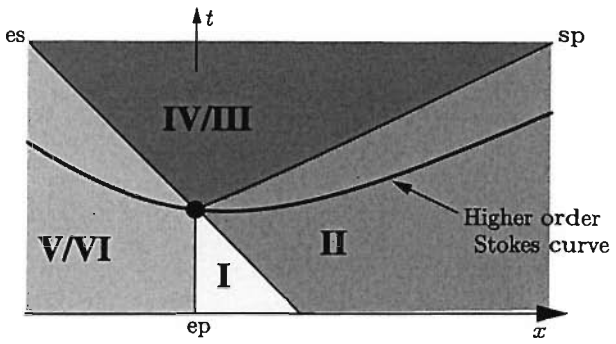

Figure 3.6: The Stokes lines and the higher order Stokes line for I_1.

calculation results in an exactly terminated expansion for each type of asymptotic expansion.

The endpoint expansion is

$$T^{(e)}(\epsilon) = \sum_{r=0}^{N-1} T_r^{(e)} \epsilon^r + R_N^{(e)}. \tag{3.45}$$

The remainder term may be written exactly as

$$R_N^{(e)} = \frac{1}{2\pi i} \sum_{m=s_1,s_2} \frac{K_{em}}{F_{em}^{N-1/2}} \int_0^\infty du \frac{u^{N-1/2} e^{-u}}{\left(1 - \frac{u\epsilon}{F_{em}}\right)} T^{(m)}\left(\frac{F_{em}}{u}\right), \tag{3.46}$$

which has within it a contribution from the pole and from the saddle. Re-writing the remainder to include these terms gives

$$\begin{aligned} T^{(e)} &= \sum_{r=0}^{N-1} T_r^{(e)} \epsilon^r - \sum_p \frac{\epsilon^N g_p}{F_{ep}^{N+1}} \int_0^\infty du \frac{e^{-u} u^N}{\left(1 - \frac{u\epsilon}{F_{ep}}\right)} \\ &\quad + \sum_m \frac{\epsilon^N}{2i\pi F_{em}^{N+1/2}} \int_0^\infty dv \frac{e^{-v} v^{N-1/2}}{\left(1 - \frac{v\epsilon}{F_{em}}\right)} T^{(m)}\left(\frac{F_{em}}{v}\right), \end{aligned} \tag{3.47}$$

where g_p is the residue of I_1 at $p = \pm 1$. Note that the integral containing F_{ep} is an explicit integral, since the contribution of a pole to the remainder term can be evaluated explicitly. In a similar way, the expansion about s can be written as

$$T^{(s_1)} = \sum_{r=0}^{M-1} T_r^{(s_1)} \epsilon^r - \sum_p \frac{\epsilon^M g_p}{F_{s_1 p}^{M+1/2}} \int_0^\infty du \frac{e^{-u} u^{M-1/2}}{\left(1 - \frac{u\epsilon}{F_{s_1 p}}\right)}$$

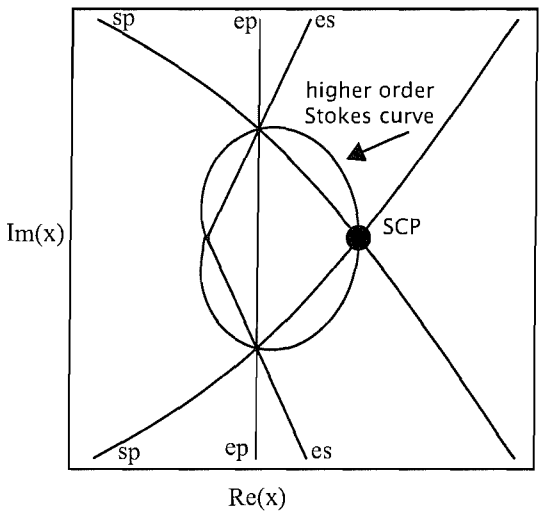

Figure 3.7: The regular Stokes lines plus the bean-shaped higher order Stokes curve plotted in the complex-x plane.

$$+\frac{\epsilon^M}{2i\pi F_{s_1s_2}^{M+1/2}}\int_0^\infty dv \frac{e^{-v}v^{M-1}}{\left(1-\frac{v\epsilon}{F_{s_1s_2}}\right)} T^{(s_2)}\left(\frac{F_{s_1s_2}}{v}\right). \qquad (3.48)$$

Note that while there is again an explicit contribution from the poles, there is now only a single further implicit s_2-dependent integral contribution. There is no contribution from the endpoint since in general saddle points do not observe endpoints. A corresponding exact expression for $T^{(s_2)}$ can be obtained by letting $s_1 \rightarrow s_2$.

The first hyperasymptotic expansion is then obtained by inserting (3.48) into (3.47), since this becomes

$$\begin{aligned} T^{(s_1)}\left(\frac{F_{es_1}}{v}\right) &= \sum_{r=0}^{M-1} T_r^{(s_1)}\left(\frac{F_{es_1}}{v}\right)^r - \sum_p \frac{\left(\frac{F_{es_1}}{v}\right)^M g_p}{F_{s_1p}^{M+1/2}}\int_0^\infty du \frac{e^{-u}u^{M-1/2}}{\left(1-\frac{uF_{es_1}}{vF_{s_1p}}\right)} \\ &+\frac{\left(\frac{F_{es_1}}{v}\right)^M}{2i\pi F_{s_1s_2}^{M+1/2}}\int_0^\infty dw \frac{e^{-w}w^{M-1}}{\left(1-\frac{wF_{es_1}}{vF_{s_1s_2}}\right)} T^{(s_2)}\left(\frac{F_{s_1s_2}}{v}\right). \qquad (3.49) \end{aligned}$$

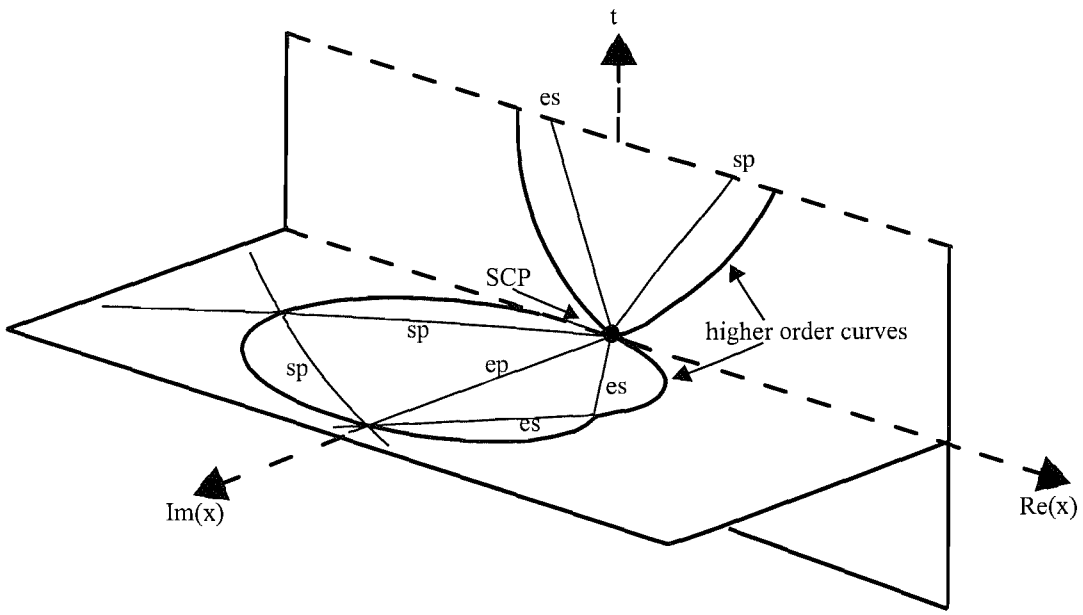

Figure 3.8: This figure shows the coincidence of the real $(x,\ t)$ plane with the complex x-plane. The higher order lines meet at the point $x = 0,\ t = 1/\sqrt{3}$, shown by the black dot.

Thus

$$
\begin{aligned}
T^{(e)}(\epsilon) \;=\; & \sum_{r=0}^{N-1} T_r^{(e)} \\
& - \sum_p \frac{\epsilon^N g_p}{F_{ep}^{N+1}} \int_0^\infty du \frac{e^{-u}u^N}{\left(1-\frac{u\epsilon}{F_{ep}}\right)} + \sum_m \frac{\epsilon^N}{2i\pi F_{em}^{N+1/2}} \int_0^\infty dv \frac{e^{-v}v^{N-1/2}}{\left(1-\frac{v\epsilon}{F_{em}}\right)} \\
& \times \left\{ \sum_{r=0}^{M-1} T_r^{(s_1)} \left(\frac{F_{es_1}}{v}\right)^r - \sum_p \left(\frac{F_{es_1}}{v}\right)^M \frac{g_p}{F_{s_1p}^{M+1/2}} \int_0^\infty du \frac{e^{-u}u^{M-1/2}}{\left(1-\frac{uF_{es_1}}{vF_{s_1p}}\right)} \right. \\
& \left. + \left(\frac{F_{es_1}}{v}\right)^M \frac{1}{2i\pi F_{s_1s_2}^M} \int_0^\infty dw \frac{e^{-w}w^{M-1}}{\left(1-\frac{wF_{es_1}}{vF_{s_1s_2}}\right)} \right\}. \qquad (3.50)
\end{aligned}
$$

The terms crucial to understanding the absence of a Stokes line at $x = 0$, $t > 1/\sqrt{3}$ are

$$
\begin{aligned}
T^{(e)}(\epsilon) = \cdots \; & - \sum_p \frac{\epsilon^N g_p}{F_{ep}^{N+1}} \int_0^\infty du \frac{e^{-u}u^N}{\left(1-\frac{u\epsilon}{F_{ep}}\right)} \\
& + \cdots \\
& - \frac{\epsilon^N}{2i\pi F_{em}^{N+1/2}} \int_0^\infty dv \frac{e^{-v}v^{N-1/2}}{(1-v\epsilon/F_{em})} \\
& \quad \times \sum_p \left(\frac{F_{es_1}}{v}\right)^M \frac{g_p}{F_{s_1p}} \int_0^\infty du \frac{e^{-u}u^{M-1/2}}{\left(1-\frac{uF_{es_1}}{vF_{s_1p}}\right)} \\
& + \cdots . \qquad (3.51)
\end{aligned}
$$

For $x = 0$, $t < 1/\sqrt{3}$, the single integral encounters a pole since $F_{ep} > 0$, and in doing so generates a Stokes phenomenon between e and $p = +1$. As t advances and crosses the higher order Stokes line where $F_{es_1}/F_{s_1p} > 0$, the double integral encounters a pole. The residue of this pole at $u = F_{s_1p}/F_{es_1}$ exactly cancels the single integral. The remainder term of $T^{(e)}(\epsilon)$ no longer contains a contribution from $p = +1$ at this exponential level and no Stokes phenomenon is generated between e and $p = +1$. This is why there is no Stokes line for $x = 0$, $t > 1/\sqrt{3}$.

A further significant consequence of this example is the necessity to include exponentially *sub*-subdominant terms in the large time asymptotic analysis. For

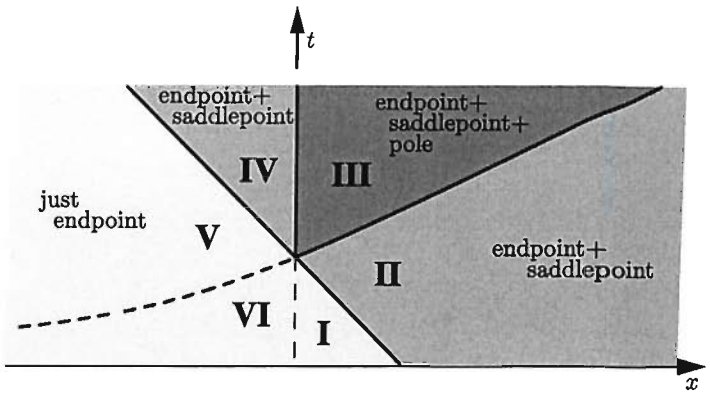

Figure 3.9: The asymptotic contributions in each region for the complete expansion of generated by the sum of integrals in (3.37)

$x > 0$, $t \approx 0$, the dominance of the asymptotic contributions is (*cf.* (3.43))

$$|e^{-f_e/\epsilon}T^{(e)}(\epsilon)| > |e^{-f_{s_1}/\epsilon}T^{(s_1)}(\epsilon)| > |e^{-f_{p_1}/\epsilon}T^{(p_1)}(\epsilon)|. \tag{3.52}$$

The long time behaviour in region 3 involves all 3 such contributions, with $e^{-f_{s_1}/\epsilon}T^{(s_1)}$ a decaying function of time but $e^{-f_{p_i}/\epsilon}T^{(p_1)}$ is independent of time. Consequently $e^{-f_{p_i}/\epsilon}T^{(p_1)}$ develops as the principle time-independent oscillatory background to the monotonic $e^{-f_e/\epsilon}T^{(e)}$. If the sub-subdominant $e^{-f_{p_i}/\epsilon}T^{(p_1)}$ had been initially neglected as irrelevant near to $t = 0$, then an incorrect large-t, finite-x behaviour would have been predicted. This can be verified by carrying out a similar analysis for the other integrals and combining the results.

Figure 3.9 shows the overall combination of terms that contribute from the sum of the four integrals. For the integrals $I_3(x;\epsilon)$ and $I_4(x;\epsilon)$, a single Stokes line exists along the whole of the t-axis. Superposing this on the integrals $I_1(x,t;\epsilon)$ and $I_2(x,t;\epsilon)$, we find that the composite expansion has a Stokes line along the t-axis for $t > 1/\sqrt{3}$. This does not alter the role of the higher order Stokes phenomenon, which has determined the constituent Stokes behaviour of $I_1(x,t;\epsilon)$ and $I_2(x,t;\epsilon)$. Hence, in regions I, VI and V, only the endpoints of the four integrals contribute to the asymptotics. In regions II and IV, there are also contributions from the saddle points, and region III is the only region where the pole also contributes.

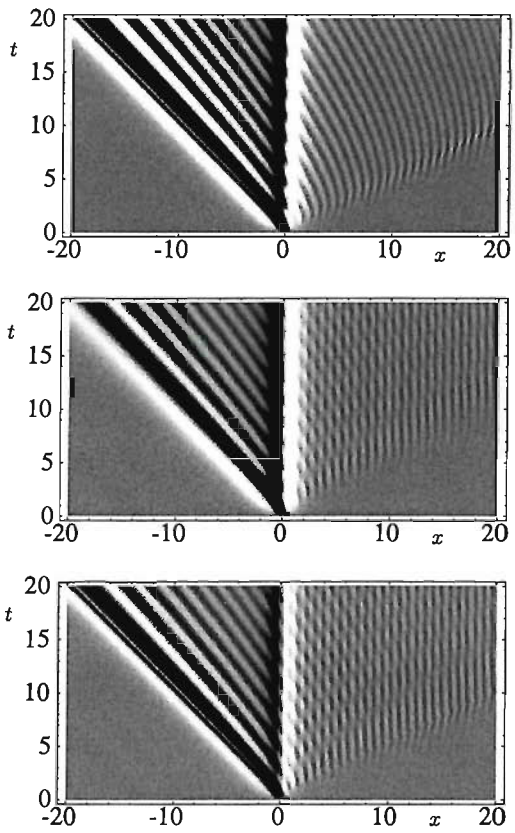

Figure 3.10: The middle plot is the solution of the PDE (3.3) minus $\arctan x$ with $\epsilon = 0.125$. The bottom plot is the result of taking leading-order behaviours of all asymptotic contributions in each region of Figure 3.9, and the top plot at the top is the same, except that the contributions from the sub-subdominant poles is omitted.

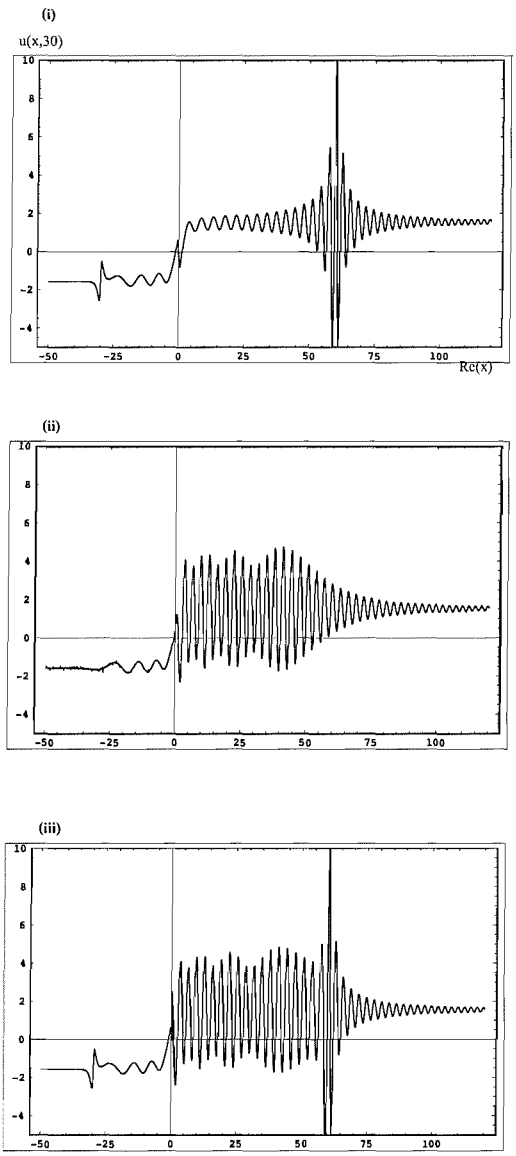

Figure 3.11: Plot (ii) shows the exact solution of equation (3.22), for $t = 30$, $\epsilon = 0.5$. The other two plots are the results of taking the leading order asymptotic contributions from each region (see Figure 3.9; plot (i), however, does not include the sub-subdominant pole contribution. It is clear that this term must be included for an accurate result. The visible 'bumps' at $x \approx -30$ and $x \approx 60$ are caused by the nearby caustics in the complex x-plane.

Figure 3.10 (see also Figure 3.11) shows a comparison of a numerical evaluation of the sum of the four integrals in (3.37) in the real (x,t)-plane against the leading order behaviours of the asymptotics within each Stokes region for $\epsilon = 0.125$. The plot in the middle of Figure 3.10 is the sum of the four integrals. The brightness indicates the height. The plot at the bottom of Figure 3.10 is the result of taking just the leading order behaviours of all asymptotic contributions in each region, as detailed in Figure 3.9. The agreement of all three is obvious in regions IV, V and VI when $x < 0$. The asymptotic approximation arising from the neglect of the sub-subdominant pole contribution (the top plot) is, however, at odds with the exact result in region III. The exact wave structure is dominated at larger times in this region by the initially sub-subdominant pole contribution. A neglect of this would have resulted in a false conclusion being drawn as to the large time behaviour. Finally, only in the neighbourhoods of the active Stokes curves do we observe that the sum of the leading order behaviours changes discontinuously.

The example presented in this section has also been studied by Chapman and Mortimer [52]; they have based an alternative approach on the work of Olde Daalhuis et al. [14].

3.4 Summary and Conclusions

In this chapter we have shown how the application of existing hyperasymptotic techniques to a PDE system reveals the higher order Stokes phenomenon. It is fair to say that it was previously known that this extra piece of information was necessary to explain the asymptotic behaviour behind some systems, but here we have presented for the first time a full explanation and reasoning for this phenomenon. Above all, we have highlighted that small exponential terms, however unimportant they may seem at first glance, should not be disregarded from an asymptotic approximation. As we have seen, they can sometimes grow to dominate the solution at a later time, and although numerically they may have a small

effect on things, they are critical to the understanding of the behaviour behind the results.

Importantly, the higher order Stokes phenomenon is not restricted to PDEs. Its generality was demonstrated by Olde Daalhuis [50], who discussed the higher order Stokes phenomena attached to a particular integral of an inhomogeneous ordinary differential equation with a large parameter.

This chapter has highlighted two interesting factors of the higher order Stokes phenomenon. The higher order Stokes phenomenon is, in fact, *just as likely* to occur as a regular Stokes phenomenon. Also, a higher order Stokes line remains invariant under changes in the small asymptotic parameter. These results stem from the fact that for a higher order Stokes phenomenon to occur, we require only that

$$\frac{F_{ij}}{F_{jk}} > 0 \tag{3.53}$$

for singularities i, j, k. Inherent in this definition is the collinearity of the 3 points, which at first may mislead us into thinking there is an extra constraint over a regular Stokes phenomenon. This is not true, since any two points lie on a straight line. The definition of a higher order Stokes phenomenon also appears independently of the asymptotic parameter, so although Stokes lines may change with a change in this parameter, a higher order line does not.

The work in this chapter appeared in print in 2004 [49].

Chapter 4

The Role of the Higher Order Stokes Phenomenon in Shock Wave Formation

4.1 Burgers' Equation

Having rigourously examined the nature of the higher order Stokes phenomenon and demonstrated its effects on a PDE system, we will now make the logical step forward of studying the effects of the higher order Stokes phenomenon on a nonlinear PDE.

In particular we will examine the role it plays in the development of smoothed shock waves via Burgers' equation [54]. Burgers' equation is well understood, and as such is a trivial example. However, the pedagogical nature of the problem will help us gain extra insight into the underlying structure of the higher order Stokes phenomenon.

Much previous work has been carried out on Burgers' equation, analysing the structure of the singularities in the problem; for example, see Senouf et al. [53]. However, the following work is approaching the problem from a new perspective.

Burgers' equation is

$$u_t + uu_x = \epsilon u_{xx}, \tag{4.1}$$
$$-\infty < x < +\infty,\ t > 0,\ 0 < \epsilon \ll 1,$$
$$u(x,0) = u_0(x).$$

It is possible to make a change of variables to transform Burgers' equation into the form of the diffusion equation, from which a solution to (4.1) can be found via a Green function [55]. Let

$$u(x,t) = v_0(s,\tau) + v_1(s,\tau) + v_2(s,\tau), \tag{4.2}$$

such that $v_0 = O(1)$, $v_1 = O(e^{-f/\epsilon})$ and $v_2 = O(e^{-2f/\epsilon})$. By substituting this back into Burgers' equation and balancing the terms at exponential orders, we find that in general

$$\partial_t v_n - \epsilon \partial_{ss} v_n = F(v_0, v_1, \ldots, v_{n-1}). \tag{4.3}$$

There is a formal solution in terms of a Green function

$$v(s,\tau;\epsilon) = \int_{-\infty}^{t}\int_{-\infty}^{\infty} G(s,\tau;X,T)F(X,T)dXdT, \tag{4.4}$$

and it can be shown that

$$G(s,\tau;X,T,\epsilon) = \frac{H(\tau - T)}{2\epsilon\sqrt{\pi(\tau - T)}} \exp\left(-\frac{(s-X)^2}{4\epsilon(\tau - T)}\right). \tag{4.5}$$

We can also solve Burgers' equation in the following way. Via the Cole-Hopf transformation ([56], [57], [58])

$$u = -2\epsilon\frac{\partial}{\partial x}\log(\phi(x,t)) \tag{4.6}$$

we can rewrite equation (4.1) as

$$\phi_t = \epsilon\phi_{xx}. \tag{4.7}$$

The initial condition

$$u(x,0) = u_0(x) \tag{4.8}$$

leads to

$$\phi(x,0) = \phi_0 = \exp\left(\frac{-1}{2\epsilon}\right)\int_0^x u_0(s)ds. \tag{4.9}$$

The solution to (4.7) is

$$\phi(x,t) = \frac{1}{\sqrt{4\pi\epsilon t}}\int_{-\infty}^{\infty}\phi_0(X)\exp\left(-\frac{(x-X)^2}{4\epsilon t}\right)dX \tag{4.10}$$

which can be derived using Fourier transforms. If we now write

$$\phi(x,t) = \frac{1}{\sqrt{4\pi\epsilon t}}\int_{-\infty}^{\infty}\exp(-f(x,X,t)/2\epsilon)dx \tag{4.11}$$

where

$$f(x,X,t) = \frac{(x-X)^2}{2t} + \int_0^X u_0(s)ds \tag{4.12}$$

then the general solution of Burgers' equation has the form

$$u(x,t) = \frac{\int_{-\infty}^{\infty}(\frac{x-X}{t})\exp\{-f(x,X,t)/2\epsilon\}dX}{\int_{-\infty}^{\infty}\exp\{-f(x,X,t)/2\epsilon\}dX}. \tag{4.13}$$

Let us split each of these integrals and write the solution as

$$u(x,t) = \frac{\int_0^{\infty}(\frac{x+X}{t})\exp\{-f(x,-X,t)/2\epsilon\}dX + \int_0^{\infty}(\frac{x-X}{t})\exp\{-f(x,X,t)/2\epsilon\}dX}{\int_0^{\infty}\exp\{-f(x,-X,t)/2\epsilon\}dX + \int_0^{\infty}\exp\{-f(x,X,t)/2\epsilon\}dX}. \tag{4.14}$$

Note the form of this solution suggests that we will have an array of Borel plane singularities (see Section 2.3.1).

4.2 Analysis of Stokes lines and Caustics

4.2.1 Steepest descent analysis

From the solution to Burgers' equation (4.13) via the Cole-Hopf transformation, we note that the saddles of the integral occur where $f_X = 0$, which means

$$x = X + u(X,0)t \tag{4.15}$$

at a saddle (cf. equation (4.12)). Note that this is also the equation of the characteristic rays. The rays of the equation passing through the point (x,t) originate at $(X,0)$. Imposing the initial condition

$$u(x,0) = \frac{1}{1+x^2} \tag{4.16}$$

means that

$$f(x,X,t) = \frac{(x-X)^2}{2t} + \int_0^X dx \frac{1}{1+x^2} \tag{4.17}$$

and

$$x = X + \frac{t}{1+X^2}, \tag{4.18}$$

that is, there are three saddles for the problem (corresponding to the 3 solutions of (4.18) for X). The saddle heights are given by

$$f_p \equiv f(x,X_p,t), \quad p = 1,2,3. \tag{4.19}$$

Figures (4.1) and (4.2) show the caustics of this integral, at which two saddle points coalesce ($f_X = f_{XX} = 0$) and the asymptotics blows up. These lines are given by the equation

$$t = \frac{2}{27}\left(x(x^2+9) \pm (x^2-3)^{3/2}\right). \tag{4.20}$$

There are two real and two complex caustics in the (x,t)-plane under consideration. We will be concerned only with the real caustics. The area 'between' these caustics in the real (x,t)-plane is where the classical smoothed shock of Burgers' equation forms.

If we take a section of Figure (4.2), constant in t, then the caustics reduce to a pair of turning points. We are interested in what happens as we cross the caustic in the (x,t)-plane and in looking at the Stokes phenomena that occur in the neighbourhood of these points. We choose the point $x_c = 5$, $t_c = \frac{2}{27}(170 - 22\sqrt{22})$ and walk around this point in the complex x-plane. Since we are on a caustic, the usual asymptotic techniques break down here, so we expand the positions of

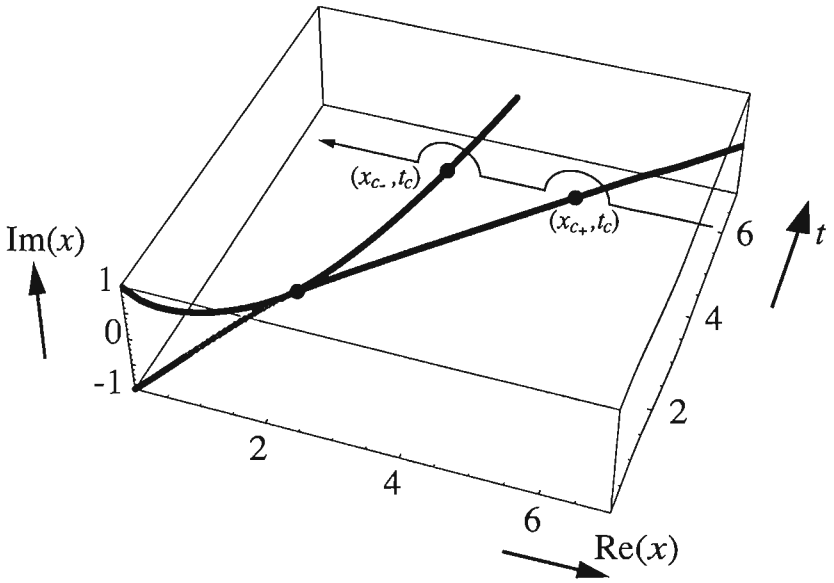

Figure 4.1: Caustics in complex-x space for real t and a path of analytic continuation around them.

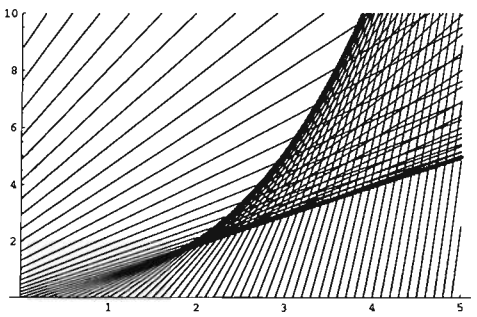

Figure 4.2: The caustics of Burgers' equation with $u(x,0) = \frac{1}{1+x^2}$ can be seen at the tangency of the rays.

the saddles and the saddle heights in a Taylor series about the point x_c on this t-section. We find that the saddles are located at

$$X_1 = \alpha + \beta(x-5) + O\left((x-5)^{3/2}\right), \tag{4.21}$$

$$X_2 = \bar{\alpha} + \gamma(x-5)^{1/2} + \bar{\beta}(x-5) + O\left((x-5)^{3/2}\right), \tag{4.22}$$

$$X_3 = \bar{\alpha} - \gamma(x-5)^{1/2} + \bar{\beta}(x-5) + O\left((x-5)^{3/2}\right), \tag{4.23}$$

where

$$\alpha = \frac{1}{3}(5+2\sqrt{22}), \tag{4.24}$$

$$\bar{\alpha} = \frac{1}{3}(5-\sqrt{22}), \tag{4.25}$$

$$\beta = \frac{1}{99}(61+10\sqrt{22}), \tag{4.26}$$

$$\bar{\beta} = \frac{1}{99}(19-5\sqrt{22}), \tag{4.27}$$

$$\gamma = \frac{i}{99}\sqrt{28\sqrt{\frac{2}{11}}-10}. \tag{4.28}$$

As usual we define the difference in saddle heights to be

$$F_{nm}(x,t) = f_m(x,t) - f_n(x,t). \tag{4.29}$$

We find that in the vicinity of the turning point it is only saddles X_2 and X_3 which are coalescing, since there is no vanishing of F_{31} or F_{21} at this point.

Having done this we can calculate the position of the potential Stokes lines, defined by

$$S_{i>j} = \{x \in C, t \in R : f_j(x,t) - f_i(x,t) > 0\}, \tag{4.30}$$

via steepest descent plots. These are shown in Figure 4.3.

The presence of the $\arctan X$ in f means that there are logarithmic branch points at $x = \pm i$, so there are an infinite number of Borel plane singularities arising from the three basic saddle points. The calculations to find the Stokes lines use only the saddles on the principal Riemann sheet.

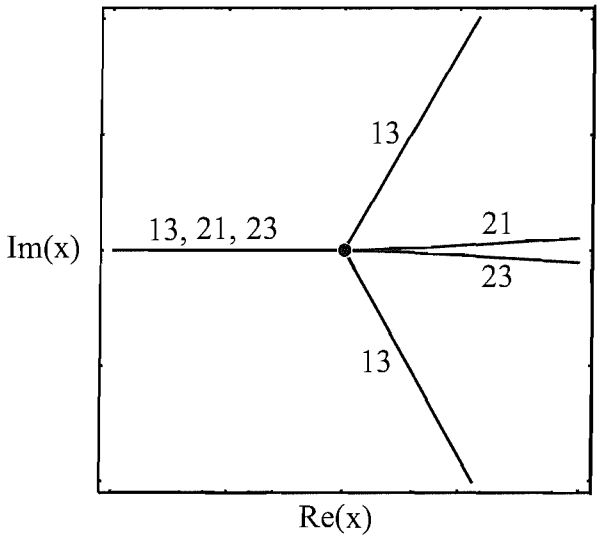

Figure 4.3: The combined Stokes lines for Burgers' equation, with $x = 5$, $t = \frac{2}{27}(170 - 22\sqrt{22})$. The notation 13, for example, represents the Stokes line where saddle 3 is switched on by saddle 1. The line running along the negative x-direction x_c is a possible Stokes line between 13, 21 and 23.

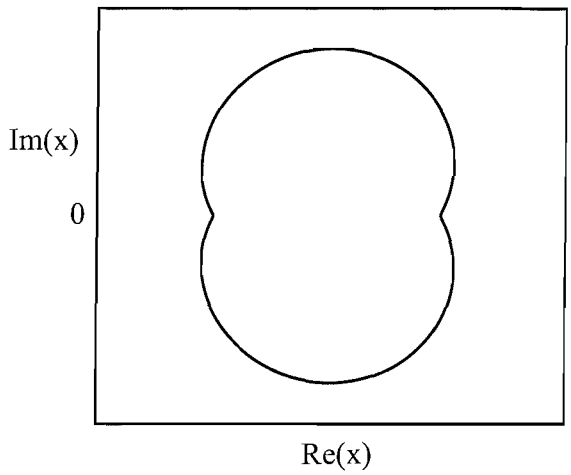

Figure 4.4: The signature bean-shaped higher order Stokes curve in the complex-x plane ($t = \frac{2}{27}(170 - 22\sqrt{22})$).

The higher order Stokes line is where the principal sheet values of f_1, f_2, f_3 are collinear in the Borel plane. The line is defined by

$$S_{ijk} = \left\{ x \in C, t \in R : \frac{f_j(x,t) - f_k(x,t)}{f_k(x,t) - f_i(x,t)} \in R \right\}, \tag{4.31}$$

for $i \neq j \neq k$. The resulting plot is shown in Figure 4.4. In order to determine the adjacency of the saddles, we plot the steepest descent contours in the complex x-plane. We walk around the turning point from $\arg x = \theta = 0$ to $\theta = \pi$. An example of a contour plot and the steepest descent lines through the saddles is shown in Figure 4.6, which represents the $\theta = \pi/18$ plot.

At first glance, this is a confusing and slightly ambiguous diagram. It can be interpreted in the following way. Since the steepest paths must run from $-\infty$ to $+\infty$, we begin in the valley at $-\infty$ and pass over saddle 2 before following around through the branch cut at $+i$. This means that we drop onto an adjacent Riemann sheet. The contour then sweeps back into the valley at $-\infty$, picking up half a contribution at saddle 2 on the way (due to the "dog-leg" encountered there [28]). In the valley, the contour connects with an another contour which

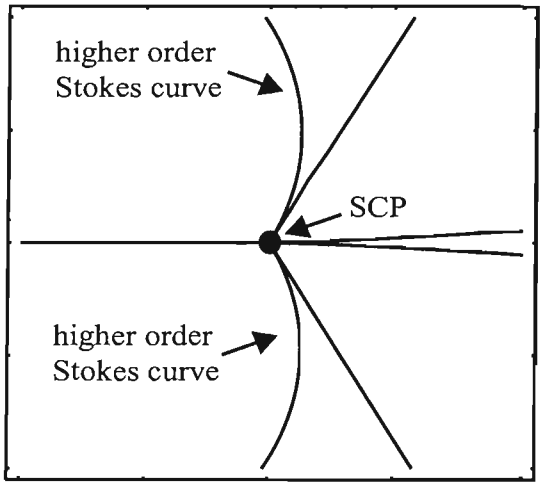

Figure 4.5: The Stokes lines in the complex-x plane with the higher order Stokes line superimposed around the SCP at x_c.

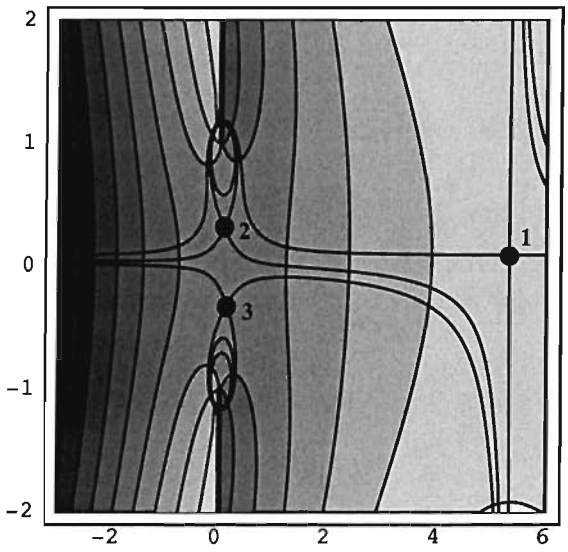

Figure 4.6: A steepest descent plot at $\theta = \pi/18$. The branch cuts at $\pm i$ are clearly shown.

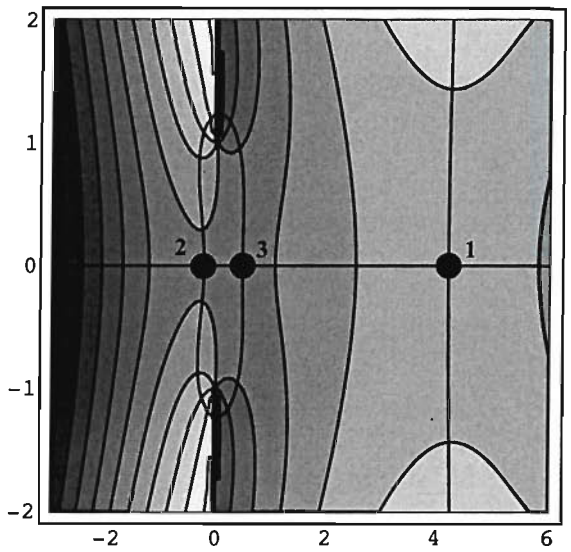

Figure 4.7: The contour plot at $\theta = \pi$, showing the apparent linking of all 3 saddles. However, there is no Stokes phenomenon taking place here. (Refer to the text for details.)

runs back through the cut (and thus back onto the principal sheet) where it passes through saddle 1 and then on to $+\infty$. Thus, only saddles 1 and 2 contribute to the asymptotics, but the branch cut means that we may have contributions from different Riemann sheets. This situation continues as we walk around the turning point, until we reach the $\theta = \pi$ position, when all 3 saddles link up.

Figure 4.7 shows this point. There appears to be a Stokes phenomenon occurring here between saddles 2 and 3, suggesting that the contour simply runs from $-\infty$ to $+\infty$ straight through each saddle. This is not the case; the way the plot must be interpreted is as follows. The contour from $-\infty$ runs straight through saddle 2, picking up a whole contribution, and then runs over saddle 3 turning through a right-angle (picking up a (directionally) negative 1/2-contribution) and across the branch cut onto an adjacent Riemann sheet. It then picks up a negative 1/2-contribution from saddle 2 before returning to the valley at $-\infty$. The contour then returns across the branch cut in the same way, picking up a positive

1/2-contribution from saddle 2. After crossing the branch cut and returning to the principal sheet, the contour picks up a final 1/2-contribution from saddle 3 before passing through 1 and on to $+\infty$. The net effect is that saddle 3 makes no contribution to the asymptotics here. Thus we see how Figure 4.7 is, in that sense, misleading.

The conclusion we can draw from the above analysis is that the Stokes line $S_{1>2}$ at $0 < \theta < \pi/18$ is an active Stokes line. At $\theta = \pi/3$ there is also an active Stokes line but the fact that saddle 3 is not involved in the asymptotics at this point makes it irrelevant. At $\theta = \pi$ we have crossed the higher order Stokes line, which has the effect of turning $S_{1>2}$ off so that at $\theta = \pi$ no Stokes phenomenon takes place (which would essentially remove 2), and again because 3 is not involved here, neither of the other possible Stokes lines is relevant at this point.

In this case, we have seen that the method of steepest descent is not necessarily the most efficient way of calculating the position of the Stokes lines, and the effect of the higher order Stokes line, due to the ambiguousness nature of some of the contour plots. For a clearer view of what is happening, let us look at the problem in the Borel plane.

4.2.2 Borel plane analysis

Since we are dealing with initial conditions that lead to 3 saddle points, Dingle [4] says that we can write the general solution (4.13) as

$$u(x,t) \sim \frac{e^{-f_0/\epsilon}T^{(0)} + e^{-f_1/\epsilon}T^{(1)} + e^{-f_2/\epsilon}T^{(2)}}{e^{-f_0/\epsilon}S^{(0)} + e^{-f_1/\epsilon}S^{(1)} + e^{-f_2/\epsilon}S^{(2)}}, \tag{4.32}$$

where

$$T^{(0)} = \sqrt{\frac{\pi}{2f''(0)}} \sum_{r=0}^{\infty} T_r^{(0)} \epsilon^r. \tag{4.33}$$

Thus

$$u(x,t) \sim \frac{T^{(0)}\left(1 + \left[e^{-(f_1-f_0)/\epsilon}T^{(1)} + e^{-(f_2-f_0)/\epsilon}T^{(2)}\right](T^{(0)})^{-1}\right)}{S^{(0)}\left(1 + \left[e^{-(f_1-f_0)/\epsilon}S^{(1)} + e^{-(f_2-f_0)/\epsilon}S^{(2)}\right](S^{(0)})^{-1}\right)}, \tag{4.34}$$

$$\sim \frac{T^{(0)}}{S^{(0)}}\left(1+\left[e^{-(f_1-f_0)/\epsilon}T^{(1)}+e^{-(f_2-f_0)/\epsilon}T^{(2)}\right](T^{(0)})^{-1}\right)$$
$$\times\left(1+\left[e^{-(f_1-f_0)/\epsilon}S^{(1)}+e^{-(f_2-f_0)/\epsilon}S^{(2)}\right](S^{(0)})^{-1}\right)^{-1}, \quad (4.35)$$

$$\sim \frac{T^{(0)}}{S^{(0)}}\left(1+\left[e^{-(f_1-f_0)/\epsilon}T^{(1)}+e^{-(f_2-f_0)/\epsilon}T^{(2)}\right](T^{(0)})^{-1}\right)$$
$$\times\sum_{r=0}^{\infty}\left(\frac{-1}{S^{(0)}}\right)^{r}\left(e^{-(f_1-f_0)/\epsilon}S^{(1)}+e^{-(f_2-f_0)/\epsilon}S^{(2)}\right)^{r}. \quad (4.36)$$

The different terms that can arise from the multiplicative expansion of (4.36) tell us where to expect the branch points in the Borel plane. Let us rename the exponents

$$f_1-f_0=f^{(1)}, \quad f_2-f_0=f^{(2)}, \quad (4.37)$$

and note that there is a third present, except that we now have $f^{(0)}=0$.

We now see that in general we should expect to find Borel branch points at:

$$0, \quad (n+1)f^{(1)}, \quad (n+1)f^{(2)}, \quad f^{(1)}+nf^{(2)}, \quad f^{(2)}+nf^{(1)}.$$

This means that we have an infinite array of singularities in the Borel plane; a figurative example is given in Figure 4.8.

Our chosen initial point is on the real x-axis, at $x=x_c+0.5$ (point 1). This point does not lie on a Stokes line. We walk around the semi-circle set out in Figure 4.9 in an anticlockwise direction; Figure 4.10 reveals the layout of the f's in the Borel plane at selected points. By the time we have reached point 2, we see that $f^{(2)}$ has risen through the branch cut emanating from 0, which tells us that a possible Stokes phenomena has occurred between 1 and 2. Topologically the Borel plane then remains the same until we reach point 3, which we know should lie on a Stokes line. Indeed, there is a potential for a Stokes phenomena to occur between $f^{(2)}$ and $f^{(1)}$, signified by the lining up of $f^{(2)}$ and $f^{(1)}$ in the Borel plane. At point 4 we are approaching the area where we expect the higher order Stokes line to be. If we compare what is happening between points 4 and 5, we see that at some stage all three singularities will have been perfectly aligned (albeit

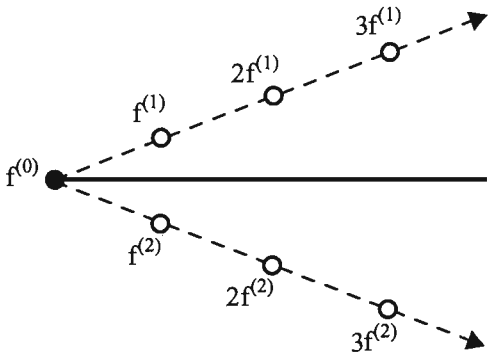

Figure 4.8: A figurative example of an array of Borel singularities, as seen from 0.

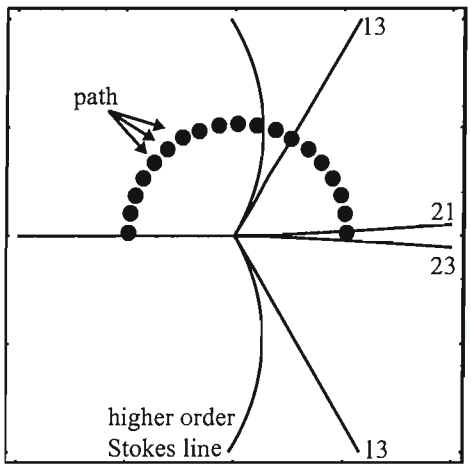

Figure 4.9: The path taken around the point x_c in the complex plane. We walk anti-clockwise from $\theta = 0$, which is the point on the real x-axis to the right of x_c.

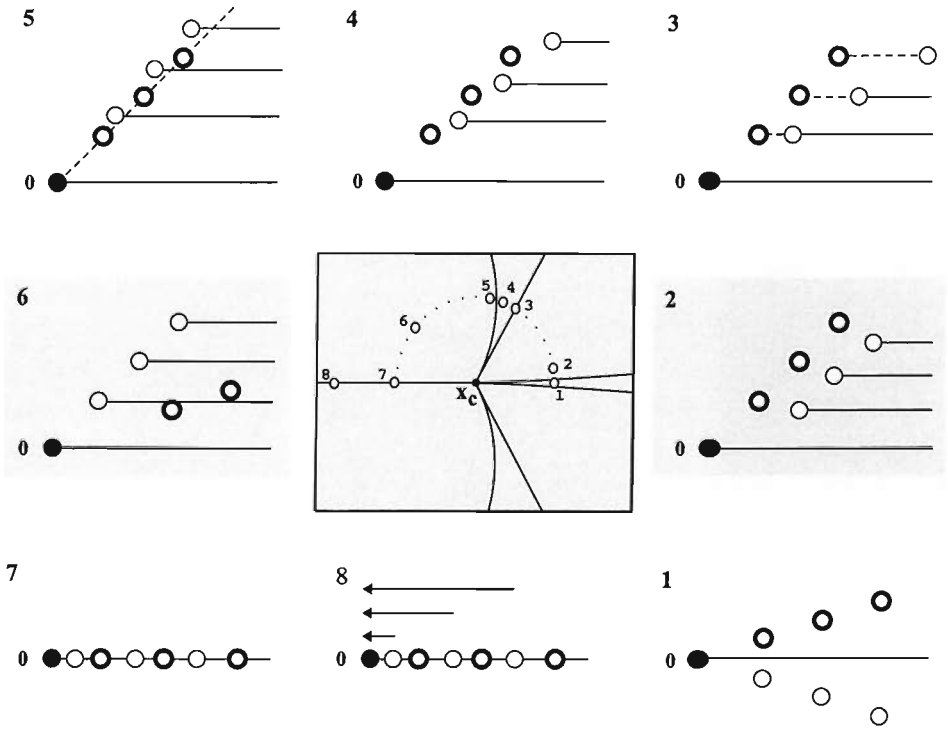

Figure 4.10: The central picture shows the complex x-plane for constant $t = \frac{2}{27}(170 - 22\sqrt{22}$, illustrating the Stokes lines, higher order Stokes lines and the chosen path around them. For each of the highlighted points 1–8, an accompanying diagram of the Borel plane is shown, each as viewed from the singularity $f^{(0)}$=0. The thick-rimmed circles are the $f^{(1)}$. Refer to the main text for an explanation of each diagram.

diagonally), confirming that a higher order Stokes phenomenon has occurred. As viewed from singularity 0, across a higher order Stokes line the singularity $f^{(2)}$ moves across a cut emanating from $f^{(1)}$ and onto a different Riemann sheet from 0.

Of course, this case is different to that in the previous chapters. Rather than having a finite number of collinear singularities, we are now dealing with an infinite set and hence an infinite number of Riemann sheets. (Similarly, across the higher order Stokes line, when viewed from $nf^{(2)}$, the singularity at $(n+1)f^{(2)}$ will move across at cut emanating from $nf^{(2)} + f^{(1)}$ and onto a different sheet from $nf^{(2)}$.) This means that it is possible for all of the singularities $f^{(2)}$, $2f^{(2)}$, $3f^{(2)}\ldots$ to be directly invisible from 0, and also that $nf^{(2)}$ cannot see $(n+1)f^{(2)}$ either.

At point 6, the singularities are no longer collinear with one another, although the $(n+1)f^{(2)}$ remain collinear with 0, even though they are are different Riemann sheets. At point 7 the singularities are again all collinear. There is the potential for a Stokes phenomenon between 0 and the $(n+1)f^{(2)}$, or between 0 and the $(n+1)f^{(1)}$. However, the $(n+1)f^{(2)}$ are now on different Riemann sheets to 0 and so cannot cross the Borel integration contour on the principal Riemann sheet, hence the Stokes line between the two singularities is inactive. There is no Stokes phenomenon between 0 and the $(n+1)f^{(1)}$ at this point either since, as we saw above, $f^{(1)}$ does not contribute to the asymptotics here. (The potential exists for a Stokes phenomenon between $f^{(2)}$ and $f^{(1)}$, or even 0 and $f^{(2)}$, but we will not concern ourselves with this here.)

On the real x-axis (where $\theta = \pi$), the conditions for a higher order Stokes line are seemingly also fulfilled: the three singularities are collinear (see plot 7 of Figure 4.10). This is a necessary but perhaps not sufficient condition for a higher order Stokes phenomenon to be taking place; the calculations above did not initially produce a higher order Stokes line at this position. Closer investigation is needed here. There is also a branch cut present in the calculations, extending from the turning point (thus far neglected from the plots of the higher order Stokes line).

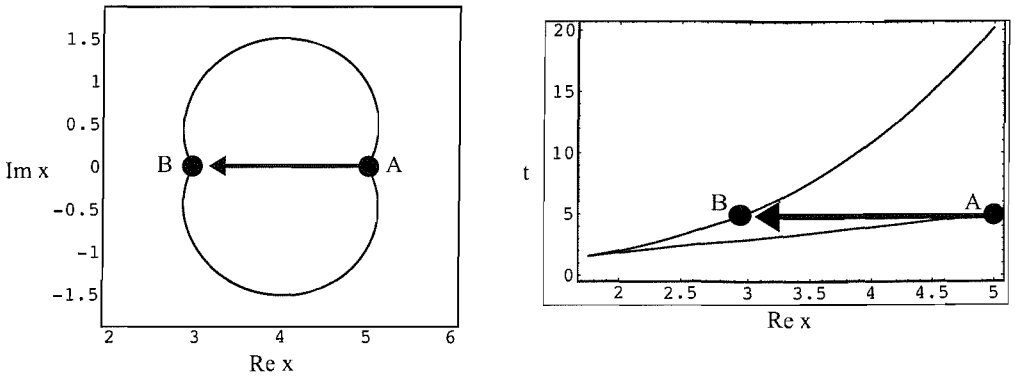

Figure 4.11: The paths indicated on the above diagrams from A to B are equivalent.

These two together mean that things are a little complicated for $\theta > \pi$, as we enter the lower half plane.

The steepest descent contour plots show that there is a smooth transition across the x-axis at $\theta = \pi$, but the singularities $f^{(2)}$ and $f^{(1)}$ instantaneously switch position, while at the same time, the adjacency of the saddles is switched as well (saddle X_3 is now adjacent to X_1, not X_2). In order for the story to make sense, the interpretation is that the branch cut accounts for the swapping of the saddle positions, whilst a higher order Stokes phenomenon accounts for the swapping of adjacency at this point. We find that if this is the case, the second Stokes line at $-\pi/18 < \theta < 0$ is active, switching saddle X_2 off and leaving saddle X_1 as the only contributing saddle. Thus the circle around the turning point is complete.

We will now show how the higher order Stokes phenomenon is crucial to the formation of smoothed shock waves in this problem. Let us move along the line $S_{0>1}$ in the negative x-direction (as indicated in Figure 4.11), which corresponds to walking away from point 7 in the direction of point 8 in Figure 4.10. At the point A in Figure 4.11, we are sat on a caustic where saddles X_2 and X_3 have

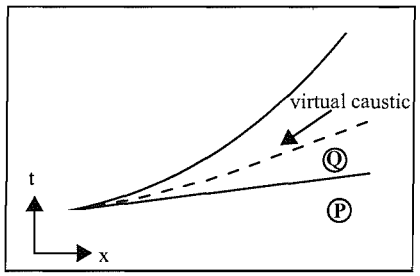

Figure 4.12: When is a caustic not a caustic? This diagram indicates the regions P and Q, and the approximate position of the virtual caustic. The form of $u(x,t)$ changes from P to Q (see equations (4.39) and (4.42) respectively).

coalesced, which of course means that $f^{(1)}$ and $f^{(2)}$ coalesce in the Borel plane. At the point B, the same saddles again coalesce.

An analysis of the Borel plane along the line between A and B reveals the following. We find that all of the $(n+1)f^{(2)}$ rush towards 0 and appear to coalesce at $x \approx 3.65$. We are tempted, therefore, to announce the presence of a third caustic. However, this is only an apparent coalescence, and in fact we have uncovered a 'virtual caustic' (Figure 4.12). The lack of a third caustic can be explained by the above analysis of the Riemann sheet structure. It must be the case that 0 and the $(n+1)f^{(2)}$ lie on mutually different Riemann sheets, and do not actually coalesce. Thus we only have a virtual turning point. Contour plots confirm that there is no saddle coalescence at this point. Classically, this is position of the smoothed shock, where the solution changes rapidly from one point to the next. The higher order Stokes phenomenon is the reason why the singularities lie on different Riemann sheets, and without it we would find that the shock would in fact be a caustic.

We now analyse the Cole-Hopf solution (4.13) in the region of the caustic.

Since we have

$$u = \frac{T^{(0)} + e^{-f^{(1)}/\epsilon}T^{(1)} + e^{-f^{(2)}/\epsilon}T^{(2)}}{S^{(0)} + e^{-f^{(1)}/\epsilon}S^{(1)} + e^{-f^{(2)}/\epsilon}S^{(2)}} \tag{4.38}$$

then it is clear that in region P of Figure 4.12, the leading order solution is just

$$u(x,t) = \frac{T^{(0)}}{S^{(0)}} + O(\epsilon) \tag{4.39}$$

since $e^{-f^{(1)}/\epsilon}T^{(1)} + e^{-f^{(2)}/\epsilon}T^{(2)}$ is exponentially small. Inside the caustics (region Q in Figure 4.12) we know from the Borel plane analysis that we are in a region where $f^{(1)}$ can approach 0. Hence, $e^{-f^{(2)}/\epsilon}T^{(2)}$ can approach $O(1)$ and interfere with other $O(1)$ terms. Terms in $e^{-f^{(1)}/\epsilon}T^{(1)}$ remain exponentially small. Thus, in region Q,

$$\begin{aligned} u(x,t) &= \frac{T^{(0)} + e^{-f^{(2)}/\epsilon}T^{(2)}}{S^{(0)} + e^{-f^{(2)}/\epsilon}S^{(2)}} + O(\epsilon) && (4.40)\\ &= \frac{T^{(0)}}{S^{(0)}}\left(1 - e^{-f^{(2)}/\epsilon}\frac{S^{(2)}}{S^{(1)}}\right) + O(\epsilon) && (4.41)\\ &= \frac{T^{(0)}}{S^{(0)}} + \left(\frac{S^{(0)2}T^{(2)} - S^{(0)}S^{(2)}T^{(0)}}{S^{(0)2}(S^{(0)} + e^{-f^{(2)}/\epsilon}T^{(2)})}\right)e^{-f^{(2)}/\epsilon} + O(\epsilon). && (4.42) \end{aligned}$$

Note that the form of $u(x,t)$ in region Q takes the form that was discussed in Section 2.3.1.

Let us return to the Cole-Hopf solution (4.13), and consider the leading order two saddle problem

$$u(x,t) = \frac{e^{-f^{(0)}/\epsilon}T^{(0)} + e^{-f^{(1)}/\epsilon}T^{(1)}}{e^{-f^{(0)}/\epsilon}S^{(0)} + e^{-f^{(1)}/\epsilon}S^{(1)}} \tag{4.43}$$

where

$$T^{(j)} = \sqrt{\frac{\pi}{2f''^{(j)}}}\sum_{r=0}^{\infty} T_r^{(j)}\epsilon^r, \tag{4.44}$$

$$S^{(j)} = \sqrt{\frac{\pi}{2f''^{(j)}}}\sum_{r=0}^{\infty} S_r^{(j)}\epsilon^r, \tag{4.45}$$

where $j = 0, 1$. From (4.13) we know that

$$q_0^{(0)} = \frac{x - X_0}{t}, \tag{4.46}$$

but at a saddle we have

$$x = X_j + a_j(X_j)t \tag{4.47}$$

(with the convention that $a_j(x,t) = a_j(x)$), thus at saddle 0 we can write

$$T_0^{(0)} = a_0(X_0), \tag{4.48}$$

and also

$$T_0^{(1)} = a_0(X_1). \tag{4.49}$$

It is also clear that

$$S_0^{(1)} = S_0^{(0)} = 1. \tag{4.50}$$

Thus the leading order solution is

$$u(x,t) \sim \frac{\sqrt{\frac{\pi}{2f''(0)}}e^{-f^{(0)}/\epsilon}T_0^{(0)} + \sqrt{\frac{\pi}{2f''(1)}}e^{-f^{(1)}/\epsilon}T_0^{(1)}}{\sqrt{\frac{\pi}{2f''(0)}}e^{-f^{(0)}/\epsilon}S_0^{(0)} + \sqrt{\frac{\pi}{2f''(1)}}e^{-f^{(1)}/\epsilon}S_0^{(1)}} \tag{4.51}$$

$$\sim \frac{\sqrt{\frac{\pi}{2f''(0)}}e^{-f^{(0)}/\epsilon}T_0^{(0)}\left[1 + \sqrt{\frac{f''(0)}{f''(1)}}\frac{T_0^{(1)}}{T_0^{(0)}}e^{-[f^{(1)}-f^{(0)}]/\epsilon}\right]}{\sqrt{\frac{\pi}{2f''(0)}}e^{-f^{(0)}/\epsilon}S_0^{(0)}\left[1 + \sqrt{\frac{f''(0)}{f''(1)}}\frac{S_0^{(1)}}{S_0^{(0)}}e^{-[f^{(1)}-f^{(0)}]/\epsilon}\right]} \tag{4.52}$$

$$\sim \frac{T_0^{(0)}}{S_0^{(0)}}\left\{1 + \sqrt{\frac{f''(0)}{f''(1)}}\frac{T_0^{(1)}}{T_0^{(0)}}e^{-[f^{(1)}-f^{(0)}]}\right\}\sum_{r=0}^{\infty}\left(-\sqrt{\frac{f''(0)}{f''(1)}}\frac{S_0^{(1)}}{S_0^{(0)}}e^{-[f^{(1)}-f^{(0)}]}\right)^r \tag{4.53}$$

$$\sim \frac{T_0^{(0)}}{S_0^{(0)}}\left\{1 + \sqrt{\frac{f''(0)}{f''(1)}}\frac{T_0^{(1)}}{T_0^{(0)}}e^{-[f^{(1)}-f^{(0)}]/\epsilon}\right\} \times \left\{1 - \sqrt{\frac{f''(0)}{f''(1)}}\frac{S_0^{(1)}}{S_0^{(0)}}e^{-[f^{(1)}-f^{(0)}]/\epsilon} + O(e^{2-[f^{(1)}-f^{(0)}]/\epsilon})\right\} \tag{4.54}$$

$$\sim \frac{T_0^{(0)}}{S_0^{(0)}}\left\{1 + \sqrt{\frac{f''(0)}{f''(1)}}e^{-[f^{(1)}-f^{(0)}]/\epsilon}\left(\frac{T_0^{(1)}}{T_0^{(0)}} - \frac{S_0^{(1)}}{S_0^{(0)}}\right)\right\} + O(e^{2-[f^{(1)}-f^{(0)}]/\epsilon}) \tag{4.55}$$

$$\approx a_0\left\{1 + \sqrt{\frac{f''(0)}{f''(1)}}\left(\frac{a_0(X_1)}{a_0(X_0)} - 1\right)\right\} + O(e^{2-[f^{(1)}-f^{(0)}]/\epsilon}) \tag{4.56}$$

We can simplify this expression since we have

$$x = X_0 + a_0(X_0)t, \tag{4.57}$$

$$x = X_1 + a_0(X_1)t, \tag{4.58}$$

$$\Rightarrow \quad t = \frac{X_1 - X_0}{a_0(X_0) - a_0(X_1)}. \tag{4.59}$$

With a little simple algebraic simplification, the result is

$$\begin{aligned} u(x,t) \quad &\sim a_0(X_0) + e^{-[f^{(1)} - f^{(0)}]/\epsilon}\,(a_0(X_1) - a_0(X_0)) \\ &\times \left\{ \sqrt{\frac{a_0(X_0) - a_0(X_1) + a_0'(X_0)(X_1 - X_0)}{a_0(X_0) - a_0(X_1) + a_0'(X_1)(X_1 - X_0)}} \right\}. \end{aligned} \tag{4.60}$$

If we repeat the above calculation for the full solution case, then (4.55) becomes

$$u(x,t) \sim \frac{\sum_r T_r^{(0)}\epsilon^r}{\sum_r S_r^{(0)}\epsilon^r} \left\{ 1 + \sqrt{\frac{f''(0)}{f''(1)}} e^{-[f^{(1)} - f^{(0)}]/\epsilon} \left(\frac{\sum_r T_r^{(1)}\epsilon^r}{\sum_r T_r^{(0)}\epsilon^r} - \frac{\sum_r S_r^{(1)}\epsilon^r}{\sum_r S_r^{(0)}\epsilon^r} \right) \right\} \tag{4.61}$$

Let

$$\frac{\sum_r T_r^{(0)}\epsilon^r}{\sum_r S_r^{(0)}\epsilon^r} = \sum_r a_r \epsilon^r, \tag{4.62}$$

then

$$\sum_r T_r^{(0)}\epsilon^r = \sum_r a_r \epsilon^r \sum_s S_s^{(0)}\epsilon^s, \tag{4.63}$$

$$\Rightarrow \quad \sum_n T_n^{(0)}\epsilon^n = \sum_{n=0}^{\infty} \sum_{s=0}^{n} a_{n-s} S_s^{(0)} \epsilon^n \qquad (n = r + s) \tag{4.64}$$

Since $S_0^{(0)} = 1$,

$$a_n = T_n^{(0)} - \sum_{s=1}^{n} a_{n-s} S_s^{(0)}. \tag{4.65}$$

So, we have

$$T_0^{(0)} = a_0 S_0^{(0)} = a_0(X_0), \tag{4.66}$$

$$T_0^{(1)} = a_0(X_1), \tag{4.67}$$

$$S_0^{(0)} = S_0^{(1)} = 1, \tag{4.68}$$

and thus

$$a_1 = T_1^{(0)} - a_0 S_1^{(0)}. \tag{4.69}$$

Let us define

$$T_r^{(0)} \sim \frac{1}{2\pi i} \frac{(r-1)!}{f_1^r} T_0^{(1)}, \tag{4.70}$$

where

$$f_1 = f^{(1)} - f^{(0)}. \tag{4.71}$$

Then

$$a_n = \frac{1}{2\pi i} \frac{(n-1)!}{f_1^n} T_0^{(1)} - \sum_{s=1}^{n} \frac{(s-1)! a_{n-s}}{2\pi i f_1^s} S_0^{(1)}, \tag{4.72}$$

$$\sim \frac{(n-1)!}{2\pi i f_1^n} T_0^{(1)} - \frac{a_0 (n-1)!}{2\pi i f_1^n} S_0^{(1)} - \frac{a_1 (n-2)!}{2\pi i f_1^{n-1}} S_0^{(1)} + \ldots \tag{4.73}$$

So

$$a_n \sim \frac{(n-1)!}{2\pi i f_1^n} \left\{ T_0^{(1)} - a_0 S_0^{(1)} - \ldots \right\}, \tag{4.74}$$

$$\sim \frac{(n-1)!}{2\pi i f_1^n} \left\{ a_0(X_1) - a_0(X_0) \right\}, \tag{4.75}$$

and as $X_1 \to X_0$ (ie., near a caustic) then

$$a_n \sim \frac{(n-1)!}{2\pi i f_1^n} a_0'(X_1)(X_1 - X_0). \tag{4.76}$$

We will not often have the luxury of an integral solution to a problem, which helps us considerably on our way to finding the higher order Stokes behaviour, be it through steepest descent methods or Borel plane methods. We have highlighted how steepest descent approaches to complicated problems may not always provide clear solutions. With this in mind we will now summarize an approach to the above problem by Howls and Olde Daalhuis (henceforth referred to as HD)([62], see also [63]), who arrived at the same results without an integral solution to Burgers' equation. We will present the outlines and important points of their work. More details and calculations are given in their paper. The extra complications introduced into the Borel analysis by nonlinearities are also discussed elsewhere; for example, see [20].

The problem is the same as equation (4.1) above, with initial condition (4.16). Since the assumption is that there is no integral solution available, HD approach the problem from an exponential asymptotics point of view, and seek a formal solution of the form

$$u(x,t;\epsilon) \sim u^{(0)}(x,t;\epsilon) + \sum_{n=1}^{\infty} C_1^n u^{(n,1)}(x,t;\epsilon) + \sum_{n=1}^{\infty} C_2^n u^{(n,2)}(x,t;\epsilon) \tag{4.77}$$

where

$$u^{(0)}(x,t;\epsilon) \sim \sum_{r=0}^{\infty} a_r(x,t)\epsilon^r, \tag{4.78}$$

$$u^{(n,j)}(x,t;\epsilon) \sim e^{-nf_j(x,t)/\epsilon} \sum_{r=0}^{\infty} a_r^{(n,j)}(x,t)\epsilon^r, \tag{4.79}$$

$$j = 1,2 \quad n = 1,2,3,\ldots.$$

By substitution into (4.1), it can be seen that $a_0(x,t)$ satisfies the inviscid Burgers' equation

$$\frac{\partial a_r}{\partial t} + a_0 \frac{\partial a_0}{\partial x} = 0, \qquad a_0(x,0) = \frac{1}{1+x^2}, \tag{4.80}$$

and for $r \geq 1$ the $a_r(x,t)$ satisfy

$$\frac{\partial a_r}{\partial t} + \sum_{s=0}^{r} a_{r-s} \frac{\partial a_s}{\partial x} = \frac{\partial^2 a_{r-1}}{\partial x^2}, \qquad a_r(x,0) = 0. \tag{4.81}$$

Similarly, balancing at $O(e^{-nf/\epsilon})$ leads to finding that the exponential functions $f_j(x,t)$ satisfy the first order nonlinear equation

$$f_t + a_0 f_x + f_x^2 = 0. \tag{4.82}$$

The boundary data for these functions can be found by consideration of the rays of (4.80). There are 3 rays through each point (x,t). These are the lines

$$x = x_j + a_0(x_j)t, \qquad j = 0,1,2 \tag{4.83}$$

where here and henceforth, $a_0(x_j,0)$ is abbreviated to $a_0(x_j)$, and the x_j are the intersection points of these rays with the complex plane $t = 0$. (They are also the

locations of the saddle points of the Cole-Hopf solution.) On these rays the a_0 take the constant values

$$a_0(x_j) = \frac{1}{1+x_j^2}, \qquad j = 0, 1, 2. \tag{4.84}$$

The root x_0 is chosen to be the one that is real for all real (x, t). The families of rays generated by the x_j are tangential at the caustics which simultaneously satisfy (4.83) and

$$0 = 1 + \frac{da_0(x_j)}{dx_j} t, \qquad j = 0, 1, 2. \tag{4.85}$$

The caustics are as before (equation (4.20)).

On the complex caustic with $\mathrm{Im}(x) > 0$ (see Figure 4.1), roots x_0 and x_1 coalesce and so the caustic is called C_{01}. On the complex caustics with $\mathrm{Im}(x) < 0$, x_0 and x_2 coalesce and is labelled C_{02}. On the real caustics C_R, x_1 and x_2 coalesce.

The exponents $f_j(x, t)$ must vanish on the complex caustics, since here they coalesce with the exponents of the leading order solution, ie., $f_0(x, t) \equiv 0$, so that the exponential correction terms there are of the same order as the first series in (4.77). Thus the boundary data for the solutions of (4.82) are

$$f_j(x, t) = 0 \quad \text{on} \quad C_{0j}, \quad j = 1, 2 \tag{4.86}$$

and

$$f_1(x, t) = f_2(x, t) \quad \text{on} \quad C_R. \tag{4.87}$$

(Note that $f_j = f^{(j)}$ from the previous section.) Direct analysis of the PDE reveals that

$$f_j(x(x_0, x_j), t(x_0, x_j)) = \frac{1}{2}\int_{x_0}^{x_j} a_0(z)dz - \frac{1}{4}(a_0(x_0) + a_0(x_j))(x_j - x_0), \quad j = 1, 2. \tag{4.88}$$

It can also be shown that

$$a_0^{(1,1)}(x_0, x_1) = (a_0(x_1) - a_0(x_0))\sqrt{\frac{a_0(x_1) - a_0(x_0) - a_0'(x_0)(x_1 - x_0)}{a_0(x_1) - a_0(x_0) - a_0'(x_1)(x_1 - x_0)}}, \tag{4.89}$$

(cf. equation (4.60)). This result holds for all values of x_0 and x_1.

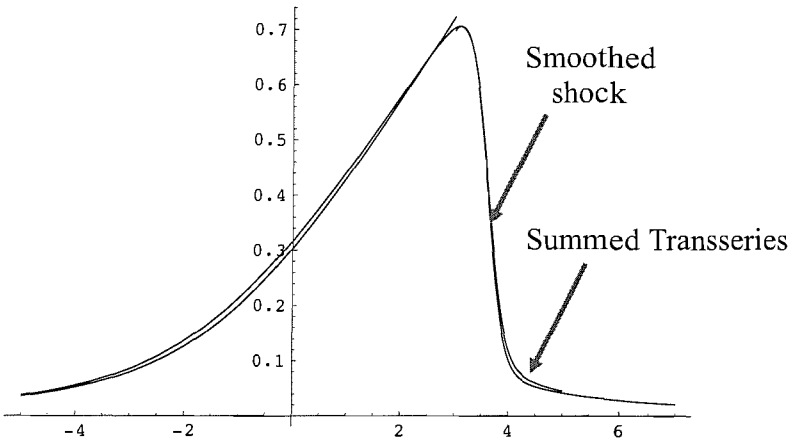

Figure 4.13: The wave produced by Burgers' equation for $t = 5$ and $\epsilon = 0.05$. The classical position of the smoothed shock is shown, as well as an indication of the position of the summed transseries.

HD now turn to the structure in the Borel plane. It is a complicated problem, but it will suffice to provide only an outline of the full picture here.

The location of the singularities visible from $\tau = f_0(x,t)$ are as indicated in Figure 4.10 in the previous section. From (4.77) it is possible to deduce that in the Borel plane (logarithmic) branch-points exist at $\tau = nf_j$, $j = 1,2$, $n = 1,2,3,\ldots$. A detailed analysis of the transseries or of the Cole-Hopf representation shows that the Borel transform of $u^{(1,1)}(x,t;\tau)$ must see a branch-point at $\tau = f_2(x,t)$. Likewise, the Borel transform of $u^{(1,2)}(x,t;\tau)$ must see a branch-point at $\tau = f_1(x,t)$. Note that for certain values of (x,t) these singularities may appear to coalesce in the Borel plane. However only when the singularities lie on the same Riemann sheet can this give rise to actual caustics and divergences in the asymptotic representations.

Now HD consider the analytic continuation of the transseries expansion in the real plane from regions outside the C_R to inside. The chosen point is x_c as above.

The path taken in the complex x-plane is as shown in Figure 4.9. This path

avoids any singular behaviour in the exponentially small transseries $u^{(n,1)}$ and $u^{(n,2)}$. (Note that $u^{(0)}$ is actually regular at C_R.)

The analysis of the Borel plane is essentially as above, and we will refer to the central diagram of Figure 4.10. At the point 1, to satisfy the decay of u as $|x| \to \infty$, comparison of the full template for the asymptotic expansion reveals that $C_1 = C_2 = 0$. Hence

$$u(1,t;\epsilon) \sim u^{(0)}(1,t;\epsilon) \tag{4.90}$$

is the complete asymptotic expansion at that point.

The Stokes lines are revealed in the same places as in the previous analysis. After crossing the first line (at point 2) the asymptotics is now a transseries that takes the form

$$u(x,t;\epsilon) \sim u^{(0)}(x,t;\epsilon) + \sum_{n=1}^{\infty} K_{01}^n u^{(n,1)}(x,t;\epsilon), \tag{4.91}$$

where K_{01} is a Stokes constant (in fact $K_{01} = 1$).

The activity of each Stokes line is examined and the results are the same as revealed above.

It is important to recall that $x = x_c$ is not a turning point/caustic for f_0 and $(n+1)f_1$. Hence the activity of the Stokes curve $S_{0>1}$ has changed at a regular point across the higher order Stokes curve that passes through $x = x_c$.

The 'dominant' part of the transseries on the real x-axis inside the caustics is

$$u(x,t;\epsilon) = a_0(x,t) + \sum_{n=1}^{\infty} K_{01}^n e^{-nf_1(x,t)/\epsilon} a_0^{(n,1)}(x,t) + O(\epsilon) \tag{4.92}$$

as $\epsilon \to 0^+$. Again, the exponentially small terms are included before the $O(\epsilon)$ because in this region $f_1(x,t)$ may decrease to zero.

By combining (4.78), (4.79) and (4.82), it can be deduced that

$$a_0^{(n,1)} = \left(a_0^{(1,1)}\right)^n \left(-2\frac{\partial f_1}{\partial x}\right)^{1-n}, \quad n = 2,3,4,\ldots. \tag{4.93}$$

From this relationship the n-sum in the transseries (4.92) may be summed to obtain

$$u(x,t;\epsilon) = a_0(x,t) + \frac{2K_{01}a_0^{(1,1)}(x,t)\frac{\partial f_1}{\partial x}e^{-f_1/\epsilon}}{2\frac{\partial f_1}{\partial x} + K_{01}a_0^{(1,1)}(x,t)e^{-f_1/\epsilon}} + O(\epsilon), \tag{4.94}$$

Comparing this result with equation (4.42) we see that both methods recover a similar form of the solution $u(x,t)$ in this region.

Continuing along from point 7 in the negative x-direction again sees the $(n)f_1$ all move towards f_0 in the Borel plane, so we see the apparent third caustic. In this case an examination of the coefficients $a_r(x,t)$ shows that individual terms in the asymptotics do not diverge at this point; it is not a true turning point. The terms themselves in the transseries do not diverge at the position of the smoothed shock.

This approach has shown that information regarding the higher order Stokes behaviour of Burgers' equation can be extracted without the integral form of solution that we used at the beginning of this chapter and in the previous chapter.

4.3 Summary

This chapter has shown how the higher order Stokes phenomenon is relevant to smoothed shock formation in a nonlinear PDE.

We began by analysing the Stokes structure of Burgers' equation using steepest descent methods. Due to the presence of branch cuts in the problem (arising form our choice of initial data), this proved to be an unsatisfactory way to approach the problem. We then changed to Borel plane analysis, which proved to be a more reliable and revealing method in extracting information on the higher order Stokes behaviour of the problem.

We found that at the position of the smoothed shock, there is no caustic or turning point. The reason for this is that the higher order Stokes phenomenon causes the singularities to lie on mutually different Riemann sheets, and there is only a virtual coalescence. It is a very subtle, yet crucial role.

Although this is a very specific example of a smoothed shock problem, chosen because of its pedagogical nature, we believe that the underlying results and analysis are general. For both the integral approach and the 'direct' approach, if a Borel

plane structure exists for a given problem with infinitely many Borel singularities, then it must be the case that these singularities lie on mutually different Riemann sheets at a shock where the asymptotics does not diverge.

The practicality of examining the effects of a higher order Stokes phenomenon should not be underestimated. The example of Burgers' equation was chosen as it is easily solved, providing a foot-up into the problem. The work included in the last section by Howls *et al.* provides an alternative which reaches the same conclusions as that of an integral approach. However, it should be noted that it is entirely dependent on being able to solve the equation (4.82), and often sufficient boundary data is lacking. In the next chapter will discuss this further.

The higher order Stokes phenomenon has clearly given a valuable extra insight into the underlying analytic structure of the asymptotics. Canonical examples such as Burgers' equation should therefore be regarded as important, even though they may be examples of PDE's that are already well studied.

Chapter 5

Discussion and Conclusions

The Borel plane approach to the higher order Stokes phenomena is, in effect, a 'plug and play' method. We have shown in this thesis that it works very well as a tool for determining the activity of Stokes lines and for determining the more subtle higher order Stokes behaviour of a given problem.

In this final chapter, we will consider ideas which could lead to further areas of research in the future. The main one of these will be what we will call the 'direct' method approach to extracting the Stokes behaviour of a problem. In essence, this is a Borel-type approach without an integral solution. We have encountered this in the previous chapter through Howls and Olde Daalhuis' work on Burgers' equation.

The new work in this thesis has focused mainly on PDE problems, both linear and nonlinear, and some interesting results have been uncovered. This should encourage further research of this type in PDEs. With this is mind, in this chapter we will briefly discuss formal methods of solving PDEs to produce integral solutions (in order to implement the integral approach, should a Borel plane structure exist), which are often hard to find or do not exist. We will then introduce and discuss at length work on the 'direct' method that has been carried out so far, and suggest future avenues of investigation.

5.1 Formal Solutions of PDE's

There are a few approaches to solving a given PDE problem that may be considered. Perhaps an exact solution is easily found, by change of variables and simple integration, etc., but this is unlikely. We might attempt to solve a PDE directly using matched asymptotic techniques for an approximate result. It may also be possible that formal integral solutions may exist. For example, hyperbolic equations may be solved formally in terms of an integral solution via Riemann's method [55]. The Riemann function $R(x, y)$ arises in the solution of the hyperbolic partial differential equation

$$\bar{L}u = u_{xy} + au_x + bu_y + cu = f, \tag{5.1}$$

$$u(0, t) = \phi(t),$$

$$u(t, 1) = \psi(t),$$

$$\phi(1) = \phi(0).$$

R(x,y) is the solution of the equation

$$R_{xy} - (aR)_x - (bR)_y + cR = 0 \tag{5.2}$$

with

$$R(\xi, y) = \exp\left[\int_\eta^y a(\xi, t)dt\right],$$

$$R(x, \eta) = \exp\left[\int_\xi^x b(t, \eta)dt\right],$$

on the characteristics $x = \xi$ and $y = \eta$. The solution is then given by the formula

$$u(x, y) = \int_0^x d\xi \int_1^y R(\xi, \eta; x, y) f(\xi, \eta)d\eta. \tag{5.3}$$

By [35] this multiple integral can be rewritten as a single integral, and thus we have an integral solution of the form (2.84).

Elliptic equations may be tackled in a similar way via Green functions, which will again lead to a formal integral solution for the problem [55]. Green functions

can also be applied to some parabolic equations, such as the diffusion equation. Consider the one-dimensional form

$$\phi(x,t)_t = \phi_{xx} + f(x,t). \tag{5.4}$$

The solution is given by

$$\phi(x,t) = \int_{-\infty}^{t}\int_{-\infty}^{\infty} G(x,t;y,\tau)f(y,\tau)dydt, \tag{5.5}$$

with the associated causal Green function $G(x,t;y,\tau)$ satisfying

$$G_t - G_{xx} = \delta(t-\tau)\delta(x-y). \tag{5.6}$$

In this case, it can be shown that

$$G(x,t;y,\tau) = \frac{H(t-\tau)}{2\sqrt{\pi(t-\tau)}}\exp\left(-\frac{(x-y)^2}{4(t-\tau)}\right), \tag{5.7}$$

where $H(t-\tau)$ is the Heaviside function

$$H(x) = \int_{-\infty}^{x}\delta(\xi)d\xi = \begin{cases} 0 & x<0 \\ 1 & x>0 \end{cases} \tag{5.8}$$

In many cases however, is it not a trivial exercise to find the value of $G(x,t;y,\tau)$.

The form of these solutions is interesting to us, because from them we may be able to develop theory linked to the areas we have discussed already. We may be able to deduce the existence of a Borel plane structure and of course this could introduce exponential asymptotic results for multiple integrals as a result.

For example, consider the work of Balian and Bloch [59] (see also [60]). They studied the Helmholtz equation

$$(\nabla^2 + k^2)\psi(\mathbf{r}) = 0, \tag{5.9}$$

where $\psi = 0$ on a specified boundary S. We will not consider the physics of the problem here, only the outline of the mathematics. The Green function satisfies

$$(\nabla^2 + k^2)G = \delta(\mathbf{r}-\mathbf{r}_0), \quad \mathbf{r},\mathbf{r}_0 \in S. \tag{5.10}$$

Thus

$$G = \int_S d\sigma_\alpha \frac{\partial G_0(\mathbf{r},\alpha)}{\partial n_\alpha} f(\alpha, \mathbf{r}_0), \tag{5.11}$$

where G_0 is known as the 'free' Green function. The variable σ measures out the boundary and n the outward normals from the boundary at a specified points α lying on the boundary. The function f is determined by the boundary conditions. Equation (5.11) is then rearranged to find an integral equation in f, whence iteration leads to the full Green solution of the form

$$\begin{aligned} G = & \int_S d\sigma_\alpha \frac{\partial G_0(\mathbf{r},\alpha)}{\partial n_\alpha} G_0(\alpha, \mathbf{r}_0) \\ + & \int_S d\sigma_\alpha d\sigma_\beta \frac{\partial G_0(\mathbf{r},\alpha)\partial G_0(\alpha,\beta)}{\partial n_\alpha} G_0(\beta, \mathbf{r}_0) \\ + & \int_S d\sigma_\alpha d\sigma_\beta d\sigma_\gamma \frac{\partial G_0(\mathbf{r},\alpha)\partial G_0(\alpha,\beta\partial G_0(\beta,\gamma)}{\partial n_\alpha} G_0(\gamma, \mathbf{r}_0) \\ + & \cdots . \end{aligned} \tag{5.12}$$

α, β, $\gamma, \ldots$ are points on the boundary S. The important thing from our point of view is that G_0 is known, and takes the following forms:

$$G_0 = \frac{-i}{4} H_0(k|\mathbf{r} - \mathbf{r}_0|) \quad \text{(2-dim)}, \tag{5.13}$$

$$G_0 = \frac{e^{ik|\mathbf{r}-\mathbf{r}_0|}}{|\mathbf{r} - \mathbf{r}_0|} \qquad \text{(3-dim)}. \tag{5.14}$$

Since the Hankel function asymptotically goes like an exponential

$$H_v(k) = \sqrt{\frac{2}{\pi x}} e^{i(x-\alpha_v)}. \quad x \to \infty, \tag{5.15}$$

(where $\alpha_v = (2v+1)\frac{\pi}{4}$ [12]) this means that the integrals in (5.12) begin to take the form that we require for our Borel plane method. If we now employ the results of Howls [35], we can reduce the string of multi-dimensional integrals to single integrals. We are then in a position to begin looking for Borel plane structures for the problem.

We see, then, that there may be scope for approaching complicated PDE problems from the point of view of an integral Borel method. But what if this is not possible? The next section will discuss this idea and develop techniques to overcome this problem.

5.2 The Direct Method

We begin by reviewing the work of Olde Daalhuis [61] (hereafter referred to as OD) who was the first to produce work on this approach.

The PDE he studies is

$$u_t - u_x = \epsilon^2 u_{xxx} - \frac{1}{1+ix}, \quad u(x,0) = -i\ln(1+ix). \tag{5.16}$$

OD first rewrites the equation in terms of new variables $s = x + t$, $\tau = t$, such that

$$u(x,t) = -i\ln(1+ix) + v(s,\tau). \tag{5.17}$$

Thus (5.16) becomes

$$v_\tau = \epsilon^2 v_{sss} - \frac{2\epsilon^2}{(1+i(s-\tau))^3}, \quad v(s,0) = 0. \tag{5.18}$$

Substituting the expansion

$$v(s,\tau) \sim \sum_{n=1}^{\infty} a_n(s,\tau)\epsilon^{2n} \tag{5.19}$$

into (5.18) obtains

$$\frac{\partial}{\partial\tau}a_1 = \frac{-2}{(1+i(s-\tau))^3}, \quad a_1(s,0) = 0 \tag{5.20}$$

and

$$\frac{\partial}{\partial\tau}a_n = \frac{\partial^3}{\partial s^3}a_{n-1}, \quad a_n(s,0) = 0, \quad n = 2,3,4,\cdots. \tag{5.21}$$

It is easy to see that

$$a_1(s,\tau) = \frac{i}{(1+i(s-\tau))^2} - \frac{i}{(1+is)^2}, \tag{5.22}$$

$$a_n(s,\tau) = \int_0^\tau \frac{\partial^3}{\partial s^3}a_{n-1}(s,\bar{\tau})d\bar{\tau}. \tag{5.23}$$

This important step in the method highlights a possible drawback at this early stage. From the form of $a_1(s,\tau)$ it can be seen that there will be blow up at $s = i$ and $s - \tau = i$, so a general form for the $a_n(s,\tau)$ can be extracted from this.

Therefore it is necessary that $a_1(s,\tau)$ can be calculated explicitly. The method from this point on is reliant on this fact.

The ansatz

$$a_n(s,\tau) \sim \frac{K(s,\tau)\Gamma(2n+\bar{\alpha})}{(f(s,\tau))^{2n+\alpha}}, \quad \text{as } n \to \infty \tag{5.24}$$

is made and substituted into (5.21), obtaining the equation

$$f_\tau = (f_s)^3. \tag{5.25}$$

Note that the Stokes multiplier K is a function of s and τ, not simply a constant. In general, $\alpha \neq \bar{\alpha}$.

Again, the derivation of equation (5.25) must be possible in order for this method to proceed.

Attention now turns to the blow up at $s = i$ in particular. Substituting a general form of $f(s,\tau)$ into (5.25) leads to

$$f(s,\tau) = \frac{(s-i)^{3/2}}{g(s,\tau)}, \tag{5.26}$$

and so now

$$a_n(s,\tau) \sim \frac{K(s,\tau)\Gamma(2n+\bar{\alpha})(g(s,\tau))^{2n+\alpha}}{(s-i)^{3n+3\alpha/2}}. \tag{5.27}$$

By comparing this term to the blow up of $a_1(s,\tau)$ it is possible to obtain the value $\alpha = -\frac{2}{3}$. Once more this step is only possible since a_1 can be found explicitly. Thus

$$a_n(s,\tau) \sim \frac{K(s,\tau)\Gamma(2n+\bar{\alpha})(g(s,\tau))^{2n-2/3}}{(s-i)^{3n-1}} \quad \text{as } n \to \infty. \tag{5.28}$$

To include the condition $a_n(s,0) = 0$, the simplest assumption to make is

$$g(s,\tau) \sim A\tau^\beta, \quad \tau \to 0. \tag{5.29}$$

Via equation (5.25) it may be seen that $\beta = \frac{1}{2}$.

At this stage, $f(s,\tau)$ is rewritten as

$$f(s,\tau) = \frac{2i(s-i)^{3/2}}{3\sqrt{3\tau}} h(s,\tau) \tag{5.30}$$

in order to simplify what follows. Upon substitution into (5.25) the following non-linear PDE is obtained:

$$(h + \frac{2}{3}(s-i)h_s)^3 = h - 2\tau h_\tau. \tag{5.31}$$

A Taylor expansion of $h(s,\tau)$ about $s = i,\ \tau = 0$

$$h(s,\tau) = h(i,0) + h_s(i,0)(s-i) + h_\tau(i,0)(\tau - 0) + \ldots \tag{5.32}$$

reveals that the only sensible solution of the PDE near $(s,\tau) = (i,0)$ is $h(s,\tau) = \pm 1$. This is seen by substituting (5.32) into (5.30) and then (5.25), and balancing terms. Hence, the first solution obtained is

$$f_1 = \frac{2i(s-i)^{3/2}}{3\sqrt{3\tau}}. \tag{5.33}$$

The same techniques are applied to the blow up at $s - \tau = i$, by setting

$$f(s,\tau) = (1 + i(s-\tau))k(s,\tau). \tag{5.34}$$

Now let $x = 1 + i(s-\tau)$, and $t = i\tau$, so that $f = xk(x,t)$ and

$$(k + xk_x)^3 = k + x(k_x - k_t). \tag{5.35}$$

In exactly the same fashion as above, it can be seen that the only analytic solution near $(x,t) = (0,0)$ is $k(x,t) = \pm 1$. Hence the second value of f is found to be

$$f_2 = 1 + i(s-\tau). \tag{5.36}$$

Relying on the fact that the $a_1(s,\tau), \cdots, a_6(s,\tau)$ are easily computable, the general form for the blow up near $s = i$ is found to be

$$a_n(s,\tau) \sim \frac{i(-\tau)^{n-1}\Gamma(3n-1)}{(s-i)^{3n-1}\Gamma(n)}, \quad \text{as } s \to i. \tag{5.37}$$

This dominant behaviour near $s = i$ also satisfies the recurrence relation in (5.21), so (5.37) holds for all n. It follows that $\bar{\alpha} = -\frac{1}{2}$. Similarly, for all n

$$a_n(s,\tau) \sim \frac{i(-1)^n\Gamma(2n)}{(s-\tau-i)^{2n}}, \quad \text{as } s - \tau \to i. \tag{5.38}$$

Note that this result cannot be valid near $\tau = 0$.

The activity of the Stoke lines can be determined using the asymptotic behaviour

$$a_n(s,\tau) \sim K_1(s,\tau)\frac{i(-\tau)^{n-1}\Gamma(3n-1)}{(s-i)^{3n-1}\Gamma(n)} + K_2(s,\tau)\frac{i(-1)^n\Gamma(2n)}{(s-\tau-i)^{2n}}, \quad \text{as } n \to \infty. \tag{5.39}$$

$K_1 \approx 1$ near $s = i$ and $K_2 \approx 1$ near $s - \tau = i$. At this stage, values of n, s and τ are substituted into the system, which is then solved for $K_1(s,\tau)$ and $K_2(s,\tau)$. Obviously the particular value of n chosen depends on the ability to calculate the corresponding $a_n(s,\tau)$.

When s is large and $s - \tau$ is bounded then the second term of the right-hand side of (5.39) is the dominant term in the asymptotics. Substituting this term into recurrence relation (5.52) gives

$$\frac{\partial K_2}{\partial \tau} + 3\frac{\partial K_2}{\partial s} = 0, \tag{5.40}$$

with general solution

$$K_2(s,\tau) = g(3\tau - s), \tag{5.41}$$

where $g(u)$ is an arbitrary function. Now take $s = \tau + d$ with τ large and d bounded. Computing the large τ asymptotics of $a_1(s,\tau), \ldots, a_6(s,\tau)$ shows that

$$a_n(s,\tau) \sim \frac{i(-1)^n\Gamma(2n)}{(d-i)^{2n}}, \quad \text{as } \tau \to \infty. \tag{5.42}$$

On comparison with (5.39), $g(2\tau - d) \sim 1$ as $\tau \to \infty$, that is,

$$K_2(s,\tau) \sim 1, \quad \text{as } t \to \infty \text{ along } x\text{=constant}, \tag{5.43}$$

where x and t are the original variables. This compares favourably with the numerical results produced above. This procedure is repeated using the first term on the right-hand side of (5.39). The equation obtained upon substituting this term into (5.52) is

$$\tau\frac{\partial K_1}{\partial \tau} + (s-i)\frac{\partial K_1}{\partial s} = 0. \tag{5.44}$$

Thus

$$K_1(s,\tau) = h\left(\frac{\tau}{s-i}\right), \tag{5.45}$$

where $h(u)$ is an arbitrary function. Take s fixed and look at the large τ asymptotics of $a_1(s,\tau),\ldots,a_6(s,\tau)$. Then

$$a_n(s,\tau) \sim \frac{i(-\tau)^n\Gamma(2n)}{(s-i)^{3n-1}}, \quad \text{as } \tau \to \infty. \tag{5.46}$$

Thus $h(\tau/(s-i)) \sim 1$ as $\tau \to \infty$, that is,

$$K_1(s,\tau) \sim 1, \quad \text{as } t \to \infty \text{ along } x+t = \text{constant} \tag{5.47}$$

This direct approach has been very successful in revealing the Stokes activity of the problem. However, we have highlighted a few questions raised by the method. It is already clear that in order for us to be successful, we require a certain amount of 'luck' to be able to proceed at each stage; in this particular case, it is in being able to calculate the a_n's explicitly.

Following the same method, we now attempt to finish off this problem by including an exponentially small term in front of the approximation for $v(s,\tau)$; thus

$$u(x,t) = -i\ln(1+ix) + v(s,\tau), \tag{5.48}$$

$$v(s,\tau) = \exp\left(-f(s,\tau)/\epsilon\right)\sum_{n=0}^{\infty} a_n(s,\tau)\epsilon^n, \tag{5.49}$$

and

$$s = x+t, \quad \tau = t. \tag{5.50}$$

In the original work, the value of f in (5.49) was zero; we had an "endpoint" expansion from which we found out about the interaction of the saddle and the pole with the endpoint. We now want to find out what the saddle and the pole know about each other.

If we substitute the above into the original equation (5.16) we recover the following equations:

$$(-f_\tau + (f_s)^3)a_0 = 0, \tag{5.51}$$

$$
\begin{aligned}
\Rightarrow a_0 &= 0 \text{ or } f_\tau = (f_s)^3 \\
(-f_\tau + (f_s)^3)a_1 &= 3f_s f_{ss} a_0 + 3(f_s)^2 \partial_s a_0 - \partial_t a_0, && (5.52) \\
(-f_\tau + (f_s)^3)a_2 &= 3f_s f_{ss} a_1 + 3(f_s)^2 \partial_s a_1 - \partial_t a_1 && (5.53) \\
&\quad - \{f_{sss} a_0 + 3f_{ss}\partial_s a_0 + 3f_s \partial_{ss} a_0\}, \\
(-f_\tau + (f_s)^3)a_{n+1} &= 3f_s f_{ss} a_n + 3(f_s)^2 \partial_s a_n - \partial_t a_n && (5.54) \\
&\quad - \{f_{sss} a_{n-1} + 3f_{ss}\partial_s a_{n-1} + 3f_s \partial_{ss} a_{n-1}\} + \partial_{sss} a_{n-2}, \\
&\quad (n \geq 3).
\end{aligned}
$$

In theory, equation (5.51) should lead us to all of the a_n, via the other equations; for example, a_1 should come from equation (5.52) since the left-hand side is zero if we assume $a_1 \neq 0$. The problem lies in the fact that finding the a_n in the above system requires that we can solve the equation

$$-f_\tau + (f_s)^3 = 0, \tag{5.55}$$

without any initial data (compare this with equation (4.82) from the previous chapter). One method we could use to try and solve it is Charpit's method [55]. Let

$$f_\tau \equiv p, \quad f_s \equiv q, \tag{5.56}$$

then

$$-p + q^3 = 0. \tag{5.57}$$

For simplicity, we set

$$s = x + t - i, \quad t = \tau. \tag{5.58}$$

The rays of the equation are as follows:

$$
\begin{aligned}
\tau &= \tau_0 - \bar{\tau}, && (5.59) \\
s &= s_0 + 3q_0^2 \bar{\tau}, && (5.60) \\
f &= f_0 + (-p_0 + 3q_0^3)\bar{\tau} \\
&= f_0 + (-q_0^3 + 3q_0^3)\bar{\tau}
\end{aligned}
$$

$$= f_0 + 2q_0^3\bar{\tau}, \tag{5.61}$$

$$\frac{df_0}{d\bar{s}} = p_0\frac{d\tau_0}{d\bar{s}} + q_0\frac{ds_0}{d\bar{s}}. \tag{5.62}$$

We must apply the initial condition $f_0 = 0$ in order to make the initial approximation (5.49) hold.

The cases $s_0 = \bar{s},\ \tau_0 = 0$ and $s_0 = 0,\ \tau_0 = \bar{s}$ both return the answer $p_0 = q_0 = 0$ (equations (5.62) and (5.57)). To avoid this, we have two other cases to consider.

Firstly we could have $s_0 = 0,\ t_0 = 0$. The rays in this case are

$$\tau = -\bar{\tau}, \tag{5.63}$$

$$s = 3q_0^2\bar{\tau}, \tag{5.64}$$

$$f = 2q_0^3\bar{\tau}. \tag{5.65}$$

This case means that the equation (5.62) becomes irrelevant $(0 = 0)$. We proceed by eliminating q_0 between the equations, giving

$$q_0 = \sqrt{\frac{-s}{3\tau}}. \tag{5.66}$$

Therefore

$$f = \sqrt{\frac{-4s^3}{27\tau}} = \pm i\sqrt{\frac{4s^3}{27\tau}} \tag{5.67}$$

$$= \pm\frac{2i(x+t-i)^{3/2}}{3\sqrt{3t}} \tag{5.68}$$

is the solution to (5.55).

The next case to look at is where $s_0 = \bar{s},\ \tau_0 = \bar{s}$. The rays in this case are

$$\tau = \bar{s} - \bar{\tau}, \tag{5.69}$$

$$s = \bar{s} + 3q_0^2\bar{\tau}, \tag{5.70}$$

$$f = 2q_0^3\bar{\tau}. \tag{5.71}$$

This time (5.62) gives us

$$0 = p_0 + q_0 \Rightarrow p_0 = -q_0. \tag{5.72}$$

Therefore from (5.57) we find that $q_0 = 0$ or $q_0 = \pm i$. Then, eliminating $\bar{s}$ and $\bar{\tau}$ from the above equations, we find that the solution to (5.55) is

$$f = \pm i(s - \tau) \tag{5.73}$$

$$= \pm(1 + ix). \tag{5.74}$$

We note here another flaw in the method we are presenting. In general we may not be able to solve the equivalent equations to (5.51) and we could not proceed any further, since we will not have enough boundary data to do so. The example of Howls and Olde Daalhuis in the previous chapter shows that, again, a certain degree of luck is required in order to solve such equations. They were able to use boundary data given on complex caustics in order to solve (4.82); in our case, there is no such information we can use.

Now, the LHS of equation (5.52) is zero, and having now found the solution to equation (5.51), we try and calculate the first few a_n terms. We face a huge problem, of course, in that we have no boundary data for the a_n at all. Consider $f = +i\sqrt{\frac{4(s)^3}{27\tau}}$. We can solve the first of our recurrence relations (5.52) to find

$$a_0 = \frac{1}{\sqrt{t}} C\left[\frac{s}{t}\right], \tag{5.75}$$

where C represents a constant function, and effectively this is as far as we can go. The same goes for $f = i(s - \tau)$ as well. Unfortunately, we cannot calculate any more information about the a_n's.

Chapman and Mortimer (hereafter referred to as CM) [52] provided an alternative approach, which we will review in this section. Even though many of the results are the same as we have have shown above, it still bears including their work in this section, as it provides a good summary of an alternative approach to this problem. CM draw on the work of Chapman *et al.* [16] and base their approach on the method of matching.

The equation they investigate is

$$\phi_t - \phi_s = \epsilon^2 \phi_{sss} - \tfrac{1}{1+s^2}, \tag{5.76}$$

$$\phi(s,0) = \tan^{-1} s, \tag{5.77}$$

$$\phi \to \pm\tfrac{\pi}{2} \quad \text{as } s \to \pm\infty. \tag{5.78}$$

Making the change of variables

$$\tau = t, \tag{5.79}$$

$$\sigma = s + t - i \quad , \tag{5.80}$$

equation (5.76) becomes

$$\phi_\tau = \epsilon^2 \phi_{\sigma\sigma\sigma} + \frac{i}{2(\sigma - \tau)}, \tag{5.81}$$

and in general

$$\phi_\tau^{(n)} = \phi_{\sigma\sigma\sigma}^{(n-1)}, \tag{5.82}$$

$$\phi^{(n)}(\sigma, 0) = 0. \tag{5.83}$$

They make the ansatz that the solution of (5.76) has the form

$$\phi^{(n)} \sim A(\sigma,\tau)\frac{\Gamma(2n + \gamma(\sigma,\tau))(-1)^n}{u(\sigma,\tau)^{2n+\gamma(\sigma,\tau)}}, \tag{5.84}$$

as $n \to \infty$. Substituting (5.84) into (5.82) obtains the following equations;

$$u_\tau + (u_\sigma)^3 = 0, \tag{5.85}$$

$$\gamma_\tau + 3\gamma_\sigma (u_\sigma)^2 = 0, \tag{5.86}$$

$$A_\tau + 3(u_\sigma)^2 A_\sigma + 3u_\sigma u_{\sigma\sigma} A = 0. \tag{5.87}$$

CM use Charpits method to solve (5.85). They note that the factorial-over-power divergence is generated by repeatedly differentiating the singularities of the early terms $\phi^{(0)}$ and $\phi^{(1)}$ and impose the condition that $u = 0$ at such a singularity. There are 2 singularities to consider, the static singularity at $s = i$ ($\sigma = \tau$) and the moving singularity at $s = i - t$ ($\sigma = 0$).

Considering first the static singularity at $s = i$, another change of variable is made

$$u = \sigma - \tau, \tag{5.88}$$

simplifying equations (5.86) and (5.87) to

$$\gamma + 3\gamma_\sigma = 0 \tag{5.89}$$

$$A_\tau + 3A_\sigma = 0 \tag{5.90}$$

respectively. Hence $\gamma = \gamma(\sigma - 3\tau)$ and $A = A(\sigma - 3\tau)$. Here they reason that since ϕ_1 has a double pole at $\sigma = \tau$ we must have that $\gamma \equiv 0$.

To determine A matching is used. A change of variables is made:

$$\sigma - \tau = \epsilon z, \tag{5.91}$$

$$\sigma - 3\tau = y, \tag{5.92}$$

$$\phi = \frac{-i}{2}\log\epsilon - \frac{i}{2}\psi, \tag{5.93}$$

The inner expansion is

$$\psi = \log z + \sum_{n=1}^{\infty} \frac{a_n(y)}{z^{2n}}, \tag{5.94}$$

as $z \to \infty$. They find

$$a_n = (-1)^n \Gamma(2n). \tag{5.95}$$

To match with the outer expansion, (5.84) is rewritten in the inner coordinates

$$\epsilon^{2n}\phi^{(n)} \sim A(y)\frac{\Gamma(2n)(-1)^n}{z^{2n}}. \tag{5.96}$$

They find that $A = i/2$ and so

$$\phi^{(n)} \sim \frac{i(-1)^n\Gamma(2n)}{2(\sigma - \tau)^{2n}}. \tag{5.97}$$

To determine the late terms of the moving singularity, CM impose the boundary conditions $\sigma = \tau = 0$ at the singularity, thus

$$u = \left(\frac{4\sigma^3}{27\tau}\right)^{1/2}. \tag{5.98}$$

The equivalent equations to (5.86) and (5.87) are

$$\gamma_\tau + \frac{\sigma}{\tau}\gamma_\sigma = 0, \tag{5.99}$$

$$A_\tau + \frac{\sigma}{\tau}A_\sigma + \frac{1}{2\tau}A = 0, \tag{5.100}$$

with solutions $\gamma = \gamma(\sigma/\tau)$ and $A = \tau^{-1/2}B(\sigma/\tau)$. Note that this is the same result that we arrived at with our method (cf. equation (5.75)). However, CM are able to go a step further with their calculations.

The functions γ and B are determined by matching with a region near the singularity. The inner coordinates are

$$y = \frac{\sigma}{\tau}, \tag{5.101}$$

$$\epsilon z = u, \tag{5.102}$$

$$\phi = -\frac{i}{2}\log\epsilon + \frac{i\psi}{2}, \tag{5.103}$$

and the inner expansion is

$$\psi = -\log\left(\frac{3^{3/2}z(y-1)}{2y^{3/2}}\right) + \sum_{n=1}^{\infty}\frac{B_n(y)}{z^{2n}}, \tag{5.104}$$

It is shown that B satisfies

$$B_n = o(y^n) \quad \text{as } y \to \infty, \tag{5.105}$$

and that the late terms will be of the form

$$B_n(y) \sim (-1)^n\Gamma(2n-1/2)b(y). \tag{5.106}$$

CM are unable to determine $b(y)$. However, they are able to 'spot' the solution for B_n from previous calculations; it is written as

$$B_n(y) = \frac{(1)^n\Gamma(2n)4^n y^{3n}}{27^n(y-1)^{2n}} + \frac{(-1)^{n+1}\Gamma(2n)4^n}{27^n}\sum_{j=0}^{n-1}\frac{\Gamma(2n+1)}{\Gamma(2n)\Gamma(j+1)}y^{n-j}. \tag{5.107}$$

So, although CM reach a solution, it is dependent on being able to spot the solution; it could not be calculated explicitly.

5.3 Summary

What we have seen in this chapter is that the direct method approach, be it from the point of view of a Borel-type approach, or from matching methods, is still very

much a 'work in progress'. However, it is most certainly a route worth pursuing further, since it could eventually allow us to investigate Stokes and higher order Stokes behaviour in complicated problems where there is no integral solution available. It is yet to be determined whether or not the problems we have encountered here can be overcome in general or not.

We have also shown, through the inclusion of work by Howls & Olde Daalhuis and Chapman & Mortimer, that we do not have to use the integral-type approaches endorsed by the work in this thesis in order to reproduce the results we have gained.

The fundamental results of this thesis do not necessarily arise from the techniques used to derive them. In Chapter 2 we introduced the notion that a 'ladder' of exponentials could be present in the solution of a boundary layer linear ODE. Coupled to this was the message that using an exponential asymptotic approach to finding approximate solutions to linear ODEs can be as good as matching techniques in terms of accuracy, and can sometimes simplify the whole process.

Chapter 3 revealed the existence of the higher order Stokes phenomenon, and crucially showed that even sub-subdominant exponentials should not be disregarded. We saw how such terms can in fact grow to dominate solutions. We showed how the Borel plane technique can handle this subtle effect, and actually illustrates the process very nicely.

In Chapter 4, we developed the ides from the previous chapter for nonlinear PDEs. Burgers' equation was a good choice because of its pedagogical nature; we had a integral solution to work with, and so progress with our integral-Borel approach was unhindered. We showed how the higher order Stokes phenomenon is a relevant effect to the behaviour of a nonlinear PDE. The classically smoothed shock of Burgers' equation is a consequence (albeit a very subtle one) of the higher order Stokes phenomenon.

We believe that future research in related areas, for example, the KdV equation

$$u_t + u_{xxx} = 6uu_x \tag{5.108}$$

may well produce similarly interesting results. Further to this, and inspired by the work of [67], it may be possible to extend the work on Burgers' equation to more general non-linear terms, and could potentially go some way to resolving some of the outstanding issues we have highlighted in this last chapter.

Appendix A

Form of the Late Terms in PDEs.

Can we see the factorial-over-power form of the late term asymptotics for PDE's? Let us consider the heat equation with the following boundary conditions:

$$\begin{gathered} u_t = u_{xx} \qquad (A.1) \\ 0 \leq x \leq b(\epsilon t),\ t > 0, \\ u(x,0) = \psi(x),\ 0 \leq x \leq b(0), \\ u(0,t) = \phi(\epsilon t),\ u(b(\epsilon t),t) = 0,\ \epsilon \to 0^+. \end{gathered}$$

Upon setting $\tau = \epsilon t$ this becomes

$$\begin{gathered} \epsilon u_\tau = u_{xx} \qquad (A.2) \\ 0 \leq x \leq b(\tau),\ \tau > 0, \\ u(x,0) = \psi(x),\ 0 \leq x \leq b(0), \\ u(0,\tau) = \phi(\tau),\ u(b(\tau),\tau) = 0,\ \epsilon \to 0^+. \end{gathered}$$

A perturbation solution of the form

$$u(x,t) \sim \sum_{n=0}^{\infty} f_n(x,t)\epsilon^n \qquad (A.3)$$

cannot satisfy all of the conditions above. Again, we could use the methods of matched asymptotic expansions, but instead we will impose the ansatz

$$u(x,\tau) \sim \sum_{n=0}^{\infty} f_n(x,\tau)\epsilon^n + \exp\left(\frac{-g(x,\tau)}{\epsilon}\right)\sum_{n=0}^{\infty} h_n(x,\tau)\epsilon^n. \tag{A.4}$$

This gives us a new set of boundary conditions to work with:

$$f_0(0,\tau) = \phi(\tau), \tag{A.5}$$

$$\begin{aligned} f_n(0,\tau) &= 0, \ n \geq 1, \\ f_n(b,\tau) &= 0 \ \forall n, \\ h_n(0,\tau) &= 0 \ \forall n, \\ h_n(b,\tau) &= 0 \ \forall n, \\ f_0(x,0) + h_0(x,0) &= \psi(x), \\ f_n(x,0) + h_n(x,0) &= 0, \ n \geq 1. \end{aligned} \tag{A.6}$$

Substituting this form of $u(x,\tau)$ into equation (A.2) and balancing at orders of ϵ and $\epsilon\exp(-g/\epsilon)$ leads to the following equations:

$$f_{0,xx} = 0, \tag{A.7}$$

$$f_{n-1,\tau} = f_{n,xx}, \tag{A.8}$$

$$-g_x^2 h_0 = 0 \ \Rightarrow g = g(\tau), \tag{A.9}$$

$$-g_\tau h_0 = h_{0,xx}, \tag{A.10}$$

$$-g_\tau h_n + h_{n-1} = h_{n,xx}. \tag{A.11}$$

Equation (A.7) can be integrated twice and using the appropriate boundary condition we find

$$f_0(x,\tau) = \phi(\tau)\left(1 - \frac{x}{b(\tau)}\right). \tag{A.12}$$

We also have enough information to tackle equation (A.10).

$$-g_\tau h_0 = h_{0,xx}, \tag{A.13}$$

$$\Rightarrow h_0 = A\sin\sqrt{g_\tau}x + B\cos\sqrt{g_\tau}x. \tag{A.14}$$

From the boundary conditions, we know that we must have

$$\begin{aligned} h_0(x,0) &= \psi(x) - f_0(x,0) \\ &= \left\{\psi(x) - \phi(0)\left(1 - \frac{x}{b(0)}\right)\right\}, \qquad \text{(A.15)} \\ h_n(0,\tau) = 0 \quad &\Rightarrow \quad B = 0, \qquad \text{(A.16)} \\ h_n(b,\tau) = 0 \quad &\Rightarrow \quad A\sin\sqrt{g_\tau}b(\tau) = 0. \qquad \text{(A.17)} \end{aligned}$$

Therefore we have that either $A = 0$ or $\sqrt{g_\tau}b(\tau) = k\pi$. Since the first result is trivial, we take the latter as true, so

$$\begin{aligned} g_\tau &= \left(\frac{k\pi}{b(\tau)}\right)^2, \qquad \text{(A.18)} \\ g(\tau) &= \int_0^\tau \frac{k^2\pi^2}{b(\xi)^2}d\xi. \qquad \text{(A.19)} \end{aligned}$$

We require $g(0) = 0$ in order to agree with the boundary data.

We now have the leading order solution to our problem.

$$\begin{aligned} u(x,\tau) &= f_0(x,\tau) + \sum_k \exp\left(-g(\tau)/\epsilon\right)h_0^{(k)}(x,\tau) \qquad \text{(A.20)} \\ &= \phi(\tau)\left(1 - \frac{x}{b(\tau)}\right) + \sum_k \exp\left[-\frac{1}{\epsilon}\int_0^\tau \left(\frac{k\pi}{b(\xi)}\right)^2 d\xi\right] A^{(k)}\sin\left(\frac{k\pi x}{b(\tau)}\right), \qquad \text{(A.21)} \end{aligned}$$

where

$$A^{(k)} = \int_0^{b(0)} \left[\psi(x) - \phi(0)\left(1 - \frac{x}{b(0)}\right)\right]\sin\left(\frac{k\pi x}{b(0)}\right)dx. \qquad \text{(A.22)}$$

Let us choose some boundary data and provide an example solution. Let

$$\begin{aligned} b(\tau) &= \sqrt{1+\tau^2}, \qquad \text{(A.23)} \\ \phi(\tau) &= 1, \qquad \text{(A.24)} \\ \psi(x) &= 0. \qquad \text{(A.25)} \end{aligned}$$

Then,

$$f_0(x,\tau) = 1 - \frac{x}{\sqrt{1+\tau^2}}, \qquad \text{(A.26)}$$

and

$$g(\tau) = \int_0^\tau \frac{k^2\pi^2}{1+\xi^2} d\xi \;=\; (k\pi)^2 \arctan\tau. \tag{A.27}$$

The leading order solution to this problem would then be

$$u(x,\tau) \sim 1 - \frac{x}{\sqrt{1+\tau^2}} + \sum_{k=1}^{\infty} e^{\{(k\pi)^2 \arctan\tau\}/\epsilon} \frac{-1}{k\pi} \sin\left(\frac{k\pi x}{\sqrt{1+\tau^2}}\right), \tag{A.28}$$

since

$$A^{(k)} \;=\; \int_0^1 (x-1)\sin(k\pi x)dx \tag{A.29}$$

$$\;=\; -\frac{1}{k\pi}, \quad k = 1,2,3,\ldots. \tag{A.30}$$

We are now free to calculate the f terms, and look to recover the factorial-over-power form

$$f_n(x,\tau) = \frac{\gamma(x,\tau)\Gamma(n+\alpha)}{F(x,\tau)^{n+\alpha}}, \; n \to \infty. \tag{A.31}$$

We calculate explicitly the values of $f_1, \ldots, f_6$ (using the relevant information from (A.6)) and by inspection we find that in general the form of the f's will be

$$f_n(x,\tau) = \frac{(-1)^{n+1}x^{2n+1}\phi(\tau)(b'(\tau))^n\Gamma(n+2)}{(b(\tau))^{n+1}(n+1)\Gamma(2n+2)}, \; b(\tau) \to 0, \; n \to \infty. \tag{A.32}$$

Using the same values of b, ϕ and ψ as in (A.23)-(A.25), the f_n's would become

$$f_n(x,\tau) = \frac{\tau^n x^{2n+1}\Gamma(n+2)}{(1+\tau^2)^{\frac{2n-1}{2}}\Gamma(2n+2)}, \; n \to \infty, \; \tau \to \pm i. \tag{A.33}$$

This demonstrates that the factorial-over-power form is also found in the late terms of series' arising from PDE's.

Appendix B

Hyperasymptotics

The infinite oriented contour $C_n(\theta_k)$ is the path of steepest descent through the nth saddle $z = z_n$, that is

$$\mathrm{Re}[k(f(z) - f_n)] > 0, \tag{B.1}$$

where $f_n \equiv f(z_n)$. Now let

$$I^{(n)}(k) \equiv k^{-\frac{1}{2}} e^{-kf_n} T^{(n)}(k), \tag{B.2}$$

$$T^{(n)}(k) = k^{\frac{1}{2}} \int_{C_n(\theta_k)} dz g(z) e^{-k[f(z)-f_n]} \tag{B.3}$$

The coefficients $T_r^{(n)}$ are required in the formal (divergent) asymptotic expansion

$$T^{(n)}(k) \sim \sum_{r=0}^{\infty} \frac{T_r^{(n)}}{k^r}. \tag{B.4}$$

A new variable

$$u(z) \equiv k[f(z) - f_n] \tag{B.5}$$

is introduced. For each point z on the contour $C_n(\theta_k)$, u is real and non-negative (by (B.1)), but for all $u \neq 0$, there are two values of z. This is because there exists a value $z_+(u)$ on the half of the steepest descent path emerging from z_n, and a value $z_-(u)$ on the half leading into z_n. Applying this transformation gives

$$T^{(n)}(k) = \int_0^{\infty} du \frac{e^{-u}}{\sqrt{k}} \left\{ \frac{g(z_+(u))}{f'(z_+(u)} - \frac{g(z_-(u))}{f'(z_-(u))} \right\}. \tag{B.6}$$

Crucially, the quantity in curly brackets can be written as the contour integral

$$\left\{\frac{g(z_+(u))}{f'(z_+(u)}-\frac{g(z_-(u))}{f'(z_-(u))}\right\}=\frac{1}{2\pi i u^{1/2}}\oint_{\Gamma_n(\theta_k)}dz\frac{g(z)[k\{(f(z)-f_n\}]^{1/2}}{f(z)-f_n-u/k} \tag{B.7}$$

where $\Gamma_n(\theta_k)$ is the positive (anticlockwise) loop surrounding $C_n(\theta_k)$, as shown in Figure 2.8. Combining (B.6) and (B.7) gives the representation

$$T^{(n)}(k)=\frac{1}{2\pi i}\int_0^\infty du\frac{e^{-u}}{u^{1/2}}\oint_{\Gamma_n(\theta_k)}dz\frac{g(z)[f(z)-f_n]^{1/2}}{f(z)-f_n-u/k}. \tag{B.8}$$

This is an exact representation of $T^{(n)}$ and provides the basis for what follows. The denominator of the second integral in (B.8) can be expanded binomially in powers of k^{-1} :

$$T^{(n)}(k)=\frac{1}{2\pi i}\int_0^\infty du\frac{e^{-u}}{u^{1/2}}\oint_{\Gamma_n(\theta_k)}dz\frac{g(z)[f(z)-f_n]^{1/2}}{(f(z)-f_n)\{1-u/k(f(z)-f_n)\}}, \tag{B.9}$$

and

$$\begin{aligned}\left(1-\frac{u}{k(f(z)-f_n)}\right)^{-1} &= \sum_{r=0}^{N-1}\left(\frac{u}{k(f(z)-f_n)}\right)^r \\ &+ \frac{u^N}{k^N(f(z)-f_n)^N}\frac{1}{(1-u/k(f(z)-f_n)},\end{aligned} \tag{B.10}$$

so

$$\begin{aligned}T^{(n)}(k) &= \sum_{r=0}^{N-1}\frac{1}{k^r}\int_0^\infty du\frac{e^{-u}u^{r-1/2}}{2\pi i}\oint_{\Gamma_n(\theta_k)}dz\frac{g(z)}{(f(z)-f_n)^{r+1/2}} \\ &+R^{(n)}(k,N)\end{aligned} \tag{B.11}$$

$$\Rightarrow T^{(n)}(k) = \sum_{r=0}^{N-1}\frac{T_r^{(n)}}{k^r}+R^{(n)}(k,N), \tag{B.12}$$

where the coefficients $T_r^{(n)}$ are defined as

$$T_r^{(n)} = \frac{(r-1/2)!}{2\pi i}\oint_n dz\frac{g(z)}{(f(z)-f_n)^{r+1/2}}. \tag{B.13}$$

The contour $\Gamma_n(\theta_k)$ has now been shrunk to a small positive loop around z_n. Integrals of this form can be evaluated exactly in terms of coefficients in the expansions of f and g about z_n, to yield explicit terms in the saddle expansion. For example, Dingle gives the leading $r = 0$ term

$$T_0^{(n)} = \sqrt{\frac{2\pi}{f_n''}} g_n. \tag{B.14}$$

Appendix C

Kuzmak's Method

Motivated by the form of (2.82) we can look for a solution that corresponds to the summation of all the p-exponentials in (2.77). This is similar to Kuzmak's method ([64], [65]) and is related to the method of multiple scales. We look for a solution of (2.63) based on the extended WKB ansatz:

$$\begin{aligned} y(x) &\sim \sum_{p=0}^{\infty} e^{-pF(1)/\epsilon} \sum_{n=0}^{\infty} f_n^{(p)}(x)\epsilon^n + \sum_{p=0}^{\infty} e^{-(F(x)+pF(1))/\epsilon} \sum_{n=0}^{\infty} h_n^{(p)}(x)\epsilon^n \\ &\sim \sum_{n=0}^{\infty} W_n(x,X)\epsilon^n + e^{-F(x)/\epsilon} \sum_{n=0}^{\infty} V_n(x,X)\epsilon^n, \end{aligned} \tag{C.1}$$

where $X = F(1)/\epsilon$. We now substitute the ansatz (C.1) into (2.63) and balance at $O(\epsilon^n)$ and $O(\exp(-F(x)/\epsilon))$, ignoring the ϵ-dependence in the X terms. Since the "variable" X is actually just a constant, we do not generate a derivative in $\partial/\partial X$, and as a consequence we simply arrive at the recurrence relations we obtained from substituting (2.65) into (2.63), but in W and V:

$$W_n(x,X) = \frac{c_n - W'_{n-1}(x,X)}{2x+1};\ V'_n(x,X) = \frac{V''_{n-1}(x,X)}{2x+1};\ n \geq 0 \tag{C.2}$$

with $W_{-1}(x,X) = V_{-1}(x,X) \equiv 0$. The constants c_n are determined from a modified set of boundary conditions. Due to the similarity of (2.65) and (C.1), again we find that (C.1) cannot satisfy the boundary condition at $x = 1$ exactly without

including further series. So, instead of (2.68) and (2.69) we have

$$W_n(0,X) + V_n(0,X) = \delta_{n0}\alpha, \tag{C.3}$$

$$W_n(1,X) + \exp(-X)V_n(1,X) = \delta_{n0}\beta. \tag{C.4}$$

Note that the exponential in (C.4) is $\exp(-F(1)/\epsilon)$, precisely of the order that was neglected in (2.69) and which lead to ansatz (2.77). We see then that had we included this exponential in (2.69) we would have avoided the need for section 2.3.1 (at the expense of missing out on the ladder structure of the problem). That we can now include this exponential term is a result of treating X as varying on a different scale to ϵ.

Using (C.3) and (C.4) we can now find the constants c_n. Some short calculations lead to

$$W_0(x,X) = \frac{(3\beta-\alpha)+\alpha(1-3\exp(-X))}{(1-3\exp(-X))(2x+1)}, \tag{C.5}$$

$$W_n(x,X) = \frac{(W'_{n-1}(1,X) - W'_{n-1}(x,X)) - 3\exp(-X)(W'_{n-1}(0,X) - W'_{n-1}(x,X))}{(1-3\exp(-X))(2x+1)}; \tag{C.6}$$

$$V_0(x,X) = \frac{(\alpha-3\beta)}{(1-3\exp(-X))}, \tag{C.7}$$

$$V_n(x,X) = \frac{W'_{n-1}(0) - W'_{n-1}(1)}{(1-3\exp(-X))}. \tag{C.8}$$

We find that we recover (2.82) if we insert the value of $\epsilon X = F(1) = 2$ at leading order in ϵ. Note that neglecting the terms in $\exp(-X)$ reduces the recurrence relations (C.5)-(C.8) to those in (2.72), as we should expect.

By addressing the issue of satisfaction of the boundary condition at $x = 1$, we derived a more sophisticated version of the WKB expansion (2.65). This is simply a more complicated ϵ-dependence in the coefficients. However we have not addressed the overall divergence of the perturbation expansion as a function of x. The series in (C.1) with coefficients according to (C.5)-(C.8) satisfy the boundary conditions at each order, but the sums of the W and V terms are still divergent.

Bibliography

[1] Hardy, G. H. 1949. *Divergent Series.* Clarendon Press, Oxford.

[2] Hyslop, J. M. 1942. *Infinite Series.* Oliver and Boyd, Edinburgh.

[3] Stokes, G. G. 1849. *Trans. Camb. Phil. Soc.,* **8**

[4] Dingle, R. B. 1973. *Asymptotic Expansions: their derivation and interpretation.* (Academic Press, New York and London)

[5] Poincaré, H. 1886. *Acta Math,* **8**, 295-344

[6] Olver, F. W. J. 1974. *Asymptotics and special functions.* (Academic Press, New York and London)

[7] Copson, E. T. 1965. *Asymptotic Expansions.* (Cambridge University Press)

[8] Wong, R. 1989. *Asymptotic Approximations of Integrals.* (Academic Press, New York and London)

[9] Berry, M. V. 1989, *Proc. Roy. Soc. Lond.,* **A422**, 7-21

[10] Howls C. J. 1991. *Exponential Asymptotics.* PhD thesis, Department of Physics, University of Bristol

[11] Berry, M. V. 1991. *Asymptotics, Superasymptotics, Hyperasymptotics* in *Asymptotics beyond all orders.* Editors: H. Segur *et al.* (Plenum Press, New York)

[12] Ablowitz, M. J. and Fokas, A. S. 1997. *Complex Variables: Introduction and Applications.* Cambridge University Press.

[13] McLeod, J. B. 1992. *Proc. Roy. Soc. Lond*, **A437**, 343-354

[14] Olde Daalhuis, A. B., Chapman S. J., King, J. R., Ockendon, J. R., & Tew, R. H. 1995. *SIAM J. Appl. Math*, **55**, 1469-1483

[15] Chapman, S. J. 1996. *Proc. Roy. Soc. Lond.*, **A452**, 2225-2230

[16] Chapman, S. J., King, J. R., Adams, K. L. 1997. *Proc. Roy. Soc. Lond.*, **A454**, 2733-2755

[17] Kruskal, S. and Segur, H. 1991. *Stud. Appl. Math.*, **85**, 129-181

[18] Amick, C. J. & McLeod, J. B. 1990. *Arch. Ration. Mech. Analysis*, **109**, 139-171

[19] Nayheh, A. H. 1973. *Perturbation Methods.* (John Wiley and Sons, New York)

[20] Costin, O. 1995. *IMRN*, **8**, 377-417

[21] Costin, O., Costin, R. D., Kohut, M. 2004. *Proc. Roy. Soc. Lond.*, **A460**, 3631-3641

[22] Costin, O., Kruskal, M. D. 199. *Proc. Roy. Soc. Lond.*, **A455**, 1931-1956

[23] Olde Daalhuis, A. B. 2005 *Hyperasymptotics for nonlinear ODEs I.* Submitted.

Hyperasymptotics for nonlinear ODEs II. Submitted.

[24] Airy, J. R. 1937. *Phil. Mag.*, **24**, 521-552

[25] Miller, J. C. P. 1952. *Proc. Camb. Phil. Soc.*, **48**, 243-254

[26] Boyd, W. G. C. 1990. *Proc. Roy. Soc. Lond.*, **A429**, 227-246

[27] Berry, M. V. and Howls, C. J. 1990. *Proc. Roy. Soc. Lond.*, **A430**, 653-668

[28] Berry, M. V. and Howls, C. J. 1991. *Proc. Roy. Soc. Lond.*, **A434**, 657-675

[29] Howls, C. J. 1992. *Proc. Roy. Soc. Lond.*, **A439**, 373-396

[30] Olde Daalhuis, A. B. 1992. *IMA J. Appl. Math.*, **49**, 203-216

[31] Olde Daalhuis, A. B. and Olver, F. J. 1995. *Methods Appl. Analysis*, **2**, 173-197,
Olde Daalhuis, A. B. and Olver, F. J. 1994. *Proc. Roy. Soc. Lond.*, **A445**, 1-29
Olde Daalhuis, A. B. and Olver, F. J. 1998. *SIAM Review*, **40**, 463-495

[32] Olde Daalhuis, A. B. 1995. *Methods Appl. Analysis*, **2**, 198-211

[33] Olde Daalhuis, A. B. 1998. *Proc. Roy. Soc. Lond.*, **A454**, 1-29

[34] Boyd, W. G. C. 1993. *Proc. Roy. Soc. Lond.*, **A440**, 493-518

[35] Howls, C. J. 1997. *Proc. Roy. Soc. Lond.*, **A453**, 2271-2294

[36] Écalle, J. 1981. *Les fonctions résurgentes.* Publ. Math. Université de Paris-Sud.

[37] Olde Daalhuis, A. B. 1996. *J. Comp. Appl. Math*, **76**, 255-264

[38] Olde Daalhuis, A. B. 1997. *J. Comp. Appl. Math.*, **89**, 87-95

[39] Berry, M. V. and Howls, C. J. 1993. *Proc. Roy. Soc. Lond*, **A443**, 107-126

[40] Berry, M.V. and Howls, C.J., 1994 *Proc. Roy. Soc. Lond*, **A444**, 201-216

[41] In *Toward the Exact WKB Analysis of Differential Equations, Linear or Non-Linear*, 2000. Editors: Howls, C. J., Kawai, T., Takei, Y. (Kyoto University Press)

[42] Pearcey, T. 1946. *Phil. Mag.*, **37**, 311-317

[43] Paris, R. B. 1991. *Proc. Roy. Soc. Lond.*, **A432**, 391-426

[44] Berk, H. L., Nevins, W. M., and Roberts, K. V. 1982. *J. Math. Phys.*, **42**, 3691-3713

[45] Aoki, T., Kawai, T., and Takei, Y. 2001. *J. Math. Phys.*, **23**, 988-1002

[46] Delabaere, E and Howls, C. J, 2002. *Duke Mathematical Journal*, **112**, 199-264

[47] de Bruijn, N. J, 1958. *Asymptotic Methods in Analysis.* (North Holland Publishing, Amsterdam)

[48] Hakim, V. and Mallick, K. 1992. *Exponentially small splitting of seperatrices, matching in the complex plane, and Borel summation*

[49] Howls, C. J., Langman, P. J., and Olde Daalhuis, A. B. 2004. *Proc. Roy. Soc. Lond.*, **A460**, 2285-2303

[50] Olde Daalhuis, A. B., 2004. *On the higher-order Stokes phenomenon of an inhomogeneous linear ordinary differential equation*, **169**, 235-246

[51] Fokas, A.S., 2002. *IMA Journal of Applied Mathematics*, **67**, 559-590

[52] Chapman, S. J., Mortimer D. 2004. In the press

[53] Senouf,D., Caflisch, R., Ercolani, N. 1996. *Nonlinearity*, **9**, 1671-1702

[54] Burgers, J. M. 1948. *Adv. Appl. Mech.*, **1**, 171-199

[55] Ockendon, J., Howison, S., Lacey, A., and Movchan, A. 1999. *Applied Partial Differential Equations.* (Oxford University Press)

[56] King, A., Billingham, J. FIND IT

[57] Cole, J. D. 1951. *Quart. Appl. Math.*, **9**, 225-236

[58] Hopf, E. 1950. *Commun. Pure Appl. Math.*, **3**, 201-230

[59] Balian, R. and Bloch, C. 1974. *Annals of Physics*, **85**, 514-545

[60] Trasler, S. A. 1998 *Higher Orders of Weyl Expansions.* PhD Thesis, Department of Mathematics and Statistics, Brunel University

[61] Olde Daalhuis, A. B. 2003. *Direct PDE Method*, Preprint

[62] Howls, C. J., & Olde Daalhuis, A. B., 2005. Preprint

[63] Howls, C.J., 2004. *Real Consequences of the Higher Order Stokes Phenomenon I, II and III.* (Kyoto University, Japan)

[64] Kuzmak, G. E. 1959. *J. Appl. Math. Mech.*, **23**, 730-744

[65] King, A. C., Billingham, J. and Otto, S. R. 2003. *Differential Equations.* (Cambridge University Press)

[66] Abramowitz, M. and Stegun, I. A. 1972. *Handbook of mathematical functions.* (National Bureau of Standards, Washington)

[67] Lee-Bapty I. P., Crighton D. G. 1987. *Phil. Trans. Roy Soc. Lond. A. Math. Phys, Sci.*, **323** , 173-209.